8-2011

Optimal Theory Applied in Integrodifference Equation Models and in a Cholera Differential Equation Model

Peng Zhong
pzhong@utk.edu

To the Graduate Council:

I am submitting herewith a dissertation written by Peng Zhong entitled "Optimal Theory Applied in Integrodifference Equation Models and in a Cholera Differential Equation Model." I have examined the final electronic copy of this dissertation for form and content and recommend that it be accepted in partial fulfillment of the requirements for the degree of Doctor of Philosophy, with a major in Mathematics.

Suzanne Lenhart, Major Professor

We have read this dissertation and recommend its acceptance:

Louis Gross, Charles Collins, Don Hinton

Accepted for the Council:
Dixie L. Thompson

Vice Provost and Dean of the Graduate School

(Original signatures are on file with official student records.)

To the Graduate Council:
I am submitting herewith a dissertation written by Peng Zhong entitled "Optimal Theory Applied in Integrodifference Equation Models and in a Cholera Differential Equation Model." I have examined the final electronic copy of this dissertation for form and content and recommend that it be accepted in partial fulfillment of the requirements for the degree of Doctor of Philosophy, with a major in Mathematics.

Suzanne Lenhart, Major Professor

We have read this dissertation
and recommend its acceptance:

Louis Gross

Don Hinton

Charles Collins

Accepted for the Council:

Carolyn R. Hodges

Vice Provost and Dean of the Graduate School

(Original signatures are on file with official student records.)

Optimal Theory Applied in Integrodifference Equation Models and in a Cholera Differential Equation Model

A Dissertation

Presented for the

Doctor of Philosophy

Degree

The University of Tennessee, Knoxville

Peng Zhong

August 2011

To my mother, Chen Fengyun

Acknowledgements

First and foremost I want to thank my advisor Suzanne Lenhart. It has been an honor to be Ph.D. student and a great pleasure working with her. I appreciate all her contributions of time, ideas, and funding to my Ph.D. experience. The joy and enthusiasm she has for her research was contagious and motivational for me, even during tough times in the Ph.D. pursuit. I am also thankful for the excellent example she has provided as a successful woman mathematician and professor.

I thank Prof. Louis Gross for the suggestions and discussions on both the harvesting and the cholera model and Prof. Elsa Scheafer and Boloye Gomero for the help with the Latin Hypercube Sampling analysis results. Prof. Don Hinton and Prof. Charles Collins are thanked for their help and general advice as committee members.

I am grateful to all my friends from the University of Tennessee, for being the surrogate family during the many years I stayed there and for their continued moral support there after.

Finally, I am forever indebted to my parents for their understanding, endless patience and encouragement when it was most required. Thank you.

Abstract

Integrodifference equations are discrete in time and continuous in space, and are used to model the spread of populations that are growing in discrete generations, or at discrete times, and dispersing spatially. We investigate optimal harvesting strategies, in order to maximize the profit and minimize the cost of harvesting. Theoretical results on the existence, uniqueness and characterization, as well as numerical results of optimized harvesting rates are obtained. The order of how the three events, growth, dispersal and harvesting, are arranged also affects the harvesting behavior.

Cholera remains a public health threat in many parts of the world and improved intervention strategies are needed. We investigate a key intervention strategy, vaccination, with optimal control applied to a cholera model. This system of differential equations has human compartments with susceptibles with different levels of immunity, symptomatic and asymptomatic infecteds, and two cholera vibrio compartments, hyperinfectious and non-hyperinfectious. The spread of the infection in the model is shown to be most sensitive to certain parameters, and the effect of varying these parameters on the optimal vaccination strategy is shown in numerical simulations. Our simulations also show the importance of the infection rate under various parameter cases.

Contents

List of Tables

List of Figures

Chapter 1

Introduction

1.1 Optimal Control Theory

This dissertation studies optimal control theory and its applications to mathematical models in biology and epidemiology, consisting of ordinary differential equations and integrodifference equations that simulate dynamics of populations and diseases. Mathematical biology is a growing branch of applied mathematics as the interest in modeling complex biological systems increases. Optimal control theory is a branch of mathematics developed to find optimal ways to control a dynamic system. Generally, the optimal control problem consists of an objective functional, a dynamic system and the control(s), which enter the dynamics in a variety of ways as coefficients, boundary terms or sources [15]. This dissertation focuses on biological applications of optimal control to integrodifference equations and to systems of ordinary differential equations. The tools used are Pontryagin's Maximum Principle and its extensions [43] . This principle was developed for optimal control of systems of ordinary differential equations.

1.2 Optimal Control of Harvesting Problems Modeled by Integrodifference Equations

Integrodifference equations model the spread of populations that are growing in discrete generations, or at discrete times, and dispersing spatially. These equations are discrete in time and continuous in space with a growth term usually followed by dispersal, represented by integration against a kernel.

The general form of an integrodifference equation is

$$N_{t+1}(x) = \int_{\Omega} k(x,y) f(N_t(y), y) dy,$$

where $N_t(x)$ is the population size or density at location x at time step t, $f(N_t(y), y)$ describes the local population growth at location y, and $k(x,y)$, often referred to as the dispersal kernel, is the probability of moving from point y to point x.

For certain species, these equations can assist in capturing the speed of the spread of populations [27, 28]. Invasive species and crops are important applications for these equations and lead to considerations about including harvesting in these models. Optimal control theory for integrodifference equations is beginning to be developed. Gaff, Joshi and Lenhart [16] worked on optimal harvesting in a crop model with a disease infestation, and Joshi, Lenhart, Gaff and Lou [21, 22] worked on optimal harvesting problems in which growth happens first, then dispersal following harvesting.

In Chapter 2 we first investigate optimal control analysis for harvesting problems in which the harvesting occurs after the growth and before the dispersal. The integrodifference model with harvesting is:

$$N_{t+1}(x) = \int_{\Omega} k(x,y)(1-\alpha_t(y)) f(N_t(y), y) dy \tag{1.1}$$

where $t = 0, 1, ..., T-1$.

The state variable N and the control α, which is the harvesting rate at the corresponding time step, are represented by

$$N = N(\alpha) = (N_0(x), N_1(x), \ldots, N_T(x)),$$

$$\alpha = (\alpha_0(x), \alpha_1(x), \ldots, \alpha_{T-1}(x)),$$

where x is the spatial variable in a bounded domain $\Omega \subset R^n$.

The harvesting profit is the objective functional to be maximized and the harvesting level is the control. The analytical part of this work includes existence, uniqueness, and characterization of the optimal control. The proofs of these results combine techniques from optimal control of partial differential equations [34] and discrete time models [45]. In $L^2(\Omega)$, weak convergence of maximizing sequences of controls and strong convergence of the corresponding state sequences are needed to justify the existence results. Differentiating the control-to-state and the control-to-objective functional maps are used to obtain the optimal control characterization.

The difference between this work and the work of Joshi et. al. [21, 22] can be seen in the different adjoint equations, the optimal control characterization, and the proof of existence of optimal control. But the differences can also be seen in numerical illustrations shown in Chapter 3. The numerical algorithm uses an iterative method of forward-backward sweeps with solving the state equations forward and the adjoint equations backwards, and updating the control with the characterization.

Since the order of events is crucial in a discrete time problem, in Chapter 4 we study all six possible orders of arranging the three events that happen during each time step - growth, dispersal and harvesting. Considering how certain orders can be obtained through transformations to other orders, we show that the six cases can be reduced to analyzing three cases.

1.3 Optimal Control of Vaccination in a Model of Cholera

Cholera, an infection of the small intestine caused by the bacterium *Vibrio choleae*, is a major cause of death in the world. Notable outbreaks happen every year, most recently in Haiti, October 2010, causing considerable losses of life and in the economy. A number of safe and effective vaccines for cholera are available.

Our research on this topic in Chapter 6 investigates the effects of vaccination in a cholera model. This model is a system of nine ordinary differential equations, tracking movement of susceptible individuals with and without partial immunities to either an asymptomatic infected class or a symptomatic infected class, then to two recovered classes with different waning rates. A vaccinated class is added into this model as well, and the vaccination rate is a control function. This model has the feature of two equations representing hyperinfectious and regular infectious *Vibrio choleae*, the concentrations in the environment which are determined by populations of infected humans. This work is an extension of models from King et al.[24], Hartley et al. [18], and Miller Neilan et al.[39].

The purpose of applying optimal control theory to the model of cholera stated above is to seek an optimal vaccination rate during a given time period that minimizes the economic and social losses. Therefore, the objective functional is to minimize the number of infected and the cost applying the vaccination control.

For illustrative numerical results, an iterative forward-backward sweep method with a fourth order Runge Kutta algorithm is used [31]. We first simulate outbreaks in a refugee camp with a population size of 10000, then construct optimal vaccination rates under various scenarios and study the effects of the parameters, initial conditions and weights of the objective functional on optimal vaccination strategies. The choice of parameters to vary is determined according to sensitivity analysis results using Latin Hypercube Sampling in collaboration with another UT student, Boloye Gomero, and with Elsa Schaefer, a professor at Emory University.

This project is a part of a collaborative project involving Elsa Schaefer, Holly Gaff, Renee Fister, Suzanne Lenhart and Boloye Gomero.

Chapter 2

Optimal Control for Harvesting Problems Modeled by Integrodifference Equations (Growth, Harvest and Dispersal)

2.1 Introduction

Integrodifference equation (IDE) models are discrete in time and continuous in space and represent populations with separate growth and dispersal stages [26, 33]. They were first formulated to study applications in physics [8] and population genetics [46, 47, 51].

Integrodifference equations were first applied to population ecology by Kot and Schaefer in 1986 [29]. IDE models have become more popular recently because of several advantages over reaction-diffusion equation models [3, 19, 38]. First, reaction-diffusion equations tend to underestimate the invading speed of some species [9, 36, 44], while integrodifference equations can provide a more accurate solution to that problem [27, 28, 32]. Second, integrodifference equations can readily incorporate a

variety of dispersal mechanisms [41], including fat-tailed kernels [5], while reaction-diffusion equations can only work with normal distributions.

Integrodifference equation models are also referred to as integral projection models [13], which were introduced as an alternative to traditional matrix population models, with the advantage of being able to eliminate the need for dividing a population into discrete classes. Populations of arthropod, multivoltine [23] and annual plant species [2] can be modeled with integrodifference equations.

The goal of the first part of this dissertation is to investigate optimal control of integrodifference equations, concentrating on harvesting problems. One application of optimal control for integrodifference equation models is a harvesting problem. For a species with separate growth and dispersal stages, harvesting can be done either before growth and after dispersal or before dispersal and after growth. The former case, on which the harvesting occurs before growth and after dispersal, was studied by Joshi, Lenhart and Gaff. They began with linear growth for the population and quadratic costs of the harvesting control [21]. Their objective functional was designed to maximize discounted revenue while minimizing a quadratic cost of the control.

They completed both analysis and numerical results on this harvesting problem, and later extended these results to the case with a convex growth function and convex cost function [22]. Their results were the first results on optimal control of IDE models. This approach was successfully used on an IDE system modeling crop disease [16]. Their approach was a combination of techniques from optimal control of partial differential equations and of discrete time models.

In this chapter, the case in which harvesting is done after growth and before dispersal, is studied. Using the same type of objective functional, we also begin with linear growth and quadratic costs, and then discuss a harvesting problem with a concave growth function and convex cost function. In both cases, the existence, characterization, and uniqueness of an optimal control are obtained.

Remark 2.1. *We refer to the harvesting problem with linear growth and quadratic costs as "the Linear Case", and the one with a concave growth function and convex cost function as "the Concave Case".*

2.2 Model with Linear Growth, Harvesting and Dispersal

2.2.1 Statement of the Problem for the Linear Case

The integrodifference model is:

$$N_{t+1}(x) = \int_{\Omega} k(x,y)(1-\alpha_t(y))f(N_t(y),y)dy \tag{2.1}$$

where $t = 0, 1, ..., T-1$.

The state variable N and the control α are represented by

$$N = N(\alpha) = (N_0(x), N_1(x), \ldots, N_T(x)),$$

$$\alpha = (\alpha_0(x), \alpha_1(x), \ldots, \alpha_{T-1}(x)),$$

where x is the spatial variable in a domain Ω.

Assumption 1. *Assume Ω is a bounded domain in R^n. The initial distribution $N_0(x)$ is given in $L^\infty(\Omega)$. Assume $\alpha_t(x)$ is Lebesgue measurable and $0 \leq \alpha_t(x) \leq M < 1$ for all $t = 0, 1, \ldots, T-1$ and $x \in \Omega$.*

Our goal is to maximize the objective functional $J(\alpha)$,

$$J(\alpha) = \sum_{t=0}^{T-1} \int_{\Omega} e^{-\delta t}[A_t\alpha_t(y)f(N_t(y),y) - \frac{B_t}{2}(\alpha_t(y))^2]dy. \tag{2.2}$$

In this problem, J represents the profit, which is the discounted revenue stream less the cost of the control, where the coefficient where A_t is the price factor and $e^{-\delta t}$ is

the discount factor with $\delta > 0$. Here we assume that the cost function is non-linear, and we will be dealing with a simple quadratic cost. The coefficient B_t is a weight factor that balances the two parts of the objective functional. The coefficients, A_t and B_t, are both positive numbers for any $t = 0, 1, \cdots, T-1$. We look for the control α^* that maximizes J, i.e.:

$$J(\alpha^*) = \max_{\alpha \in U} J(\alpha)$$

where the control set is $U = \left\{\alpha \in \left(L^\infty(\Omega)\right)^T | 0 \leq \alpha_t(x) \leq M, t = 0, 1, \ldots, T-1\right\}$ for $M < 1$.

Assumption 2. *We begin with a linear growth function:*

$$f(N_t(y), y) = rN_t(y).$$

Assumption 3. *Assume that the kernels are bounded and measurable such that*

$$\int_\Omega k(x, y)dy \leq 1$$

for all $x \in \Omega$, and

$$0 \leq k(x, y) \leq \Gamma$$

for $(x, y) \in \Omega \times \Omega$ and $\Gamma < 1$.

Note that integrodifference equations do not have boundary conditions on $\partial\Omega$ like in reaction-diffusion equations. No individuals enter the population from outside Ω. If x is near the $\partial\Omega$, the individuals who disperse outside $\partial\Omega$ are not counted in our population in Ω.

Assuming $N_0(x) \in L^\infty(\Omega)$, with $N_0(x) \geq 0$, we will show that the corresponding state $N = N(\alpha)$ satisfies $0 \leq N_t(\alpha) \leq C_T$, where C_T is a constant that depends on the number of discrete time steps considered in the process and the constant r.

Denote $\|\cdot\|$ by $\|\cdot\|_{L^\infty}$. Then we have

$$\|N_1\| = \|\int_\Omega k(1-\alpha)rN_0\| \leq r \cdot \|1-\alpha_0\| \cdot \|N_0\| \leq r\|N_0\|$$

$$\|N_2\| \leq r \cdot \|1-\alpha_1\| \cdot \|N_1\| \leq r^2\|N_0\|.$$

Continuing like this, we have

$$\|N_{t+1}\| \leq r \cdot \|1-\alpha_t\| \cdot \|N_t\| \leq r^{t+1}\|N_0\|.$$

Observing the state equations, we see that $k(x,y)$, $1-\alpha_t(y)$ are positive for any x, y, and f is positive whenever N_t is positive. By induction, we know the population can not be negative at anytime, i.e., $N_t(x) \geq 0$, for all t, x.

2.2.2 Existence for State System for the Linear Case

We first prove the existence of an optimal control.

Theorem 2.2. *Under Assumption 1, 2 and 3, there exists an optimal control α^* in U that maximizes the functional $J(\alpha)$.*

Proof. Let $\{\alpha^n\}$ be a maximizing sequence for the objective functional J in (2) and $N^n = N(\alpha^n)$ be the corresponding state sequence.

Since those two sequences are L^∞ bounded, there exists $\alpha^* \in U$ and $N^* \in (L^\infty(\Omega))^T$ such that on a subsequence, we have the following weak convergences,

$$N_t^n \rightharpoonup N_t^* \text{ in } L^2(\Omega), t = 1, \cdots, T$$

$$\alpha_t^n \rightharpoonup \alpha_t^* \text{ in } L^2(\Omega), t = 0, \cdots, T-1.$$

We want to show

$$\int_\Omega k(x,y)(1-\alpha_t^n(y))rN_t^n(y)dy \to \int_\Omega k(x,y)(1-\alpha_t^*(y))rN_t^*(y)dy$$

pointwise for each $x \in \Omega$.

It is known that $\alpha_t^n \rightharpoonup \alpha_t^*$ in $L^2(\Omega)$, and we want to show $N_t^n \to N_t^*$ strongly in $L^2(\Omega)$. For $k = 1$, we have

$$N_1^n(x) = \int_\Omega k(x,y)(1 - \alpha_0^n(y))rN_0(y)dy$$

since $N_0^n(x) = N_0(x)$ for all n.

From the assumption $0 \leq k(x,y) \leq 1$, $\int_\Omega k(x,y)^2 dy \leq 1$. So we know that $k(x,y) \in L^2(\Omega)$, and $k(x,y)rN_0^*(y) \in L^2(\Omega)$ as a function of y, for each x. Since $1 - \alpha_0^n(y) \rightharpoonup 1 - \alpha_0^*(y)$ in L^2, we have

$$\int_\Omega k(x,y)(1 - \alpha_0^n(y))rN_0^n(y)dy \to \int_\Omega k(x,y)(1 - \alpha_0^*(y))rN_0^*(y)dy,$$

which means $N_1^n \to N_1^*$ pointwise for each $x \in \Omega$.

We know the sequence N_1^n is uniformly L^∞ bounded and pointwise converge to N_1^*, which gives $|N_1^n(x) - N_1^*(x)|^2 \leq C$ and $|N_1^n(x) - N_1^*(x)|^2 \to 0$ *a.e.* for all n. From Lebesgue's Dominated Convergence Theorem, we have

$$\int_\Omega |N_1^n(x) - N_1^*(x)|^2 dx \to 0,$$

i.e., $N_1^n \to N_1^*$ in L^2. Using

$$N_2^n(x) = \int_\Omega k(x,y)(1 - \alpha_1^n(y))rN_1^n(y)dy,$$

$$1 - \alpha_1^n(y) \rightharpoonup 1 - \alpha_1^*(y),$$

$$N_1^n(y) \to N_1^*(y) \text{ in } L^2,$$

and k, and the sequences, α^n, N_1^n are L^∞ bounded, we obtain

$$N_2^n \to N_2^* \text{ pointwise},$$

and then $N_2^n \to N_2^*$ in L^2.

Continuing, we get $N_t^n \to N_t^*$ in L^2 for each $t = 1, 2, \cdots, T$. The weak L^2 convergence of $1 - \alpha_t^n$ sequence, the strong L^2 convergence of N_t^n sequence, and the L^∞ bounds on both sequences and k, give us

$$\int_\Omega k(x,y)(1-\alpha_t^n(y))rN_t^n(y)dy \to \int_\Omega k(x,y)(1-\alpha_t^*(y))rN_t^*(y)dy$$

for each x. Since

$$\int_\Omega k(1-\alpha_t^n)rN_t^n dy \to \int_\Omega k(1-\alpha_t^*)rN_t^* dy$$

for each x, we conclude $N^* = N(\alpha^*)$.

Here we use Corollary 2.2 from Ekeland and Témam's book. [14] By the weak L^2 convergence of α_t^n sequence, for each $t = 0, 1, \cdots, T-1$, we have

$$\int_\Omega (\alpha_t^*(x))^2 dx \leq \liminf_{n\to\infty} \int_\Omega (\alpha_t^n(x))^2 dx.$$

This inequality together with the convergence of the integral terms discussed above gives

$$J(\alpha^*) \geq \limsup_{n\to\infty} J(\alpha_t^n).$$

Thus the maximum of J is attained at α^*. □

2.2.3 Characterization of an Optimal Control for the Linear Case

To characterize an optimal control, we must differentiate the map $\alpha \to J(\alpha)$, which requires first the differentiation of the solution map $\alpha \to N(\alpha)$. The directional derivative of this solution map is called the sensitivity of the state with respect to the control.

Theorem 2.3. *Under Assumption 1, 2 and 3, the mapping* $\alpha \in U \to N \in (L^\infty(\Omega))^{T+1}$ *is differentiable in the following sense: For any* $\alpha \in U$ *and* $l \in (L^\infty(\Omega))^T$*, such that* $(\alpha + \epsilon l) \in U$ *for* ϵ *small, where* $N^\epsilon = N(\alpha + \epsilon l)$ *and* $N = N(\alpha)$*, there exists a sensitivity* $\psi \in (L^\infty(\Omega))^{T+1}$ *such that*

$$\frac{N_t^\epsilon(x) - N_t(x)}{\epsilon} \rightharpoonup \psi_t(x)$$

weakly in $L^2(\Omega)$*, as* $\epsilon \to 0$ *for each* t*. Also* ψ*, depending on* N*,* α *and* l*, satisfies:*

$$\psi_{t+1}(x) = \int_\Omega rk(x,y)[(1-\alpha_t(y))\psi_t(y) - l_t(y)N_t(y)]dy \tag{2.3}$$

$$\psi_0(x) = 0,$$

for $t = 0, 1, \cdots, T$*.*

Remark 2.4. *Since the sensitivity function depends on* N*,* α *and* l*, we can use* $\psi(\alpha, N(\alpha), l)$ *to denote the directional derivative of* $N(\alpha)$ *along vector* l *with respect to* α*.*

Proof. We form the difference quotient for the directional derivative of N with respect to α in the direction l:

$$\begin{aligned}\frac{N_{t+1}^\epsilon(x) - N_{t+1}(x)}{\epsilon} &= \frac{1}{\epsilon}\int_\Omega rk(x,y)[(1-\alpha_t(y))(N_t^\epsilon(y) - N_t(y)) - \epsilon l_t(y)N_t^\epsilon(y)]dy \\ &= \int_\Omega rk(x,y)[(1-\alpha_t(y))\frac{(N_t^\epsilon(y) - N_t(y))}{\epsilon} - l_t(y)N_t^\epsilon(y)dy\end{aligned}$$

Using $N_0^\epsilon = N_0$ and

$$\frac{N_1^\epsilon(x) - N_1(x)}{\epsilon} = \int_\Omega rk(x,y)l_0(y)N_0(y)dy,$$

we have

$$|\frac{N_1^\epsilon(x) - N_1(x)}{\epsilon}| \le C_1 \qquad \text{for all } x \in \Omega.$$

And then by iteration,

$$|\frac{N_t^\epsilon(x) - N_t(x)}{\epsilon}| \leq C_t \qquad \text{for all } x \in \Omega, t = 1, 2, \cdots, T.$$

From the *a priori* estimate, we have

$$\frac{N_t^\epsilon(x) - N_t(x)}{\epsilon} \rightharpoonup \psi_t(x) \qquad \text{weakly in } L^2(\Omega).$$

Similarly as in Theorem 1, by iteration, we have $\frac{N_t^\epsilon(x) - N_t(x)}{\epsilon}$ converges pointwise, and also strongly in L^2, which gives us the existence of $\psi \in (L^\infty(\Omega))^{T+1}$ such that

$$\psi_0(x) = 0$$

and

$$\int_\Omega rk(x,y)[(1-\alpha_t(y))\frac{(N_t^\epsilon - N_t)(y)}{\epsilon} - l_t N_t^\epsilon]dy \to \int_\Omega rk(x,y)[(1-\alpha_t(y))\psi_t(y) - l_t N_t]dy$$

Passing to the limit, we get

$$\psi_{t+1}(x) = \int_\Omega rk(x,y)[(1-\alpha_t(y))\psi_t(y) - l_t(y)N_t(y)]dy,$$

for $t = 0, \cdots, T$. □

Now we differentiate the map $\alpha \to J(\alpha)$ to obtain a characterization of an optimal control.

Theorem 2.5. *Under Assumption 1, 2 and 3, given an optimal control α^* and corresponding state solution $N^* = N(\alpha^*)$, there exists a solution $p \in (L^\infty(\Omega))^T$ satisfying the adjoint system:*

$$\begin{aligned} p_{t-1}(x) &= r(1-\alpha_{t-1}^*(x))\int_\Omega p_t(y)k(y,x)dy + e^{-\delta t}rA_{t-1}\alpha_{t-1}^*(x) \\ p_T(x) &= 0 \end{aligned} \tag{2.4}$$

where $t = T, \cdots, 2, 1$. *Furthermore, for* $t = 0, 1, 2, \cdots, T-1$*;*

$$\alpha_t^*(x) = min(max(\frac{(\int_\Omega -p_{t+1}(y)k(y,x)dy + e^{-\delta t}A_t)rN_t^*(x)}{e^{-\delta t}B_t}, 0), M) \tag{2.5}$$

Proof. Let α^* be an optimal control (which exists by Theorem 1) and $N^* = N(\alpha^*)$ be the corresponding state. For variation l with $(\alpha^* + \epsilon l) \in U$ for $\epsilon > 0$ sufficiently small, let N^ϵ be the corresponding solution of the state equation. Since the adjoint system is linear, there exists a solution p. We compute the directional derivative of the functional $J(\alpha)$ with respect to α in the direction l at α^*. Since $J(\alpha^*)$ is the maximum value, we have

$$\begin{aligned}
0 \geq & \lim_{\epsilon \to 0^+} \frac{J(\alpha^* + \epsilon l) - J(\alpha^*)}{\epsilon} \\
= & \lim_{\epsilon \to 0^+} \sum_{t=0}^{T-1} \frac{1}{\epsilon} \Big\{ \int_\Omega e^{-\delta t} \big[A_t r(\alpha_t^* + \epsilon l_t) N_t^\epsilon(y) - \frac{B_t}{2}(\alpha_t^* + \epsilon l_t)^2 \big] dy \\
& - \int_\Omega e^{-\delta t} \big[A_t r(\alpha_t^*) N_t^*(y) - \frac{B_t}{2}(\alpha_t^*)^2 \big] dy \Big\} \\
= & \lim_{\epsilon \to 0^+} \sum_{t=0}^{T-1} \int_\Omega e^{-\delta t} \big[A_t r \alpha_t^* \frac{N_t^\epsilon(y) - N_t^*(y)}{\epsilon} + A_t l_t r N_t^\epsilon(y) - \frac{B_t}{2} \epsilon l_t^2 - B_t \alpha_t l_t \big] dy \\
= & \sum_{t=0}^{T-1} \int_\Omega e^{-\delta t} A_t r \alpha_t^*(y) \psi_t(y) dy + \sum_{t=0}^{T-1} \int_\Omega e^{-\delta t} A_t l_t r N_t^*(y) dy \\
& - \sum_{t=0}^{T-1} \int_\Omega e^{-\delta t} B_t \alpha_t^*(y) l_t(y) dy.
\end{aligned}$$

We use the coefficient of the ψ_t term as the non-homogeneous term in the adjoint system and transform that term:

$$\begin{aligned}
&\sum_{t=0}^{T-1}\int_\Omega e^{-\delta t}A_t r\alpha_t^*(y)\psi_t(y)dy \\
&=\sum_{t=0}^{T-1}\int_\Omega [p_t(y)-r(1-\alpha_t^*(y))\int_\Omega p_{t+1}(x)k(x,y)dx]\psi_t(y)dy \\
&=\sum_{t=0}^{T-1}\int_\Omega p_t(y)\psi_t(y)dy-\sum_{t=0}^{T-1}\int_\Omega r(1-\alpha_t^*(y))\psi_t(y)\int_\Omega p_{t+1}(x)k(x,y)dxdy \\
&=\sum_{t=0}^{T-1}\int_\Omega p_{t+1}(y)\psi_{t+1}(y)dy-\int_\Omega p_T(y)\psi_T(y)dy+\int_\Omega p_0(y)\psi_0(y)dy \\
&-\sum_{t=0}^{T-1}\int_\Omega p_{t+1}(x)\int_\Omega r(1-\alpha_t^*(y))\psi_t(y)k(x,y)dydx \\
&=\sum_{t=0}^{T-1}\int_\Omega p_{t+1}(x)[\psi_{t+1}(x)-\int_\Omega rk(x,y)(1-\alpha_t^*(y))\psi_t(y)dy]dx \\
&=\sum_{t=0}^{T-1}\int_\Omega p_{t+1}(x)[-r\int_\Omega k(x,y)l_t(y)N_t^*(y)dy]dx
\end{aligned}$$

where we used $p_T(x)\equiv 0$, $\psi_0(x)\equiv 0$, and the sensitivity equation (2.3). Substituting out for the first term from our quotient calculation,

$$\begin{aligned}
0\geq&\sum_{t=0}^{T-1}\int_\Omega p_{t+1}(x)[-r\int_\Omega k(x,y)l_t(y)N_t^*(y)dy]dx+\sum_{t=0}^{T-1}\int_\Omega e^{-\delta t}A_t l_t r N_t^*(y)dy \\
&-\sum_{t=0}^{T-1}\int_\Omega e^{-\delta t}B_t\alpha_t^*(y)l_t(y)dy \\
&=\sum_{t=0}^{T-1}\int_\Omega[(\int_\Omega -p_{t+1}(x)k(x,y)dx+e^{-\delta t}A_t)rN_t^*(y)-e^{-\delta t}B_t\alpha_t^*(y)]l_t(y)dy.
\end{aligned}$$

For any $t=0,1,\cdots,T-1$, on the set $\{(x:0<\alpha_t^*(x)<M\}$, the variation l_t can be taken with support on this set, and have any sign, because the optimal control can be modified a little up or down and still stay inside the bounds. Thus, on this set,

the rest of the integrand must be zero, so that

$$\alpha_t^*(x) = \frac{(\int_\Omega -p_{t+1}(y)k(y,x)dy + e^{-\delta t}A_t)rN_t^*(x)}{e^{-\delta t}B_t}.$$

By taking the upper and lower bounds into account we now show

$$\alpha_t^*(x) = min(max(\frac{(\int_\Omega -p_{t+1}(y)k(y,x)dy + e^{-\delta t}A_t)rN_t^*(x)}{e^{-\delta t}B_t}, 0), M).$$

We now show how we handle the bounds.

For any $t = 0, 1, \cdots, T-1$, on the set $\{x : \alpha_t^*(x) = 0\}$, take l_t with support on this set and l_t can only be nonnegative, and

$$0 \leq \sum_{t=0}^{T-1} \int_\Omega [(\int_\Omega -p_{t+1}(x)k(x,y)dx + e^{-\delta t}A_t)rN_t^*(y)]l_t(y)dy,$$

that indicates

$$\frac{(\int_\Omega -p_{t+1}(y)k(y,x)dy + e^{-\delta t}A_t)rN_t^*(x)}{e^{-\delta t}B_t} \leq 0.$$

Hence on this set, we have

$$\alpha_t^*(x) = min(max(\frac{(\int_\Omega -p_{t+1}(y)k(y,x)dy + e^{-\delta t}A_t)rN_t^*(x)}{e^{-\delta t}B_t}, 0), M) = 0.$$

On the other hand, on the set $\{x : \alpha_t^*(x) = M\}$, then l_t with support on this set can only be non-positive, and

$$0 \leq \sum_{t=0}^{T-1} \int_\Omega [(\int_\Omega -p_{t+1}(x)k(x,y)dx + e^{-\delta t}A_t)rN_t^*(y) - e^{-\delta t}B_t M]l_t(y)dy,$$

that indicates

$$\frac{(\int_\Omega -p_{t+1}(y)k(y,x)dy + e^{-\delta t}A_t)rN_t^*(x)}{e^{-\delta t}B_t} \geq M.$$

Hence on this set,

$$\alpha_t^*(x) = min(max(\frac{(\int_\Omega -p_{t+1}(y)k(y,x)dy + e^{-\delta t}A_t)rN_t^*(x)}{e^{-\delta t}B_t}, 0), M) = M.$$

So $\alpha_t^*(x) = min(max(\frac{(\int_\Omega -p_{t+1}(y)k(y,x)dy + e^{-\delta t}A_t)rN_t^*(x)}{e^{-\delta t}B_t}, 0), M)$ is our characterization of an optimal control. □

2.2.4 Uniqueness Result for the Linear Case

We obtain uniqueness of the optimal control under the assumption of largeness of the cost coefficients, B_t, using a strict concavity argument. See [21] for similar arguments.

Remark 2.6. *In both linear and concave cases, note for $\alpha = 0$, we have $J(\alpha) = 0$. This implies $0 \leq \max_{\alpha \in U} J(\alpha)$. Thus $J(\alpha^*) \geq 0$, even if B_t's are large.*

Theorem 2.7. *Under Assumption 1, 2 and 3, if B_t, $t = 0, 1, \cdots, T-1$ are sufficiently large, then the optimal control is unique.*

Proof. We show uniqueness by showing strict concavity of the map:

$$\alpha \in U \to J(\alpha).$$

The strict concavity follows from showing for all α, $l \in U$, and $0 < \epsilon < 1$,

$$g''(\epsilon) < 0$$

where $g(\epsilon) = J(\epsilon l + (1-\epsilon)\alpha)) = J(\alpha + \epsilon(l - \alpha))$.

For convenience we denote

$$N_t^\epsilon = N(\alpha + \epsilon(l - \alpha))$$

for $t = 0, 1, \cdots, T-1$, and similarly

$$N_t^{\epsilon+\tau} = N(\alpha + (\epsilon+\tau)(l-\alpha)),$$

for $t = 0, 1, \cdots, T-1$. First, we calculate

$$\begin{aligned}
g'(\epsilon) &= \lim_{\tau\to 0} \frac{J(\alpha + (\epsilon+\tau)(l-\alpha)) - J(\alpha+\epsilon(l-\alpha))}{\tau} \\
&= \lim_{\tau\to 0} \sum_{t=0}^{T-1} \frac{1}{\tau} \Big(\int_\Omega e^{-\delta t}[A_t(\alpha_t + (\epsilon+\tau)(l_t-\alpha_t))rN_t^{\epsilon+\tau} \\
&\quad -\frac{B_t}{2}(\alpha_t + (\epsilon+\tau)(l_t-\alpha_t))^2]dy \\
&\quad - \int_\Omega e^{-\delta t}[A_t(\alpha_t+\epsilon(l_t-\alpha_t))rN_t^\epsilon - \frac{B_t}{2}(\alpha_t+\epsilon(l_t-\alpha_t))^2]dy\Big) \\
&= \lim_{\tau\to 0} \sum_{t=0}^{T-1} \int_\Omega e^{-\delta t}[A_t(\alpha_t+\epsilon(l_t-\alpha_t))r\frac{N_t^{\epsilon+\tau}-N_t^\epsilon}{\tau} + A_t(l_t-\alpha_t)rN_t^{\epsilon+\tau} \\
&\quad -\frac{B_t}{2}\tau(l_t-\alpha_t)^2 - B_t(\alpha_t+\epsilon(l_t-\alpha_t))(l_t-\alpha_t)]dy \\
&= \sum_{t=0}^{T-1} \int_\Omega e^{-\delta t}[A_t(\alpha_t+\epsilon(l_t-\alpha_t))r\psi_t^\epsilon + A_t(l_t-\alpha_t)rN_t^\epsilon \\
&\quad -B_t(\alpha_t+\epsilon(l_t-\alpha_t))(l_t-\alpha_t)]dy.
\end{aligned}$$

Remark 2.4 indicates that the directional derivative of $N(\alpha+\epsilon(l-\alpha))$ along vector $l-\alpha$ with respect to $\alpha+\epsilon(l-\alpha)$ is $\psi(\alpha+\epsilon(l-\alpha), N(\alpha+\epsilon(l-\alpha)), l-\alpha)$. For convenience we use the following notation

$$\psi^\epsilon = \psi(\alpha+\epsilon(l-\alpha), N(\alpha+\epsilon(l-\alpha)), l-\alpha),$$

and similarly

$$\psi^{\epsilon+\tau} = \psi(\alpha+(\epsilon+\tau)(l-\alpha), N(\alpha+(\epsilon+\tau)(l-\alpha)), l-\alpha).$$

From Theorem 2.3 we obtain

$$\frac{N_t^{\epsilon+\tau} - N_t^{\epsilon}}{\tau} \rightharpoonup \psi_t^{\epsilon} \text{ as } \tau \to 0$$

with

$$\begin{aligned} \psi_{t+1}^{\epsilon}(x) &= \int_{\Omega} rk(x,y)[(1-(\alpha_t(y)+\epsilon(l_t-\alpha_t)))\psi_t^{\epsilon}(y) - (l_t-\alpha_t)N_t^{\epsilon}(y)]dy \qquad (2.6) \\ \psi_0^{\epsilon}(x) &\equiv 0. \end{aligned}$$

Similarly,

$$\begin{aligned} \psi_{t+1}^{\epsilon+\tau}(x) &= \int_{\Omega} rk(x,y)[(1-(\alpha_t(y)+(\epsilon+\tau)(l_t-\alpha_t)))\psi_t^{\epsilon+\tau}(y) - (l_t-\alpha_t)N_t^{\epsilon+\tau}(y)]dy \qquad (2.7) \\ \psi_0^{\epsilon}(x) &\equiv 0. \end{aligned}$$

Estimate $\psi_t^{\epsilon}(x)$ in terms of $l-\alpha$:

$$\begin{aligned} |\psi_1^{\epsilon}(x)| &= \left| \int_{\Omega} rk(x,y)(l_0-\alpha_0)N_0^{\epsilon}(y)dy \right| \\ &\leq D_1 \int_{\Omega} |l_0-\alpha_0|\, dy, \end{aligned}$$

$$\begin{aligned} |\psi_2^{\epsilon}(x)| &= \left| \int_{\Omega} rk(x,y)[(1-(\alpha_1+\epsilon(l_1-\alpha_1)))\psi_1^{\epsilon}(y) - (l_1-\alpha_1)N_1^{\epsilon}(y)]dy \right| \\ &\leq D_2\Big(\int_{\Omega} |l_0-\alpha_0|\, dy + \int_{\Omega} |l_1-\alpha_1|\, dy \Big), \end{aligned}$$

and continuing to estimate, we obtain

$$\left|\psi_{t+1}^{\epsilon}(x)\right| \leq D_{t+1} \sum_{i=0}^{t} \int_{\Omega} |l_i-\alpha_i|\, dy,$$

where the sequence D_{t+1} does not depend on ϵ.

Given (2.6) and (2.7), and $\psi_0^{\epsilon+\tau} \equiv \psi_0^{\epsilon} \equiv 0$, we use σ_t^{ϵ} to represent the difference quotient for directional derivative of ψ with respect to $\alpha + \epsilon(l-\alpha)$ in the direction $l - \alpha$:

$$\begin{aligned}
&\frac{\psi_{t+1}^{\epsilon+\tau}(x) - \psi_{t+1}^{\epsilon}(x)}{\tau} = \\
&\quad \int_\Omega rk(x,y)[(1-\alpha_t(y) - \epsilon(l_t-\alpha_t)(y))\frac{\psi_t^{\epsilon+\tau}(y) - \psi_t^{\epsilon}(y)}{\tau}dy \\
&\quad - \int_\Omega rk(x,y)(l_t-\alpha_t)(y)\psi_t^{\epsilon,\tau}(y)dy \\
&\quad - \int_\Omega rk(x,y)(l_t(y)-\alpha_t(y))\frac{N_t^{\epsilon+\tau}(y) - N_t^{\epsilon}(y)}{\tau}dy.
\end{aligned}$$

Using $N_0^{\epsilon} = N_0$, $\psi_0^{\epsilon} \equiv 0$ and

$$\frac{\psi_1^{\epsilon+\tau}(x) - \psi_1^{\epsilon}(x)}{\tau} = \int_\Omega rk(x,y)(\alpha_t(y) + (\epsilon+\tau)(l_t-\alpha_t)(y))N_0^{\epsilon+\tau}(y)dy,$$

we have

$$|\frac{\psi_1^{\epsilon+\tau}(x) - \psi_1^{\epsilon}(x)}{\tau}| \le E_1 \qquad \text{for all } x \in \Omega.$$

From the estimate above, the bounds on $\{\psi_t^{\epsilon+\tau}(x)\}$ and the bounds on $\{\frac{N_t^{\epsilon+\tau}(y) - N_t^{\epsilon}(y)}{\tau}\}$ obtained from (5.2), we have

$$\begin{aligned}
&|\frac{\psi_2^{\epsilon+\tau}(x) - \psi_2^{\epsilon}(x)}{\tau}| \\
&\quad \le |\int_\Omega rk(x,y)[(1-\alpha_1(y) - \epsilon(l_1-\alpha_1)(y))\frac{\psi_1^{\epsilon+\tau}(y) - \psi_1^{\epsilon}(y)}{\tau}dy| \\
&\quad + |\int_\Omega rk(x,y)(l_1-\alpha_1)(y)\psi_1^{\epsilon+\tau}(y)dy| \\
&\quad + |\int_\Omega rk(x,y)(l_1(y)-\alpha_1(y))\frac{N_1^{\epsilon+\tau}(y) - N_1^{\epsilon}(y)}{\tau}dy| \\
&\quad \le E_2, \qquad \text{for all } x \in \Omega, t = 1, 2, \cdots, T.
\end{aligned}$$

Then by iteration, we obtain

$$|\frac{\psi_t^{\epsilon+\tau}(x)-\psi_t^{\epsilon}(x)}{\tau}| \leq E_t \qquad \text{for all } x \in \Omega, t = 1, 2, \cdots, T,$$

where the bounding sequence E_{t+1} does not depend on τ or ϵ. From the *a priori* estimates, we have the existence of $\sigma^{\epsilon} \in (L^{\infty}(\Omega))^{T+1}$ such that

$$\frac{\psi_t^{\epsilon+\tau}(x)-\psi_t^{\epsilon}(x)}{\tau} \rightharpoonup \sigma_t^{\epsilon}(x) \qquad \text{weakly in } L^2(\Omega), \text{ as } \tau \to 0,$$

where

$$\sigma_{t+1}^{\epsilon}(x) = \int_{\Omega} rk(x,y)[(1-\alpha_t(y)+\epsilon(l_t-\alpha_t)(y)]\sigma_t^{\epsilon}(y)dy - 2\int_{\Omega} rk(x,y)(l_t-\alpha_t)(y)\psi_t^{\epsilon}(y)dy$$

$$\sigma_0^{\epsilon}(x) \equiv 0$$

for $t = 0, 1, \cdots, T-1$.

Now we obtain

$$g''(\epsilon) = \sum_{t=0}^{T-1} \int_{\Omega} e^{-\delta t}[2A_t(l_t-\alpha_t)r\psi_t^{\epsilon} + A_t(\alpha_t+\epsilon(l_t-\alpha_t))r\sigma_t^{\epsilon} - B_t(l_t-\alpha_t)^2]dy.$$

We now use the iterative method to estimate σ_{t+1}^{ϵ} in terms of $(l_k-\alpha_k)^2$, $k = 0, 1, \cdots, T-1$:

$$\int_{\Omega} |\sigma_t^{\epsilon}(y)|\, dy \leq F_t \sum_{k=0}^{t-1} \int_{\Omega} (l_k-\alpha_k)^2 dy,$$

Where the sequence of constants F_{t+1} does not depend on ϵ.

First, using $\sigma_0^{\epsilon} \equiv 0$ and $\psi_0^{\epsilon} \equiv 0$, we obtain $\sigma_1^{\epsilon}(x) \equiv 0$.

And

$$\begin{aligned}|\sigma_2^\epsilon(x)| &= \left|2\int_\Omega rk(x,y)(l_1-\alpha_1)(y)\psi_1^\epsilon(y)dy\right| \\ &\le L_1\left|\int_\Omega (l_1-\alpha_1)(y)dy\int_\Omega (l_0-\alpha_0)(y)dy\right| \\ &\le L_2(\left|\int_\Omega (l_1-\alpha_1)(y)dy\right|^2+\left|\int_\Omega (l_0-\alpha_0)(y)dy\right|^2) \\ &\le F_1(\int_\Omega |(l_1-\alpha_1)(y)|^2\,dy+\int_\Omega |(l_0-\alpha_0)(y)|^2\,dy),\end{aligned}$$

where L_1, L_2, and F_1 are constants that do not depend on ϵ. Continuing the iteration, we can get the estimate for σ_t^ϵ. Using the estimates, we obtain a constant H independent of ϵ, such that

$$g''(\epsilon) \le \sum_{t=0}^{T-1}(H-B_t)\int_\Omega (l_t-\alpha_t)^2dy,$$

which gives the desired concavity for B_t's sufficiently large. □

2.3 Model with Concave Growth and Control Cost

2.3.1 Problem Statement for the Concave Case

We consider the harvest of the following integrodifference model with a concave growth function:

$$N_{t+1}(x) = \int_\Omega k(x,y)(1-\alpha_t(y))f(N_t(y),y)dy \tag{2.8}$$

where $t = 0, 1, ..., T-1$.

Assumption 4. *We assume f is twice differentiable in $N_t(y)$ and measurable in y. And for almost all y, $f(\cdot, y)$ is nondecreasing in the N variable, $\dfrac{\partial f(N_t(x),x)}{\partial N}$ is*

decreasing and nonnegative, and

$$f(N_t(y), y) \geq 0, \quad \textit{for all} \;\; N_t(y) \geq 0, y \in \Omega$$

$$|f(N_t(y), y)| \leq C_t < \infty, \quad \textit{for all} \;\; 0 \leq N_t(y), y \in \Omega$$

We also assume that the partial derivatives, $\dfrac{\partial f(N_t(x), x)}{\partial N}$ *and* $\dfrac{\partial^2 f(N_t(x), x)}{\partial N^2}$ *are both* L^∞ *bounded for any* $N \in L^\infty(\Omega)$.

The control set is defined as $U = \left\{\alpha \in \left(L^\infty(\Omega)\right)^T | 0 \leq \alpha_t(x) \leq M, t = 0, 1, \ldots, T-1\right\}$ *for* $M < 1$.

Assumption 4 together with $N_0 \in L^\infty(\Omega)$ and $N_0(x) \geq 0$ implies that given $\alpha \in U$, the corresponding state $N = N(\alpha)$ satisfies

$$0 \leq N_t(x) \leq C_{f(N_0)},$$

where $C_{f(N_0)}$ is a constant that depends on the growth function value at N_0.

Assumption 5. *The kernels are bounded and measurable such that*

$$\int_\Omega k(x, y)dx \leq C \leq 1$$

for all $x \in \Omega$ *and* $0 \leq k(x, y) \leq k_1$ *for* $(x, y) \in \Omega \times \Omega$.

We define the objective functional as:

$$J(\alpha) = \sum_{t=0}^{T-1} \int_\Omega e^{-\delta t}[A_t \alpha_t(y) f(N_t(y), y) - \frac{B_t}{2} V(\alpha_t(y))]dy, \tag{2.9}$$

Again J represents the profit, which is the discounted revenue stream less the cost of the control, where the coefficient where A_t is the price factor and $e^{-\delta t}$ is the discount factor with $\delta > 0$.

Assumption 6. *We assume the cost of harvesting is a nonlinear function V, and assume that the C^2 function $V : [0, M] \to R$ is increasing and convex with*

$$V''(\alpha) \geq b > 0$$

for all α in $[0, M]$ [6]. The coefficient B_t is a weight factor that balances the two parts of the objective functional. The coefficients, A_t and B_t, are both positive numbers for any $t = 0, 1, \cdots, T-1$.

2.3.2 Existence for State System for the Concave Case

We first prove the existence of an optimal control for the case with a nonlinear growth function and concave cost function.

Theorem 2.8. *Under Assumption 4, 5 and 6, there exists an optimal control α^* in U that maximizes the functional $J(\alpha)$.*

Proof. Let $\{\alpha^n\}$ be a maximizing sequence for the objective functional J in (2) and $N^n = N(\alpha^n)$ be the corresponding state sequence. From the bounded assumption on control and state, those sequences are L^∞ bounded. Then there exists $\alpha^* \in U$ and $N^* \in (L^\infty(\Omega))^T$ such that on a subsequence, we have the following weak convergences,

$$N_t^n \rightharpoonup N_t^* \text{ in } L^2(\Omega), t = 1, \cdots, T$$

$$\alpha_t^n \rightharpoonup \alpha_t^* \text{ in } L^2(\Omega), t = 0, \cdots, T-1.$$

We want to show that $N(\alpha^*) = N^*$. First we want to show

$$\int_\Omega k(x,y)(1-\alpha_t^n(y))f(N_t^n(y),y)dy \to \int_\Omega k(x,y)(1-\alpha_t^*(y))f(N_t^*(y),y)dy$$

pointwise for each $x \in \Omega$. It is known that $\alpha_t^n \rightharpoonup \alpha_t^*$ in $L^2(\Omega)$, we want to show $f(N_t^n) \to f(N_t^*)$ in $L^2(\Omega)$. For $t = 1$, we have

$$N_1^n(x) = \int_\Omega k(x,y)(1 - \alpha_0^n(y))f(N_0(y), y)dy$$

since $N_0^n(x) = N_0(x)$ for all n. From the assumption $0 \le k(x,y) \le 1$, $\int_\Omega k(x,y)^2 dy \le 1$, we know that $k(x,y) \in L^2(\Omega)$ for each x. Since $1 - \alpha_0^n(y) \rightharpoonup 1 - \alpha_0^*(y)$ in L^2, we have

$$\int_\Omega k(1 - \alpha_0^n)f(N_0^n(y), y)dy \to \int_\Omega k(1 - \alpha_0^*)f(N_0^*(y), y)dy,$$

which means $N_1^n \to N_1(\alpha^*)$, the first component of $N(\alpha^*)$, pointwise for each $x \in \Omega$. Since $f(N)$ is a continuous function, we have $f(N_1^n)) \to f(N_1(\alpha^*))$ pointwise.

We know the sequence $f(N_1^n)$ is uniformly L^∞ bounded and pointwise convergent to $f(N_1^*)$, which give $|f(N_1^n) - f(N_1(\alpha^*))|^2 \le C$ and $|f(N_1^n) - f(N_1(\alpha^*))|^2 \to 0$ *a.e.* for all n. From Lebesgue's Dominated Convergence Theorem, we have

$$\int_\Omega |f(N_1^n) - f(N_1(\alpha^*))|^2 dx \to 0,$$

i.e., $f(N_1^n) \to f(N_1(\alpha^*))$ in L^2.

Using

$$N_2^n(x) = \int_\Omega k(x,y)(1 - \alpha_1^n(y))f(N_1^n(y), y)dy,$$

$$1 - \alpha_1^n(y) \rightharpoonup 1 - \alpha_1^*(y),$$

$$f(N_1^n(y), y) \to f(N_1(\alpha^*)(y), y) \text{ in } L^2,$$

and $k, \alpha^n, f(N_1^n)$ are L^∞ bounded, we obtain

$$N_2^n \to N_2(\alpha^*) \text{ pointwise},$$

and then $f(N_2^n) \to f(N_2(\alpha^*))$ in L^2. Continuing, we get $f(N_t^n) \to f(N_t(\alpha^*))$ in L^2 for each $t = 1, 2, \cdots, T$. The weak L^2 convergence of $1 - \alpha_t^n$ sequence, the strong L^2 convergence of $f(N_t^n)$ sequence, and the L^∞ bounds on both sequences and k, give

us

$$\int_\Omega k(x,y)(1-\alpha_t^n(y))f(N_t^n(y),y)dy \to \int_\Omega k(x,y)(1-\alpha_t^*(y))f(N_t(\alpha^*),y)dy$$

for each x. Since

$$\int_\Omega k(1-\alpha_t^n)f(N_t^n(y),y)dy \to \int_\Omega k(1-\alpha_t^*)f(N_t(\alpha^*)(y),y)dy$$

for each x, we conclude $N^* = N(\alpha^*)$. Now we show that α^* achieves the maximum of J.

$$\begin{aligned}
J(\alpha^*) &= \sum_{t=0}^{T-1}\int_\Omega e^{-\delta t}[A_t\alpha_t^*(y)f(N(\alpha^*)_t(y),y) - \frac{B_t}{2}V(\alpha_t^*(y))]dy \\
&= \sum_{t=0}^{T-1}\int_\Omega e^{-\delta t}[A_t\alpha_t^*(y)f(N_t^*(y),y) - \frac{B_t}{2}V(\alpha_t^*(y))]dy \\
&\geq \limsup_{n\to\infty}\sum_{t=0}^{T-1}\int_\Omega e^{-\delta t}[A_t\alpha_t^n(y)f(N_t^n(y),y) - \frac{B_t}{2}V(\alpha_t^n(y))]dy \\
&= \lim_{n\to\infty} J(\alpha^n)
\end{aligned}$$

The inequality we got above is obtained by

$$\int_\Omega V(\alpha_t^*(y))dy \leq \liminf_{n\to\infty}\int_\Omega V(\alpha_t^n(y))dy,$$

for $t = 0, 1, ..., T-1$, which is given by the weak convergence of α_t^n and convexity of V.

□

2.3.3 Characterization of an Optimal Control for the Concave Case

To characterize an optimal control, we must again differentiate the map $\alpha \to J(\alpha)$, which requires first the differentiation of the solution map $\alpha \to N = N(\alpha)$.

Theorem 2.9. *Under Assumption 4, 5 and 6, the mapping $\alpha \in U \to N \in (L^\infty(\Omega))^T$ is differentiable in the following sense:*

$$\frac{N_t^\epsilon(x) - N_t(x)}{\epsilon} \rightharpoonup \psi_t(x)$$

weakly in $L^2(\Omega)$ as $\epsilon \to 0$ for any $\alpha \in U$ and $l \in (L^\infty(\Omega))^T$ such that $(\alpha + \epsilon l) \in U$ for ϵ small, where $N^\epsilon = N(\alpha + \epsilon l)$. Also ψ, depending on N, α and l, satisfies:

$$\psi_{t+1}(x) = \int_\Omega k(x,y)(1-\alpha_t(y))\frac{\partial f(N_t(y),y)}{\partial N}\psi_t(y)dy - \int_\Omega k(x,y)l_t(y)f(N_t(y),y)dy \tag{2.10}$$

$$\psi_0(x) = 0$$

for $t = 0, 1, \cdots, T-1$.

Proof. Consider the control-to-solution map: $\alpha \to J(\alpha)$.

Let $N^\epsilon = N(\alpha + \epsilon l)$, then

$$\begin{aligned}\frac{N_{t+1}^\epsilon(x) - N_{t+1}(x)}{\epsilon} = & \\ \int_\Omega k(x,y)(1-\alpha_t(y))\frac{f(N_t^\epsilon(y),y) - f(N_t(y),y)}{\epsilon}dy & \\ - \int_\Omega k(x,y)l_t(y)f(N_t^\epsilon(y),y)dy. &\end{aligned}$$

Using $N_0^\epsilon \equiv N_0$, and

$$\frac{N_1^\epsilon(x) - N_1(x)}{\epsilon} = \int_\Omega k(x,y)l_0(y)f(N_0^\epsilon(y),y)dy.$$

We have

$$|\frac{N_1^\epsilon(x) - N_1(x)}{\epsilon}| \leq C_1,$$

for all $x \in \Omega$. And that quotient is independent of ϵ,

$$\frac{N_1^\epsilon(x) - N_1(x)}{\epsilon} = \psi_1.$$

This gives uniform convergence of N_1^ϵ to N_1.

$$\begin{aligned}\frac{N_2^\epsilon(x) - N_2(x)}{\epsilon} = \\ \int_\Omega k(x,y)(1-\alpha_1(y))\frac{f(N_1^\epsilon(y),y) - f(N_1(y),y)}{N_1^\epsilon - N_1(y)}\psi_1 dy \\ - \int_\Omega k(x,y) l_1(y) f(N_1^\epsilon(y),y) dy.\end{aligned}$$

From the uniform convergence of N_1^ϵ to N_1, we can pass the limit and get pointwise convergence for the quotient

$$\frac{N_2^\epsilon(x) - N_2(x)}{\epsilon}.$$

Also we can get

$$|\frac{N_2^\epsilon(x) - N_2(x)}{\epsilon}| \leq C_2.$$

By iteration, we obtain:

$$|\frac{N_t^\epsilon(x) - N_t(x)}{\epsilon}| \leq C_t,$$

$$\frac{N_t^\epsilon(x) - N_t(x)}{\epsilon} \to \psi_t$$

pointwise, and N_t^ϵ convergent to N_t uniformly. Passing to the limit using the pointwise convergence of the quotients, we obtain that ψ satisfies the equation in the theorem.

□

Theorem 2.10. *Under Assumption 4, 5 and 6, given an optimal control α^* and corresponding state solution $N(\alpha^*) = N^*(\alpha)$, there exists a weak solution $p \in$*

$(L^\infty(\Omega))^T$ *satisfying the adjoint system:*

$$\begin{aligned} p_{t-1}(x) &= \frac{\partial f(N_{t-1}(x),x)}{\partial N}(1-\alpha^*_{t-1}(x))\int_\Omega p_t(y)k(y,x)dy \\ &\quad +\frac{\partial f(N_{t-1}(x),x)}{\partial N}e^{-\delta t}A_{t-1}\alpha^*_{t-1}(x) \\ p_T(x) &= 0 \end{aligned} \tag{2.11}$$

where $t = T, \cdots, 2, 1$. *Furthermore, for* $t = 0, 1, \cdots, T-1$,

$$V'(\alpha^*_t(x)) = \frac{2}{B_t}(A_t - \int_\Omega e^{\delta t}p_{t+1}(y)k(y,x)dy)f(N^*_t(x),x)$$

on the interior of the control set.

Proof. Let α^* be an optimal control (which exists by Theorem 1) and $N^* = N(\alpha^*)$ be the corresponding state. For variation l with $(\alpha^* + \epsilon l) \in U$ for $\epsilon > 0$ sufficiently small, let N^ϵ be the corresponding solution of the state equation. Since the adjoint system is linear, there exists a solution p.

We compute the directional derivative of the functional $J(\alpha)$ with respect to α in the direction l at α^*. Since $J(\alpha^*)$ is the maximum value, we have

$$
\begin{aligned}
0 \geq & \lim_{\epsilon \to 0^+} \frac{J(\alpha^* + \epsilon l) - J(\alpha^*)}{\epsilon} \\
= & \lim_{\epsilon \to 0^+} \sum_{t=0}^{T-1} \frac{1}{\epsilon} \Big\{ \int_\Omega e^{-\delta t} \big[A_t(\alpha_t^* + \epsilon l_t) f(N_t^\epsilon(y), y) - \frac{B_t}{2} V(\alpha_t^*(y) + \epsilon l_t(y)) \big] dy \\
& - \int_\Omega e^{-\delta t} \big[A_t(\alpha_t^*) f(N_t^*(y), y) - \frac{B_t}{2} V(\alpha_t^*(y)) \big] dy \Big\} \\
= & \lim_{\epsilon \to 0^+} \sum_{t=0}^{T-1} \int_\Omega e^{-\delta t} \big[A_t \alpha_t^* \frac{f(N_t^\epsilon(y), y) - f(N_t^*(y), y)}{\epsilon} + A_t l_t f(N_t^\epsilon(y), y) \\
& - \frac{B_t}{2} \frac{V((\alpha_t^* + \epsilon l_t)(y)) - V(\alpha_t^*(y))}{\epsilon} \big] dy \\
= & \sum_{t=0}^{T-1} \int_\Omega e^{-\delta t} A_t \alpha_t^*(y) \frac{\partial f(N_t^*(y), y)}{\partial N} \psi_t(y) dy + \sum_{t=0}^{T-1} \int_\Omega e^{-\delta t} A_t l_t f(N_t^*(y), y) dy \\
& - \sum_{t=0}^{T-1} \int_\Omega e^{-\delta t} \frac{B_t}{2} V'(\alpha_t^*) l_t(y) dy.
\end{aligned}
$$

We use the coefficient of the ψ_t term as the non-homogeneous term in the adjoint system.

$$
\begin{aligned}
&\sum_{t=0}^{T-1}\int_\Omega e^{-\delta t}A_t\alpha_t^*(y)\frac{\partial f(N_t^*(y),y)}{\partial N}\psi_t(y)dy\\
&=\sum_{t=0}^{T-1}\int_\Omega [p_t(y)-\frac{\partial f(N_t^*(y),y)}{\partial N}(1-\alpha_t^*(y))\int_\Omega p_{t+1}(x)k(x,y)dx]\psi_t(y)dy\\
&=\sum_{t=0}^{T-1}\int_\Omega p_t(y)\psi_t(y)dy-\sum_{t=0}^{T-1}\int_\Omega \frac{\partial f(N_t^*(y),y)}{\partial N}(1-\alpha_t^*(y))\psi_t(y)\int_\Omega p_{t+1}(x)k(x,y)dxdy\\
&=\sum_{t=0}^{T-1}\int_\Omega p_{t+1}(y)\psi_{t+1}(y)dy-\int_\Omega p_T(y)\psi_T(y)dy+\int_\Omega p_0(y)\psi_0(y)dy\\
&-\sum_{t=0}^{T-1}\int_\Omega p_{t+1}(x)\int_\Omega \frac{\partial f(N_t^*(y),y)}{\partial N}(1-\alpha_t^*(y))\psi_t(y)k(x,y)dydx\\
&=\sum_{t=0}^{T-1}\int_\Omega p_{t+1}(x)[\psi_{t+1}(x)-\int_\Omega \frac{\partial f(N_t^*(y),y)}{\partial N}k(x,y)(1-\alpha_t^*(y))\psi_t(y)dy]dx\\
&=\sum_{t=0}^{T-1}\int_\Omega p_{t+1}(x)[-\int_\Omega k(x,y)l_t(y)f(N_t^*(y),y)dy]dx
\end{aligned}
$$

where we used $p_T(x)\equiv 0$, $\psi_0(x)\equiv 0$ and the sensitivity equation (2.10).

Substituting out for the first term from our quotient calculation,

$$
\begin{aligned}
0\geq&\sum_{t=0}^{T-1}\int_\Omega p_{t+1}(x)[-\int_\Omega k(x,y)l_t(y)f(N_t^*(y),y)dy]dx+\sum_{t=0}^{T-1}\int_\Omega e^{-\delta t}A_t l_t f(N_t^*(y),y)dy\\
&-\sum_{t=0}^{T-1}\int_\Omega e^{-\delta t}\frac{B_t}{2}V'(\alpha_t^*(y))l_t(y)dy\\
&=\sum_{t=0}^{T-1}\int_\Omega[(\int_\Omega -p_{t+1}(x)k(x,y)dx+e^{-\delta t}A_t)f(N_t^*(y),y)-e^{-\delta t}\frac{B_t}{2}V'(\alpha_t^*(y))]l_t(y)dy.
\end{aligned}
$$

For any $t=0,1,\cdots,T-1$, on the set $\{(x:0<\alpha_t^*(x)<M\}$, the variation l_t can be taken with support on this set, and have any sign, because the optimal control can be modified a little up or down and still stay inside the bounds. Thus on this set, the

rest of the integrand must be zero, so that

$$V'(\alpha_t^*(x)) = \frac{2}{B_t}(A_t - \int_\Omega e^{\delta t} p_{t+1}(y)k(y,x)dy)f(N_t^*(x),x)$$

on the interior of the control set. □

Remark 2.11. *In the simplest case, if V is a quadratic function as $V(\alpha_t) = \alpha_t^2$ (the coefficient of α_t^2 can be included in B_t), then the characterization result before imposing bounds can be written as:*

$$\alpha_t^*(x) = \frac{1}{B_t}(A_t - \int_\Omega e^{\delta t} p_{t+1}(y)k(y,x)dy)f(N_t^*(x),x) \tag{2.12}$$

2.3.4 Uniqueness Result for the Concave Case

We again obtain uniqueness of the optimal control when the cost coefficients are large.

Theorem 2.12. *Under Assumption 4, 5 and 6, if B_t, $t = 0, 1, \cdots, T-1$ are sufficiently large, then the optimal control is unique.*

Proof. We show uniqueness by showing strict concavity of the map:

$$\alpha \in U \to J(\alpha).$$

The concavity follows from showing for all α, $l \in U$, and $0 < \epsilon < 1$,

$$g''(\epsilon) < 0$$

where $g(\epsilon) = J(\epsilon l + (1-\epsilon)\alpha)) = J(\alpha + \epsilon(l - \alpha))$.

For convenience we denote

$$N_t^\epsilon = N(\alpha + \epsilon(l - \alpha))$$

for $t = 0, 1, \cdots, T-1$, and similarly

$$N_t^{\epsilon+\tau} = N(\alpha + (\epsilon+\tau)(l-\alpha)),$$

for $t = 0, 1, \cdots, T-1$. First, we calculate

$$\begin{aligned}
g'(\epsilon) &= \lim_{\tau\to 0} \frac{J(\alpha + (\epsilon+\tau)(l-\alpha)) - J(\alpha+\epsilon(l-\alpha))}{\tau} \\
&= \lim_{\tau\to 0} \sum_{t=0}^{T-1} \frac{1}{\tau}\Big(\int_\Omega e^{-\delta t}[A_t(\alpha_t + (\epsilon+\tau)(l_t-\alpha_t))f(N_t^{\epsilon+\tau}(y), y)]dy \\
&\quad \int_\Omega e^{-\delta t} - \frac{B_t}{2} V(\alpha_t + (\epsilon+\tau)(l_t-\alpha_t))dy \\
&\quad - \int_\Omega e^{-\delta t}[A_t(\alpha_t + \epsilon(l_t-\alpha_t))f(N_t^{\epsilon}(y), y) - \frac{B_t}{2} V(\alpha_t + \epsilon(l_t-\alpha_t))]dy\Big) \\
&= \lim_{\tau\to 0} \sum_{t=0}^{T-1} \int_\Omega e^{-\delta t}[A_t(\alpha_t + \epsilon(l_t-\alpha_t)) \frac{f(N_t^{\epsilon+\tau}(y), y) - f(N_t^{\epsilon}(y), y)}{\tau}]dy \\
&\quad + \int_\Omega e^{-\delta t} A_t(l_t-\alpha_t) f(N_t^{\epsilon+\tau}(y), y)dy \\
&\quad - \int_\Omega e^{-\delta t} \frac{B_t}{2} \frac{V(\alpha_t + (\epsilon+\tau)(l_t-\alpha_t)) - V(\alpha_t+\epsilon(l_t-\alpha_t))}{\tau} dy \\
&= \sum_{t=0}^{T-1} \int_\Omega e^{-\delta t}[A_t(\alpha_t + \epsilon(l_t-\alpha_t)) \frac{\partial f(N_t^{\epsilon}(y))}{\partial N_t^{\epsilon}} \psi_t^{\epsilon} + A_t(l_t-\alpha_t) f(N_t^{\epsilon}(y), y) \\
&\quad - \frac{B_t}{2} V'(\alpha_t + \epsilon(l_t-\alpha_t))(l_t-\alpha_t)]dy.
\end{aligned}$$

Remark 2.4 indicates that the directional derivative of $N(\alpha+\epsilon(l-\alpha))$ along vector $l-\alpha$ with respect to $\alpha+\epsilon(l-\alpha)$ is $\psi(\alpha+\epsilon(l-\alpha), N(\alpha+\epsilon(l-\alpha)), l-\alpha)$. For convenience we use the following notation

$$\psi^{\epsilon} = \psi(\alpha + \epsilon(l-\alpha), N(\alpha+\epsilon(l-\alpha)), l-\alpha),$$

and similarly

$$\psi^{\epsilon+\tau} = \psi(\alpha + (\epsilon+\tau)(l-\alpha), N(\alpha+(\epsilon+\tau)(l-\alpha)), l-\alpha).$$

From Theorem 2.3 we obtain

$$\frac{N_t^{\epsilon+\tau} - N_t^{\epsilon}}{\tau} \rightharpoonup \psi_t^{\epsilon} \text{ as } \tau \to 0$$

with

$$\psi_{t+1}^{\epsilon}(x) = \int_{\Omega} rk(x,y)[(1-(\alpha_t + \epsilon(l_t - \alpha_t)))\frac{\partial f(N_t^{\epsilon})}{\partial N_t^{\epsilon}}\psi_t^{\epsilon} - (l_t - \alpha_t)f(N_t^{\epsilon})]dy \quad (2.13)$$
$$\psi_0^{\epsilon}(x) \equiv 0.$$

Similarly,

$$\psi_{t+1}^{\epsilon+\tau}(x) = \int_{\Omega} rk(x,y)[(1-(\alpha_t + (\epsilon+\tau)(l_t - \alpha_t)))\frac{\partial f(N_t^{\epsilon+\tau})}{\partial N_t^{\epsilon+\tau}}\psi_t^{\epsilon+\tau} - (l_t - \alpha_t)N_t^{\epsilon+\tau}]dy \quad (2.14)$$
$$\psi_0^{\epsilon}(x) \equiv 0.$$

Estimate $\psi_t^{\epsilon}(x)$ in terms of $l - \alpha$:

$$\begin{aligned} |\psi_1^{\epsilon}(x)| &= \left| \int_{\Omega} rk(x,y)(l_0 - \alpha_0)f(N_0^{\epsilon})dy \right| \\ &\leq C_1 \int_{\Omega} |l_0 - \alpha_0|\, dy \end{aligned}$$

$$\begin{aligned} |\psi_2^{\epsilon}(x)| &= \left| \int_{\Omega} k(x,y)[(1-(\alpha_1 + \epsilon(l_1 - \alpha_1)))\frac{\partial f(N_1^{\epsilon})}{\partial N_1^{\epsilon}}\psi_1^{\epsilon} - (l_1 - \alpha_1)f(N_1^{\epsilon})]dy \right| \\ &\leq C_2\Big(\int_{\Omega} |l_0 - \alpha_0|\, dy + \int_{\Omega} |l_1 - \alpha_1|\, dy \Big) \end{aligned}$$

Continuing to estimate, we obtain

$$\left|\psi_{t+1}^{\epsilon}(x)\right| \leq C_{t+1} \sum_{i=0}^{t} \int_{\Omega} |l_i - \alpha_i|\, dy.$$

For

$$\psi^\epsilon = \psi(\alpha + \epsilon(l - \alpha))$$

and

$$\psi_t^{\epsilon+\tau} = \psi(\alpha + (\epsilon + \tau)(l - \alpha)),$$

we use σ_t^ϵ to represent the difference quotient for directional derivative of ψ with respect to $\alpha + \epsilon(l - \alpha)$ in the direction $l - \alpha$:

$$\begin{aligned}\sigma_{t+1}^\epsilon(x) = &\int_\Omega k(x,y)[(1 - \alpha_t + \epsilon(l_t - \alpha_t)]\big(\frac{\partial^2 f(N_t^\epsilon)}{\partial^2 N_t^\epsilon}(\psi_t^\epsilon)^2 + \frac{\partial f(N_t^\epsilon)}{\partial N_t^\epsilon}\sigma_t^\epsilon\big)dy \\ &- 2\int_\Omega k(x,y)(l_t - \alpha_t)\frac{\partial f(N_t^\epsilon)}{\partial N_t^\epsilon}\psi_t^\epsilon dy\end{aligned}$$

$$\sigma_0^\epsilon(x) \equiv 0$$

for $t = 0, 1, \cdots, T - 1$.

Now we obtain

$$\begin{aligned}g''(\epsilon) = \sum_{t=0}^{T-1}\int_\Omega e^{-\delta t}[&2A_t(l_t - \alpha_t)\frac{\partial f(N_t^\epsilon)}{\partial N_t^\epsilon}\psi_t^\epsilon \\ &+ A_t(\alpha_t + \epsilon(l_t - \alpha_t))\big(\frac{\partial^2 f(N_t^\epsilon)}{\partial^2 N_t^\epsilon}(\psi_t^\epsilon)^2 + \frac{\partial f(N_t^\epsilon)}{\partial N_t^\epsilon}\sigma_t^\epsilon\big) \\ &- \frac{B_t}{2}V''(\alpha_t + \epsilon(l_t - \alpha_t))(l_t - \alpha_t)^2]dy\end{aligned}$$

Next, we use the iterative method to estimate σ_{t+1}^ϵ in terms of $(l_k - \alpha_k)^2$, $k = 0, 1, \cdots, T - 1$:

$$\int_\Omega |\sigma_t^\epsilon|\, dy \le C\sum_{k=0}^{t-1}\int_\Omega (l_k - \alpha_k)^2 dy \tag{2.15}$$

Notice $\sigma_1^\epsilon(x) \equiv 0$, since $\sigma_0^\epsilon(x) \equiv 0$ and $\psi_0^\epsilon(x) \equiv 0$. Using that to estimate σ_2^ϵ gives

$$\begin{aligned}
|\sigma_2^\epsilon(x)| &= \left| \int_\Omega k(x,y)[(1-\alpha_1+\epsilon(l_1-\alpha_1)] \frac{\partial^2 f(N_1^\epsilon)}{\partial^2 N_1^\epsilon} (\psi_1^\epsilon)^2 dy \right| \\
&+ 2 \left| \int_\Omega (x,y)(l_1-\alpha_1) \frac{\partial f(N_1^\epsilon)}{\partial N_1^\epsilon} \psi_1^\epsilon dy \right| \\
&\leq C_1 \left| \int_\Omega (\psi_1^\epsilon)^2 dy + \int_\Omega (l_1-\alpha_1)\psi_1^\epsilon dy \right| \\
&\leq C_2 (\int_\Omega |(l_1-\alpha_1)|^2 \, dy + \int_\Omega |(l_0-\alpha_0)|^2 \, dy)
\end{aligned}$$

In the derivation above we used the L^∞ boundedness of $\dfrac{\partial f}{\partial N}$ and $\dfrac{\partial^2 f}{\partial N^2}$ are used. Continuing the iteration, we can get the estimate (2.15) for σ_t^ϵ.

Using the above estimates,

$$g''(\epsilon) \leq \sum_{t=0}^{T-1} (K - b\frac{B_t}{2}) \int_\Omega (l_t - \alpha_t)^2 dy < 0,$$

which gives the desired concavity for B_t's sufficiently large. □

2.4 Conclusion

The application of optimal control theory in integrodifference equation models is a new area. In this chapter, we formulated an optimal control problem for integrodifference equation models with harvesting before dispersal and after growth.

We started with a problem with a linear growth function and a quadratic cost term, and obtained existence, uniqueness and characterization results for the optimal control in Section 2.2. Boundedness of controls and states, weak convergence in L^2 of control sequences, and strong convergence of state sequences are used to show the existence of the optimal control. We first differentiated the map $\alpha \to N(\alpha)$ to derive the sensitivity system ψ_t, and then differentiated the map $\alpha \to J(\alpha)$ to obtain the adjoint system and the characterization of the optimal control. The uniqueness of the optimal control was proven by showing the strict concavity of the map $\alpha \to N(\alpha)$.

In Section 2.3 we extended the theoretical analysis results to a problem with a concave growth function and a convex cost term. We used similar techniques as applied in Section 2.2 to obtain existence, characterization and uniqueness of the optimal control. Additionally, for the proof of uniqueness in 2.3.4, we used lower semi-continuity with respect to weak convergence in L^2 for concave functions.

These results are important for the control application of optimal harvesting, to species for which an integrodifference equation model is appropriate. For organisms such as insects and many plants, the assumption of harvesting before dispersal and after growth is reasonable, e.g. if harvesting is applied to reduce impact of harmful insects or plants. The results in this chapter provide explicit guidance on optimal harvesting given a particular dispersal kernel.

Chapter 3

Comparison with Another Order of Events (Growth, Dispersal and Harvest)

3.1 Optimality System for Growth, Dispersal and Harvest

In models with discrete time, the order of events within a time step is crucial. In this chapter we explore the differences arising due to the order of growth, harvest and dispersal, by comparing the two different cases, one following a growth-harvesting-dispersal order, which is discussed in Chapter 2, with the another one following a growth-dispersal-harvesting order, which was discussed by Joshi, Lenhart, Lou and Gaff [21, 22].

In this section, we state the harvesting problem together with the adjoint system and the characterization of the optimal control for a growth-dispersal-harvesting order. We use the same assumptions and control set as in Chapter 2.

$$N_{t+1}(x) = (1 - \alpha_t(x)) \int_\Omega k(x, y) r N_t(y) dy \tag{3.1}$$

where $t = 0, 1, \cdots, T-1$. The state variable N and the control α are:

$$N = N(\alpha) = (N_0(x), N_1(x), \ldots, N_T(x)),$$

$$\alpha = (\alpha_0(x), \alpha_1(x), \ldots, \alpha_{T-1}(x)).$$

The objective functional is:

$$J(\alpha) = \sum_{t=0}^{T-1} \int_\Omega e^{-\delta t} [A_t \alpha_t(x) \int_\Omega k(x, y) N_t(y) dy - \frac{B_t}{2} (\alpha_t(x))^2] dx,$$

From the results in [21], for $t = 0, 1, 2, \cdots, T-1$, the characterization for the optimal control is

$$\alpha_t^*(x) = min(max(\frac{(-p_{t+1}(x) + e^{-\delta t} A_t) \int_\Omega r k(x, y) N_t^*(y) dy}{e^{-\delta t} B_t}, 0), M), \tag{3.2}$$

with the following adjoint system:

$$\begin{aligned} p_{t-1}(x) &= r \int_\Omega (1 - \alpha_{t-1}^*(y)) p_t(y) k(y, x) dy + r \int_\Omega A_{t-1} e^{-\delta(t-1)} \alpha_{t-1}^*(y) k(y, x) dy \\ p_T(x) &= 0 \end{aligned} \tag{3.3}$$

where $t = T, \cdots, 2, 1$.

For a concave growth function and a convex cost function, the population is modeled by the following integrodifference model:

$$N_{t+1}(x) = (1 - \alpha_t(x)) \int_\Omega k(x, y) f(N_t(y), y) dy \tag{3.4}$$

where $t = 0, 1, \cdots, T-1$. The state variable N and the control α are:

$$N = N(\alpha) = (N_0(x), N_1(x), \ldots, N_T(x)),$$

$$\alpha = (\alpha_0(x), \alpha_1(x), \ldots, \alpha_{T-1}(x)).$$

The objective functional is:

$$J(\alpha) = \sum_{t=0}^{T-1} e^{-\delta t} \int_\Omega \Big[A_t \alpha_t(x) \int_\Omega k(x,y) f(N_t(y), y) dy - \frac{B_t}{2} V(\alpha_t(x))\Big] dx,$$

From the results in [22], for $t = 0, 1, 2, \cdots, T-1$, the characterization for the optimal control on the interior of the control set is

$$V'(\alpha_t^*(x)) = \frac{2}{B_t}\big(A_t - p_{t+1}(x) e^{\delta t}\big) \int_\Omega k(x,y) f(N_t^*(y), y) dy.$$

If $V(\alpha) = \alpha^2$, then we have

$$\alpha_t^*(x) = min\Big(max\Big(\big(\frac{1}{B_t}(A_t - p_{t+1}(x)e^{\delta t}) \int_\Omega k(x,y) f(N_t^*(y), y) dy\Big), 0\Big), M\Big), \tag{3.5}$$

with the following adjoint system:

$$\begin{aligned} p_{t-1}(x) &= r \int_\Omega (1 - \alpha_{t-1}^*(y)) p_t(y) k(y,x) dy + r \int_\Omega A_{t-1} e^{-\delta(t-1)} \alpha_{t-1}^*(y) k(y,x) dy \\ p_T(x) &= 0 \end{aligned} \tag{3.6}$$

where $t = T, \cdots, 2, 1$.

The optimality system for the growth-dispersal-harvesting case in the linear growth or nonlinear growth consists of state (3.1)/(3.4), adjoint (3.3)/(3.6), and characterization (3.2)/(3.5). Compared with the optimality system of the other order, with state (2.1)/(2.8), adjoint (2.4)/(2.11), and characterization (2.5)/(2.12), we can clearly see the differences in the expressions for the optimality systems for

the two cases. When deciding to harvest in an optimal way, the order of the events must be decided in advance to obtain the appropriate necessary conditions, and thus calculating the appropriate optimal control.

3.2 Numerical Examples

We further illustrate the importance of considering the order of events in these problems by numerically calculating the optimal controls for two cases from state equations (2.8) and (3.4) and corresponding objective functionals (2.9) and (3.1) respectively. We numerically calculate the optimal controls for these two cases, using specific growth rates, balancing constants, and kernels.

Starting with a given initial population distribution and a guess for the control, an iterative method is used to solve the optimality system. Given initial condition of the state and an initial guess of control, we start with solving the state equations forward. Using the new state value, we solve backwards the adjoint equations, and calculate the characterization. We then update the control by taking a convex combination of the old control values and the new value from control characterization. We use a tolerance of 0.1%, and when relative errors in control, state and adjoint values all fall below the tolerance, the iteration stops. We use $V(\alpha) = \alpha^2$ as cost function. The trapezoidal rule is used here to get integral approximations.

The work by Hackbush [17] shows that the type of numerical algorithm for forward-backward sweeps is stable for parabolic partial differential equations. We found that our numerical simulations always converged in 50 iterations.

Remark 3.1. *We note that the trapezoidal rule requires C^2 regularity in space which holds for our examples.*

If x is near the $\partial\Omega$, then the part of the dispersal that would go outside Ω is not included in the integral.

See [21, 22] for more details on such a numerical method.

In this section we show figures comparing optimal harvesting rates and corresponding populations from the two orders of events. We use kernels and growth functions chosen from those used in applications [26, 41]

We first use a linear growth function

$$N_{t+1} = rN_t,$$

with a growth rate r of 1.8, and a normal dispersal kernel

$$k(x, y) = \sqrt{\frac{\beta}{\pi}} \exp\big(-\beta(x-y)^2\big),$$

with a β value of 5. We study the harvesting strategy over a one dimensional space with size 1 during 5 time steps. Here the space gird size is 0.01. We use a parabola curve $100x(1-x)$ for the initial population. Possible maximum harvesting rate is 0.4, and the discount factor δ is set to be 0.04, indicating an interest rate of 4%. We assume the weights in the objective functionals A_t and B_t to be constant for each time step, taking values of 10 and 1000, respectively. Numerical results are shown in Figure 3.1.

Figure 3.1 shows clear differences between how the two orders affect both harvesting rates and populations. First, for the G-D-H order, the harvesting curve is smoother and varies in a smaller value range, since the harvesting is done after dispersal, when the population distribution is more even. Second, for both cases the harvesting strategy is to harvest less population in the center of the region in early time steps. The explanation could be that it is more likely to have population loss near boundaries of the region due to dispersal. We observe a lower harvesting rate in general for the G-D-H order, which could be the effect caused by the population loss after dispersal. As a result, the population is slightly larger than the case with G-H-D order. Third, in both cases, although a time discount factor δ is included the model, indicating money is worth more at an earlier time step, it is still more profitable to

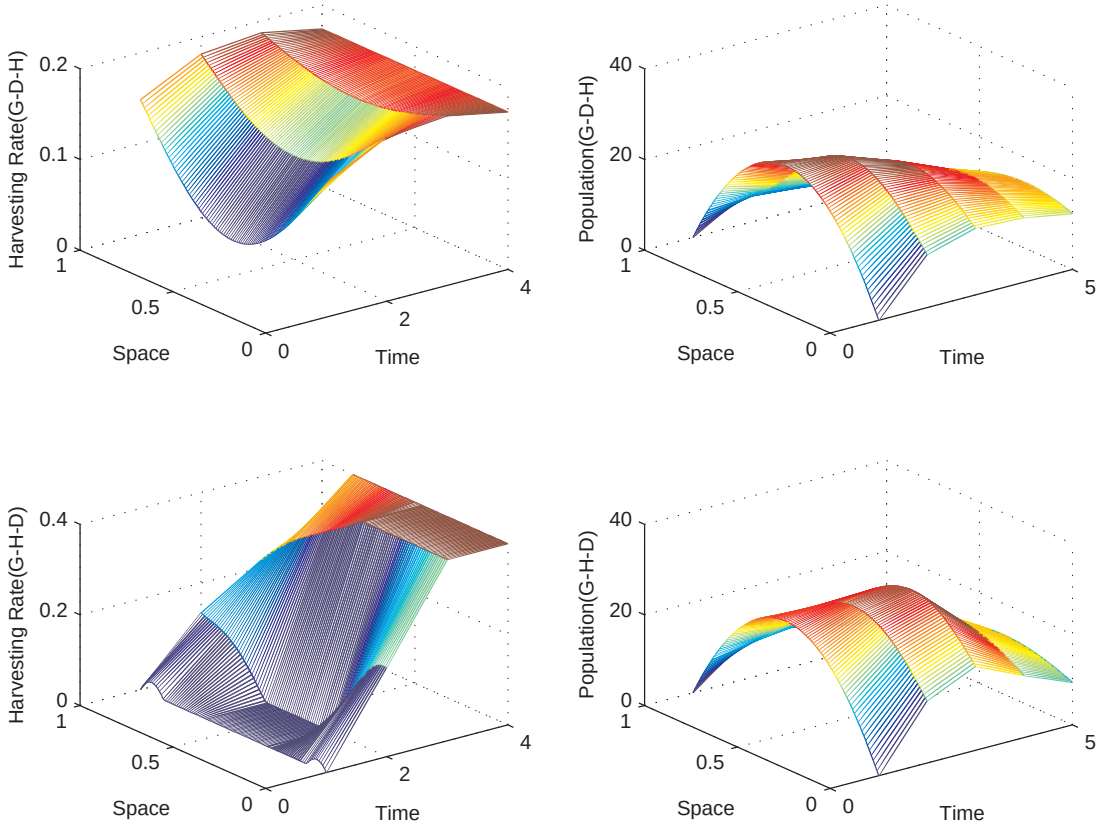

Figure 3.1: Normal kernel, $\beta = 5$, Linear growth function, $r = 1.8$, $A_t = 10$, $B_t = 500$, $L = 1$, $T = 5$, $\delta = 0.04$.

let the population grow first and perform a larger scale of harvesting at later time steps.

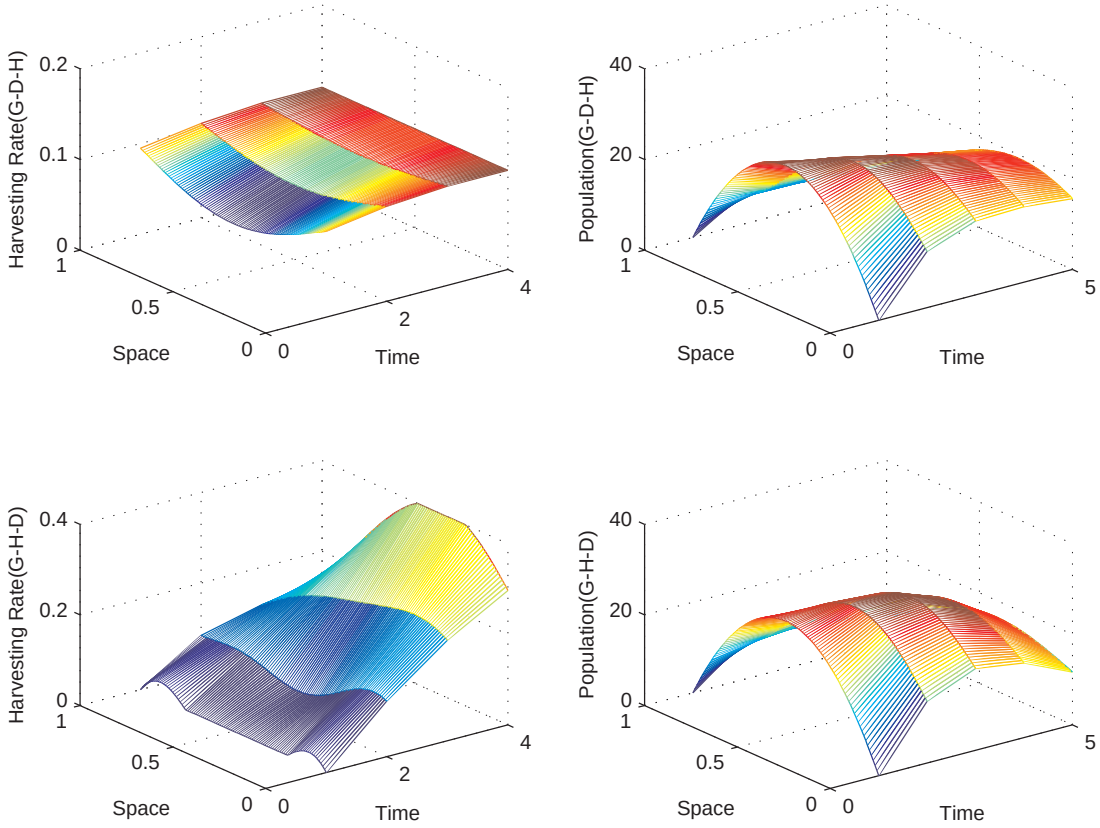

Figure 3.2: Normal kernel, $\beta = 5$, Linear growth function, $r = 1.8$, $A_t = 10$, $B_t = 1000$, $L = 1$, $T = 5$, $\delta = 0.04$.

Here we change B_t from 500 to 1000. Figure 3.2 shows how weights in the objective functionals affect harvesting decisions. Now with a larger harvesting cost, optimal harvesting rates for both orders decrease, compared to Figure 3.1, and reach the maximum threshold 0.4 at the final time step. Meanwhile, the harvesting rates show less variation in time as compared to Figure 3.1.

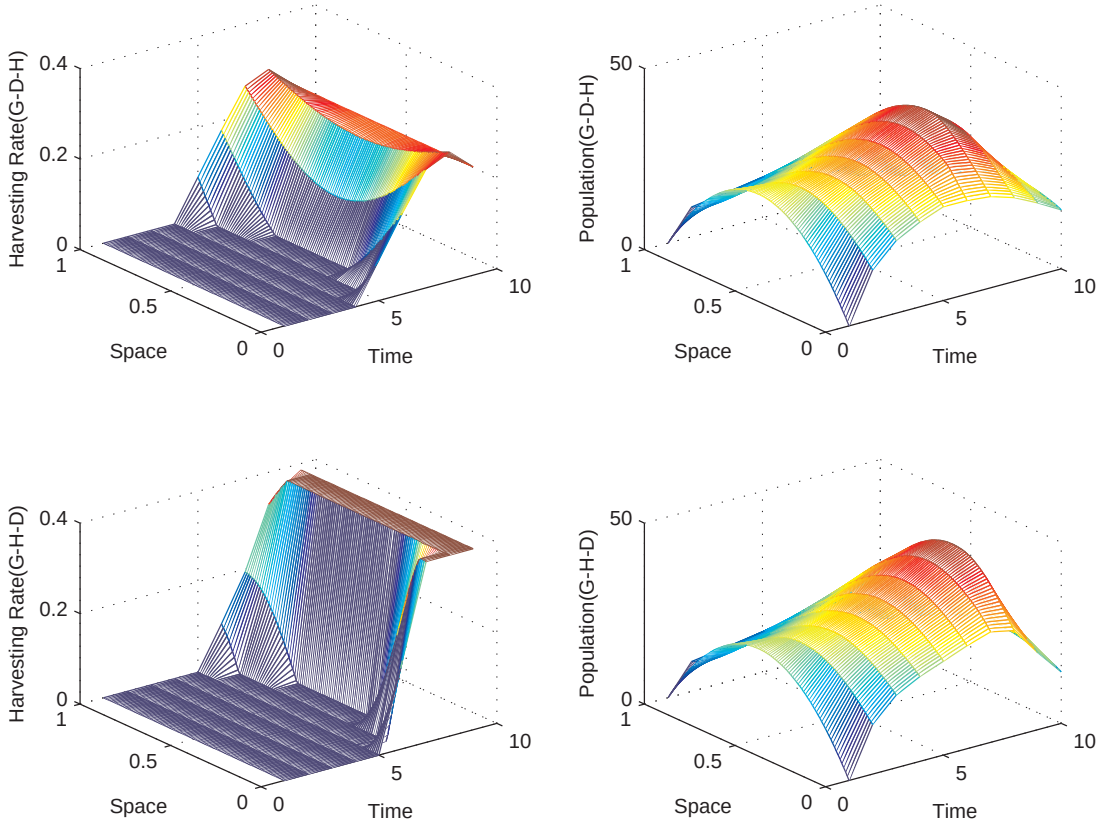

Figure 3.3: Normal kernel, $\beta = 5$, Linear growth function, $r = 1.8$, $A_t = 10$, $B_t = 500$, $L = 1$, $T = 10$, $\delta = 0.04$.

Here we extend the time range. In both cases in Figure 3.3 we observe no harvesting in the first several time steps. For order G-H-D, little harvesting is done most of the time and major effort is made during the last time step. For order G-D-H, however, harvesting is performed earlier on a larger scale and the harvesting rate levels off at the last time step.

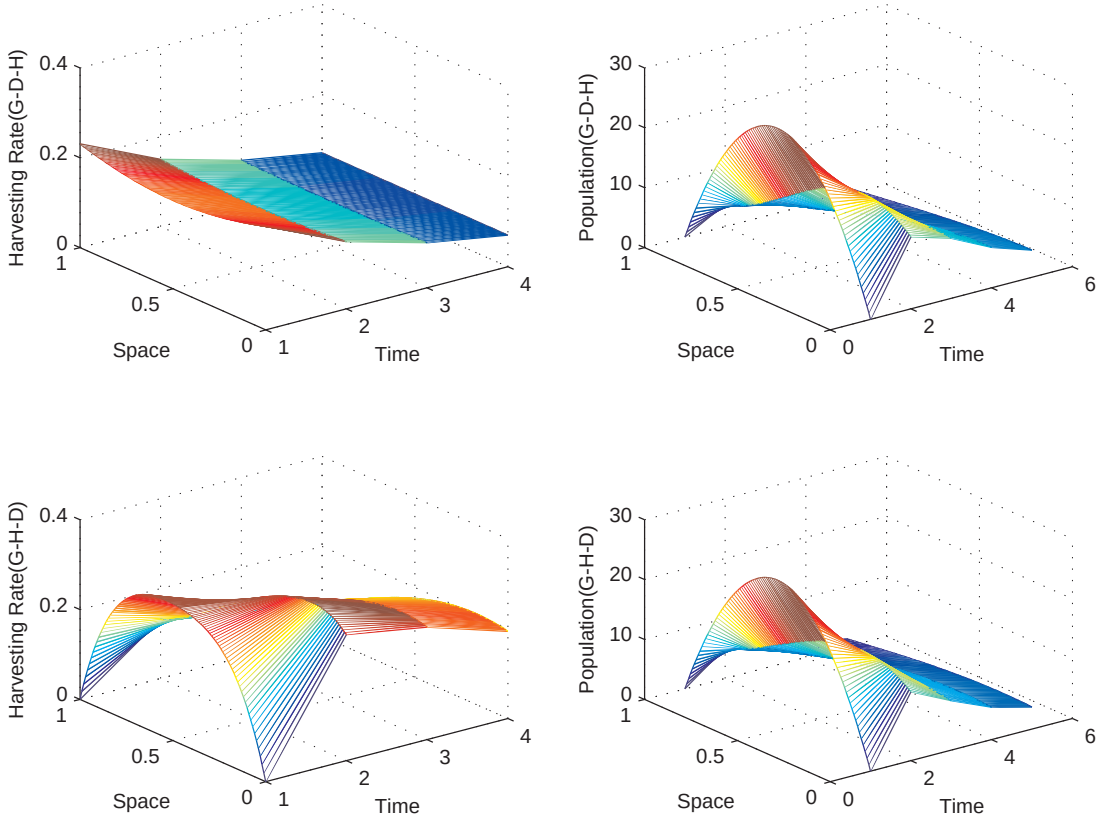

Figure 3.4: Finite range kernel, $R = 1$, Linear growth function, $r = 1.8$, $A_t = 10$, $B_t = 500$, $L = 1$, $T = 10$, $\delta = 0.04$.

We use a finite dispersal kernel

$$k(x,y) = \begin{cases} 0, & \text{if } x \leq y - R \\ \frac{\pi}{4R} cos\left[\frac{\pi}{2R}|x-y|\right], & \text{if } y - R < x < y + R \\ 0, & \text{if } x \geq y + R \end{cases}$$

to study how dispersal range affects the results. In Figure 3.4 a dispersal range $R = 1$ is used, which is the same size with the spatial region.

In Figure 3.5 a dispersal range $R = 2$ is used, which is twice the size of the spatial region.

In Figure 3.6 a dispersal range $R = 0.25$ is used, which is 1/4 the size of the spatial region.

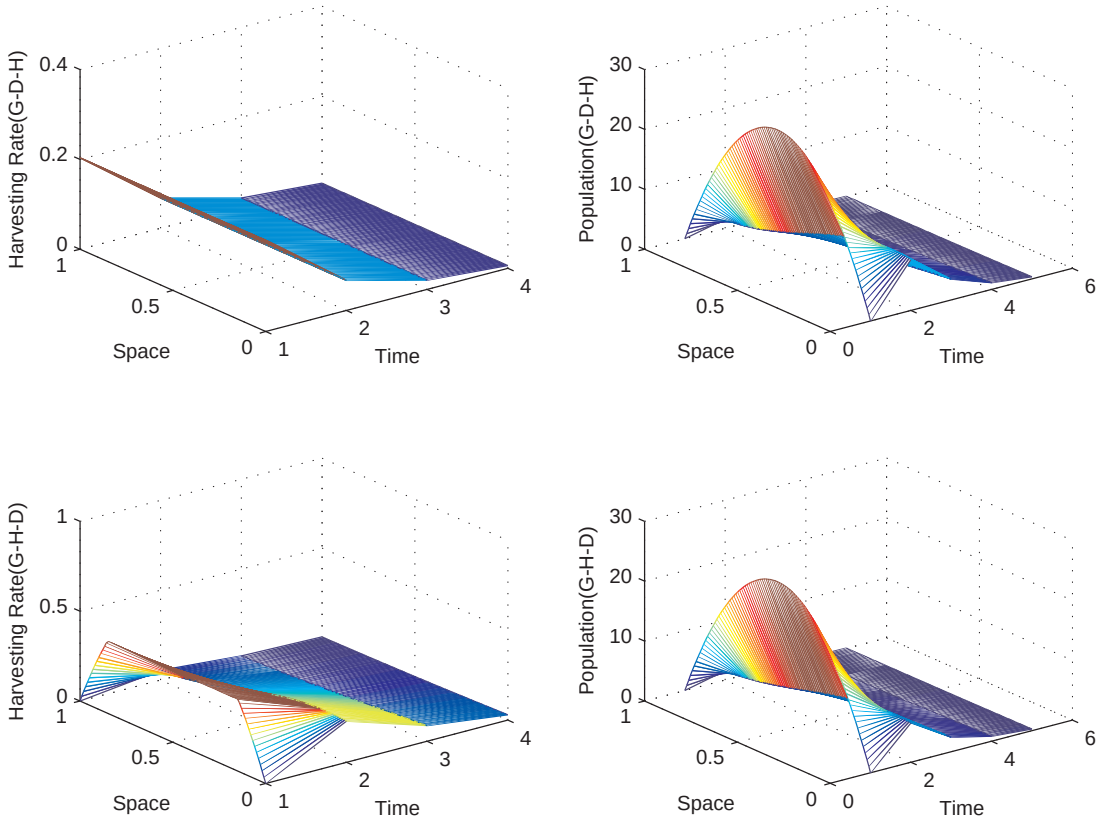

Figure 3.5: Finite range kernel, $R = 2$, Linear growth function, $r = 1.8$, $A_t = 10$, $B_t = 500$, $L = 1$, $T = 10$, $\delta = 0.04$.

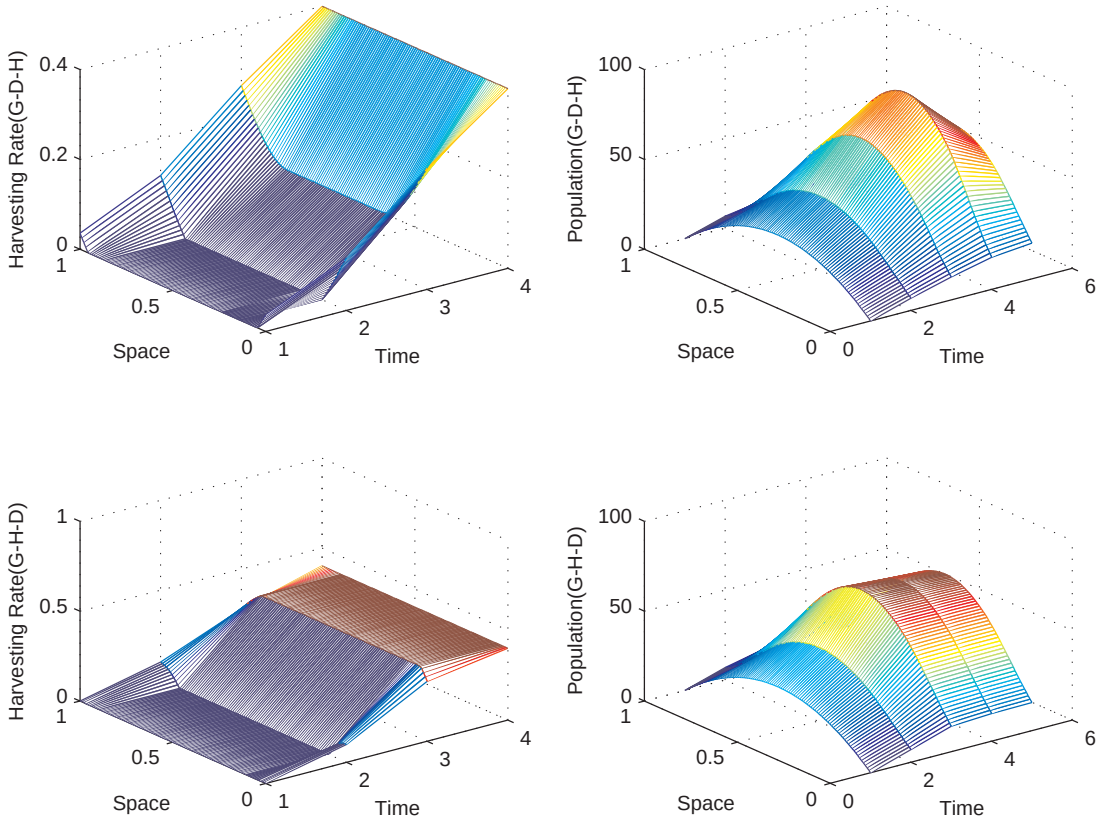

Figure 3.6: Finite range kernel, $R = 0.25$, Linear growth function, $r = 1.8$, $A_t = 10$, $B_t = 500$, $L = 1$, $T = 10$, $\delta = 0.04$.

3.3 Conclusion

In Chapter 2 we studied the harvesting problem with an order of growth, harvesting and dispersal. The discrete structure in our model naturally raised the question about the effects on the optimal results by changing order of events. In this chapter we compared the order in Chapter 2 with the order of growth, dispersal and harvesting studied by Joshi et al. [21, 22]. Section 3.1 compared the adjoint systems and characterization of optimal controls, for both linear and concave cases under the two orders. Section 3.2 showed numerical results of the optimal harvesting rates and populations under the two orders, with various dispersal kernels and parameters. With orders Growth-Harvesting-Dispersal and Growth-Dispersal-Harvesting, our optimality systems and numerical results show clearly the differences between the optimal controls.

Stability results for numerical computations of such optimality systems is an interesting open question. One could consider specifically the stability of the forward-backward sweep method.

Results in this chapter verify the importance of order of events in this discrete harvesting model, and motivates the study in Chapter 4, in which the relations among all the six possible ways of ordering events are discussed.

Chapter 4

Study of Six Different Harvesting Orders

4.1 List of Six Orders

In this chapter we study how the optimal control and state will be impacted by changing the order of growth, dispersal and harvesting.

Here we use G, H and D to denote growth, harvesting and dispersal.

In total, there are 6 ways to order these three events:

$$G \to H \to D \tag{4.1}$$

$$H \to D \to G \tag{4.2}$$

$$D \to G \to H \tag{4.3}$$

$$G \to D \to H \tag{4.4}$$

$$D \to H \to G \tag{4.5}$$

$$H \to G \to D. \tag{4.6}$$

In fact, the first 3 cases follows the same order as the chain

$$\cdots G \to H \to D \to G \to H \cdots$$

except with different starting points. Similarly, the last 3 cases follows the same order as the chain

$$\cdots G \to D \to H \to G \to D \cdots$$

except with different on starting points. We will investigate the relationships among those cases.

We next list the state equations and objective functionals using a monotone growth function f. We use $N_t^{[i]}$ to denote N_t for Case i.

For Case 1 with order $G \to H \to D$, the state equations are

$$\int_\Omega k(x,y)(1-\alpha_t(y))f(N_t^{[1]}(y))dy = N_{t+1}^{[1]}(x); \tag{4.7}$$

and the objective functional is

$$J(\alpha) = \sum_{t=0}^{T-1} \int_\Omega e^{-\delta t}[A_t\alpha_t(y)f(N_t^{[1]}(y)) - \frac{B_t}{2}V(\alpha_t(y))]dy. \tag{4.8}$$

For Case 2 with order $H \to D \to G$, the state equations are

$$f(\int_\Omega k(x,y)(1-\alpha_t(y))N_t^{[2]}(y)dy) = N_{t+1}^{[2]}(x); \tag{4.9}$$

and the objective functional is

$$J(\alpha) = \sum_{t=0}^{T-1} \int_\Omega e^{-\delta t}[A_t\alpha_t(y)N_t^{[2]}(y) - \frac{B_t}{2}V(\alpha_t(y))]dy. \tag{4.10}$$

For Case 3 with order $D \to G \to H$, the state equations are

$$(1-\alpha_t(x))f(\int_\Omega k(x,y)N_t^{[3]}(y)dy) = N_{t+1}^{[3]}(x). \tag{4.11}$$

and the objective functional is

$$J(\alpha) = \sum_{t=0}^{T-1}\int_\Omega e^{-\delta t}[A_t\alpha_t(x)f(\int_\Omega k(x,y)N_t^{[3]}(y)dy) - \frac{B_t}{2}V(\alpha_t(y))]dy. \tag{4.12}$$

For Case 4 with order $G \to D \to H$, the state equations are

$$(1-\alpha_t(x))\int_\Omega k(x,y)f(N_t^{[4]}(y))dy = N_{t+1}^{[4]}(x). \tag{4.13}$$

and the objective functional is

$$J(\alpha) = \sum_{t=0}^{T-1}\int_\Omega e^{-\delta t}[A_t\alpha_t(x)\int_\Omega k(x,y)f(N_t^{[4]}(y))dy - \frac{B_t}{2}V(\alpha_t(y))]dy. \tag{4.14}$$

For Case 5 with order $D \to H \to G$, the state equations are

$$f\big((1-\alpha_t(x))\int_\Omega k(x,y)N_t^{[5]}(y)dy\big) = N_{t+1}^{[5]}(x). \tag{4.15}$$

and the objective functional is

$$J(\alpha) = \sum_{t=0}^{T-1}\int_\Omega e^{-\delta t}[A_t\alpha_t(x)\int_\Omega k(x,y)N_t^{[5]}(y)dy - \frac{B_t}{2}V(\alpha_t(y))]dy. \tag{4.16}$$

For Case 6 with order $H \to G \to D$, the state equations are

$$\int_\Omega k(x,y)f\big((1-\alpha_t(y))N_t^{[6]}(y)\big)dy = N_{t+1}^{[6]}(x). \tag{4.17}$$

and the objective functional is

$$J(\alpha) = \sum_{t=0}^{T-1} \int_{\Omega} e^{-\delta t}[A_t \alpha_t(y) N_t^{[6]}(y) - \frac{B_t}{2} V(\alpha_t(y))]dy. \tag{4.18}$$

4.2 Relations among all the Six Cases

4.2.1 The First Three Cases

The following diagram shows the procedure of case 1 with an initial population of $N_0^{[1]}$,

$$N_0^{[1]} \underset{G\to H\to D}{\longrightarrow} N_1^{[1]} \underset{G\to H\to D}{\longrightarrow} N_2^{[1]} \cdots \underset{G\to H\to D}{\longrightarrow} N_T^{[1]}.$$

With the control $\alpha = (\alpha_0, \alpha_1, \cdots, \alpha_{T-1})$ applied during T time steps.

For case 2, with the control $\alpha = (\alpha_0, \alpha_1, \cdots, \alpha_{T-1})$ applied during T time steps, the objective functional in terms of $N_t^{[2]}$ is written below, as in (4.10).

$$J(\alpha) = \sum_{t=0}^{T-1} \int_{\Omega} e^{-\delta t}[A_t \alpha_t(y) N_t^{[2]}(y) - \frac{B_t}{2} V(\alpha_t(y))]dy.$$

We now try to write (4.10) in terms of $N_t^{[1]}$. From previous proof as in Section 2.2.1, all state functions are L^∞ bounded. That is, there exits an C such that $\| N_t^{[2]} \| \leq C$ for any $t = 1, 2, \cdots, T$. Thus the growth function f is a monotone map from $[0, C]$ to $[0, C]$. For $t = 0, 1, \cdots, T$, we construct functions $N_t : \Omega \to [0, C]$ such that $N_t(x) = f^{-1}(N_t^{[2]}(x))$ for any x in Ω.

The harvest at each time step at location y is $\alpha_t(y) N_t^{[2]}(y)$, i.e., $\alpha_t(y) f(N_t(y))$. Thus we can rewrite the objective functional for Case 2 as

$$J(\alpha) = \sum_{t=0}^{T-1} \int_{\Omega} e^{-\delta t}[A_t \alpha_t(y) f(N_t(y), y) - \frac{B_t}{2} V(\alpha_t(y))]dy.$$

We now show that N_t here is just $N_t^{[1]}$, the population at time step t under Case 1 order with control $\alpha = (\alpha_0, \alpha_1, \cdots, \alpha_{T-1})$ applied, only by showing N_t is a sequence

satisfying the state equations (4.7) of Case 1.

$$\begin{aligned} N_{t+1}(x) &= f^{-1}(N_{t+1}^{[2]}(x)) \overset{(4.9)}{=} f^{-1}(f(\int_\Omega k(x,y)(1-\alpha_t(y))N_t^{[2]}(y)dy)) \\ &= \int_\Omega k(x,y)(1-\alpha_t(y))N_t^{[2]}(y)dy \\ &= \int_\Omega k(x,y)(1-\alpha_t(y))f(N_t(y))dy. \end{aligned}$$

Thus we could conclude that a problem starting with a $N_0^{[2]}$ population under Case 2 order has exactly the same objective functional with the one starting with a population of $N_0^{[1]} = f^{-1}(N_0^{[2]})$ under Case 1 order, if the same control was applied at each time step. In other words, a harvesting problem under Case 2 order with an initial population of $N_0^{[2]}$, is equivalent to one under Case 1 order with an initial population of $N_0^{[1]} = f^{-1}(N_0^{[2]})$. The following diagram indicates this correspondence.

$$N_0^{[1]} \underset{G\to}{\dashrightarrow} N_0^{[2]} \underset{H\to D\to}{\longrightarrow} N_1^{[1]} \underset{G\to}{\to} N_1^{[2]} \underset{H\to D\to}{\longrightarrow} N_2^{[1]} \cdots \underset{H\to D\to}{\longrightarrow} N_T^{[1]} \underset{G\to}{\to} N_T^{[2]}$$

We use a similar approach for case 3. First we construct functions $N_t : \Omega \to [0, C]$, where $t = 0, 1, \cdots, T$, such that

$$N_t(x) = \int_\Omega k(x,y)N_t^{[3]}(y)dy.$$

for any x in Ω.

With the control $\alpha = (\alpha_0, \alpha_1, \cdots, \alpha_{T-1})$ applied during T time steps, The harvest at each time step is

$$\alpha_t(x)f(\int_\Omega k(x,y)N_t^{[3]}(y)dy),$$

i.e., $\alpha_t(x)f(N_t(x))$.

The objective functional in terms of $N_t^{[3]}$ is written below, as in (4.2.1).

$$J(\alpha) = \sum_{t=0}^{T-1} \int_\Omega e^{-\delta t}[A_t\alpha_t(x)f(\int_\Omega k(x,y)N_t^{[3]}(y)dy) - \frac{B_t}{2}V(\alpha_t(y))]dy.$$

We show that N_t is just the population at time step t under Case 1 order with control $\alpha = (\alpha_0, \alpha_1, \cdots, \alpha_{T-1})$ applied, only by showing N_t is a sequence satisfying the state equations (4.7) of Case 1.

$$\begin{aligned} N_{t+1}(x) &= \int_\Omega k(x,y) N_t^{[3]}(y) dy \overset{(4.11)}{=} \int_\Omega k(x,y)(1-\alpha_t(y)) f(\int_\Omega k(y,x) N_t^{[3]}(x) dx) dy \\ &= \int_\Omega k(x,y)(1-\alpha_t(y)) f(N_t(y)) dy \end{aligned}$$

Thus we could conclude that a problem starting with a $N_0^{[3]}$ population under Case 3 order has exactly the same objective functional with the one starting with

$$N_0^{[1]}(x) = \int_\Omega k(x,y) N_0^{[3]}(y) dy$$

population under Case 1 order, if the same control was applied at each time step. The following diagram indicates the corresponding procedure.

$$N_0^{[3]} \underset{D\rightarrow}{\rightarrow} N_0^{[1]} \underset{G\rightarrow H\rightarrow}{\longrightarrow} N_1^{[3]} \underset{D\rightarrow}{\rightarrow} N_1^{[1]} \underset{G\rightarrow H\rightarrow}{\longrightarrow} N_2^{[3]} \cdots \underset{G\rightarrow H\rightarrow}{\longrightarrow} N_T^{[3]} \underset{D\rightarrow}{\dashrightarrow} N_T^{[1]}$$

The comparison above indicates that harvesting problems under the first three Cases of orders are equivalent to each other given a specific relationship between the initial populations. The results on existence, characterization, and uniqueness of the optimal control in Case 1 could be applied to Cases 2 and 3.

4.2.2 The Last Three Cases

Following the same logic we show that Cases 4, 5 and 6 have a similar kind of relationship.

The following diagram shows the procedure of case 4 with an initial population of $N_0^{[4]}$.

$$N_0^{[4]} \underset{G\to D\to H}{\longrightarrow} N_1^{[4]} \underset{G\to D\to H}{\longrightarrow} N_2^{[4]} \cdots \underset{G\to D\to H}{\longrightarrow} N_T^{[4]}$$

with the control $\alpha = (\alpha_0, \alpha_1, \cdots, \alpha_{T-1})$ applied during T time steps, the objective functional in terms of $N_t^{[5]}$ is written below, as in (4.16).

For case 5, again all state functions are L^∞ bounded. That is, there exists an C such that $\| N_t^{[5]} \| \leq C$ for any $t = 1, 2, \cdots, T$. Thus the growth function f is a monotone map from $[0, C]$ to $[0, C]$. For $t = 0, 1, \cdots, T$, we construct functions $N_t : \Omega \to [0, N]$ such that $N_t(x) = f^{-1}(N_0^{[5]}(x))$ for any x in Ω.

Since the growth function is monotone, for each $t = 0, 1, \cdots, T$, there exists an N_t such that $N_t^{[5]}(x) = f(N_t(x))$ for any x in Ω.

The harvest at each time step is

$$\alpha_t(x) \int_\Omega k(x, y) N_t^{[5]}(y) dy,$$

i.e., $\alpha_t(x) \int_\Omega k(x, y) f(N_t(y)) dy$.

Then the objective function in terms of N_t is:

$$J(\alpha) = \sum_{t=0}^{T-1} \int_\Omega e^{-\delta t} [A_t \alpha_t(x) \int_\Omega k(x, y) f(N_t(y)) dy - \frac{B_t}{2} V(\alpha_t(x))] dx.$$

We now show that N_t is just the population at time step t under Case 4 order with control $\alpha = (\alpha_0, \alpha_1, \cdots, \alpha_{T-1})$ applied, only by showing N_t is a sequence satisfying (4.13),

$$\begin{aligned} N_{t+1}(x) &= f^{-1}(N_{t+1}^{[5]}(x)) \overset{(4.15)}{=} f^{-1}\left(f\big((1 - \alpha_t(x)) \int_\Omega k(x, y) N_t^{[5]}(y) dy\big) \right) \\ &= (1 - \alpha_t(x)) \int_\Omega k(x, y) N_t^{[5]}(y) dy \\ &= (1 - \alpha_t(x)) \int_\Omega k(x, y) f(N_t(y)) dy \end{aligned}$$

Thus we could conclude that a problem starting with a $N_0^{[5]}$ population under Case 5 order has exactly the same objective functional with the one starting with a $N_0^{[4]} = f^{-1}(N_0^{[5]})$ population under Case 4 order, if the same control was applied at each time step. The following diagram indicates the corresponding procedure.

$$N_0^{[4]} \underset{G\rightarrow}{\dashrightarrow} N_0^{[5]} \underset{D\rightarrow H\rightarrow}{\longrightarrow} N_1^{[4]} \underset{G\rightarrow}{\rightarrow} N_1^{[5]} \underset{D\rightarrow H\rightarrow}{\longrightarrow} N_2^{[4]} \cdots \underset{D\rightarrow H\rightarrow}{\longrightarrow} N_T^{[4]} \underset{G\rightarrow}{\rightarrow} N_T^{[5]}$$

Now we explain the complexity of Case 6. The two diagrams (4.19) and (4.20) below indicates the only two possible ways to obtain a correspondence between Case 4 and Case 6.

$$N_0^{[6]} \underset{H\rightarrow}{\rightarrow} N_0^{[4]} \underset{G\rightarrow D\rightarrow}{\longrightarrow} N_1^{[6]} \underset{H\rightarrow}{\rightarrow} N_1^{[4]} \underset{G\rightarrow D\rightarrow}{\longrightarrow} N_2^{[6]} \cdots \underset{G\rightarrow D\rightarrow}{\longrightarrow} N_T^{[6]} \underset{H\rightarrow}{\dashrightarrow} N_T^{[4]} \tag{4.19}$$

$$N_0^{[4]} \underset{G\rightarrow D\rightarrow}{\longrightarrow} N_1^{[6]} \underset{H\rightarrow}{\rightarrow} N_1^{[4]} \underset{G\rightarrow D\rightarrow}{\longrightarrow} N_2^{[6]} \underset{H\rightarrow}{\rightarrow} N_2^{[4]} \cdots \underset{G\rightarrow D\rightarrow}{\longrightarrow} N_T^{[6]} \underset{H\rightarrow}{\dashrightarrow} N_T^{[4]} \tag{4.20}$$

The diagram (4.19) shows a relation of

$$\big((1-\alpha_0)\big) N_0^{[6]} = N_0^{[4]}, \tag{4.21}$$

which does not provide helpful information because of the control term.

The diagram (4.19) shows a relation of

$$N_t^{[6]}(x) = \int_\Omega k(x,y) f(N_t^{[4]}(y)) dy, \tag{4.22}$$

but it is hard to find $N_0^{[4]}$ explicitly in term of $N_0^{[6]}$ from this equation.

Thus we can not get the the characterization result of existence, characterization and uniqueness result for Case 6 by transforming it into Case 4. Case 6 is studied separately in the following chapter.

4.3 Conclusion

There are totally six ways of ordering the three events, growth, harvesting and dispersal in this harvesting problem. In Section 4.1 we listed the six orders ((4.1)-(4.6)) and their state equations together with the objective functionals for the concave case. In Section 4.2 we discussed the relations among those orders. In fact, similarity in the first three orders is observable because they can all be viewed as one part on this chain of events:

$$\cdots G \to H \to D \to G \to H \cdots ,$$

and the only difference exists in the beginning and ending points. The ending points are not a concern since the population at the final time step is not included in the objective functional.

In 4.2.1 we give a rigorous proof of the equivalence among the first three cases under certain transformations of initial populations. Following the same idea, in 4.2.2 we are able to show the equivalence between Case 4 and Case 5. However, Case 6 can not be transformed into Case 4, due to the complexity of the two relations (4.21) and (4.22). This leads to the study in Chapter 5 about the existence, characterization and uniqueness of optimal control for Case 6.

From considering the six cases of order of events, transformations show that analysis and necessary conditions only are needed for three cases. The other three cases can be obtained from those three cases.

Chapter 5

Study of Case 6: Harvest, Growth and Dispersal

We now consider a model with the order of events being harvest, growth and dispersal.

We consider the harvest of the following integrodifference model with concave growth function:

$$N_{t+1}(x) = \int_\Omega k(x,y) f((1-\alpha_t)N_t(y), y)dy,$$

for $t = 0, 1, \cdots, T-1$.

Here f is twice differentiable in $N_t(y)$ and measurable in y. For almost all y, $f(\cdot, y)$ is nondecreasing and concave in the N variable, $\dfrac{\partial f_W(N_t(x), x)}{\partial N}$ is decreasing and nonnegative, and

$$f(N_t(y), y) \geq 0, \quad \text{for all} \quad N_t(y) \geq 0, y \in \Omega,$$

$$|f(N_t(y), y)| \leq C_r < \infty, \quad \text{for all} \quad 0 \leq N_t(y), y \in \Omega.$$

We assume that for almost all y, $f(\cdot, y)$ is Lipschitz continuous in $L^2(\Omega)$. We also assume that the partial derivatives, $f_W(N_t(x), x)$ and $f_{WW}(N_t(x), x)$ are both L^∞ bounded for any $N \in L^\infty(\Omega)$. Here f_W and f_{WW} denote the first and second partial derivatives of $f(\cdot, y)$ with respect to the first variable.

The assumption for the initial population is $N_0 \in L^\infty(\Omega)$ and $N_0(x) \geq 0$. The control set is defined as $U = \left\{\alpha \in \left(L^\infty(\Omega)\right)^T | 0 \leq \alpha_t(x) \leq M, t = 0, 1, \ldots, T-1\right\}$ for $M < 1$. Given $\alpha \in U$ the corresponding state $N = N(\alpha)$ satisfies

$$0 \leq N_t(x) \leq C_{f(N_0)},$$

where $C_{f(N_0)}$ is a constant that depends on the growth function value at N_0.

The kernels are bounded and measurable such that

$$\left| \int_\Omega k(x, y) dx \right| \leq C \leq 1$$

for all $x \in \Omega$ and $0 \leq k(x, y) \leq k_1$ for $(x, y) \in \Omega \times \Omega$.

We define the objective functional as:

$$J(\alpha) = \sum_{t=0}^{T-1} \int_\Omega e^{-\delta t} [A_t \alpha_t(y) N_t(y) dy - \frac{B_t}{2} V(\alpha_t(y))] dy.$$

Here J represents the profit, which is the discounted revenue stream less the cost of the control, where the coefficient where A_t is the price factor and $e^{-\delta t}$ is the discount factor with $\delta > 0$. We assume the cost of harvesting is a nonlinear function V, and assume that the C^2 function $V : [0, M] \to R$ is increasing and convex with

$$V''(\alpha) \geq b > 0$$

for all α in $[0, M]$. The coefficient B_t is a weight factor that balances the two parts of the objective functional. The coefficients, A_t and B_t, are both positive numbers for any $t = 0, 1, \cdots, T-1$. All other assumptions are the same with previous linear cases.

We seek $\alpha^* \in U$ such that

$$J\alpha = \max_{\alpha \in U} J(U)$$

.

5.1 Existence of an Optimal Control

First we prove the existence of an optimal control using a convex combination technique from [52].

Theorem 5.1. *There exists an optimal control α^* in U that maximizes the functional $J(\alpha)$.*

Proof. Let $\{\alpha^n\}$ be a maximizing sequence for the objective functional J in (2) and $N^n = N(\alpha^n)$ be the corresponding state sequence. From the bounded assumption on control, state, and $f(N)$, the sequences $\{\alpha^n\}$ and $f((1-\alpha^n)N^n)$ are L^∞ bounded. Then there exists $\alpha^* \in U$ and $F \in \left(L^\infty(\Omega)\right)^T$ such that on a subsequence, we have the following weak convergence,

$$\alpha_t^n \rightharpoonup \alpha_t^* \text{ in } L^2(\Omega), t = 0, \cdots, T-1,$$

$$f((1-\alpha_t^n)N_t^n(y), y) \rightharpoonup F_t(y) \text{ in } L^2(\Omega), t = 0, \cdots, T-1.$$

Thus for almost every $x \in \Omega$,

$$N_{t+1}^n(x) = \int_\Omega k(x,y) f((1-\alpha_t^n)N_t^n(y), y)dy \to \int_\Omega k(x,y)F_t(y)dy \tag{5.1}$$

for any $t = 0, \cdots, T-1$.

From dominated convergence theorem, the pointwise convergence above becomes strong L^2 convergence, i.e.,

$$\int_\Omega k(x,y) f((1-\alpha_t^n)N_t^n(y), y)dy \to \int_\Omega k(x,y)F_t(y)dy \tag{5.2}$$

strongly in $L^2(\Omega)$, for any $t = 0, \cdots, T-1$.

Let $N_0^* = N_0$, and

$$N_{t+1}^*(x) = \int_\Omega k(x,y)F_t(y)dy$$

for $t = 0, \cdots, T-1$. Then from (5.2) we know that

$$N_t^n \to N_t^*$$

strongly in $L^2(\Omega)$, for any $t = 0, \cdots, T$.

Given $N_0^* = N_0 = N_0(\alpha^*)$, we want to show by induction that $N_{t+1}^*(\alpha) \leq N_{t+1}(\alpha^*)$ holds for any $t = 0, \cdots, T-1$ and any $\alpha \in U$, with the induction assumption $N_t^*(\alpha) \leq N_t(\alpha^*)$. i.e., we want to show that

$$\int_\Omega k(x,y)F_t(y)dy \leq \int_\Omega k(x,y)f((1-\alpha_t^*)N_t(\alpha^*), y)dy \tag{5.3}$$

for any $t = 0, \cdots, T-1$.

From weak convergence of $\{\alpha_t^n\}$ and strong convergence of $\{N_t^n\}$, and the L^∞ boundedness of both sequences, we have

$$(1-\alpha_t^n)N_t^n \rightharpoonup (1-\alpha_t^*)N_t^*$$

weakly in $L^2(\Omega)$.

Mazur's Theorem [52] gives us that there exists constants β_j^n, $j = n, \cdots, m_n$, such that:

$$\sum_{j=n}^{m_n} \beta_j^n = 1, \ \ n = 1, 2, \cdots,$$

$$\beta_j^n \geq 0, \ \ n = 1, 2, \cdots, \ \ j = n, \cdots, m_n,$$

$$\sum_{j=n}^{m_n} \beta_j^n (1-\alpha_t^j)N_t^j \to (1-\alpha_t^*)N_t^* \text{ strongly in } L^2(\Omega). \tag{5.4}$$

From the concavity of $f(\cdot, y)$, we have

$$\sum_{j=n}^{m_n} \beta_j^n \int_\Omega k(x,y) f((1-\alpha_t^j) N_t^j(y), y) dy$$
$$\leq \int_\Omega k(x,y) f(\sum_{j=n}^{m_n} \beta_j^n (1-\alpha_t^j) N_t^j(y), y) dy. \tag{5.5}$$

From the Lipschitz Continuity of $f(\cdot, y)$ in $L^2(\Omega)$, we have

$$\int_\Omega k(x,y) f(\sum_{j=n}^{m_n} \beta_j^n (1-\alpha_t^j) N_t^j(y), y) dy \to \int_\Omega k(x,y) f((1-\alpha_t^*) N_t^*(y), y) dy,$$

almost everywhere for x. Also from (5.1),

$$\int_\Omega k(x,y) f((1-\alpha_t^n) N_t^n(y), y) dy \to \int_\Omega k(x,y) F_t(y) dy$$

for almost every $x \in \Omega$ and any $t = 0, \cdots, T-1$. Thus a convex combination of the left hand side sequence also converges to the right hand side function for almost every $x \in \Omega$ and any $t = 0, \cdots, T-1$. i.e.,

$$\sum_{j=n}^{m_n} \beta_j^n \int_\Omega k(x,y) f((1-\alpha_t^j) N_t^j(y), y) dy \to \int_\Omega k(x,y) F_t(y) dy.$$

for almost every $x \in \Omega$ and any $t = 0, \cdots, T-1$.

From (5.5), (5.6), and (5.6), we conclude that

$$\int_\Omega k(x,y) F_t(y) dy \leq \int_\Omega k(x,y) f((1-\alpha_t^*) N_t^*(y), y) dy. \tag{5.6}$$

for almost every $x \in \Omega$ and any $t = 0, \cdots, T-1$.

Induction Hypothesis $N_t^*(\alpha) \leq N_t(\alpha^*)$ and f being an increasing function gives

$$\int_\Omega k(x,y) f((1-\alpha_t^*) N_t^*(y), y) dy \leq \int_\Omega k(x,y) f((1-\alpha_t^*) N_t(\alpha^*), y) dy. \tag{5.7}$$

So we have

$$N^*_{t+1}(x) = \int_\Omega k(x,y)F_t(y)dy \le \int_\Omega k(x,y)f((1-\alpha^*_t)N_t(\alpha^*),y)dy = N_{t+1}(\alpha^*)(x) \tag{5.8}$$

for almost every $x \in \Omega$ and any $t = 0, \cdots, T-1$, which completes our induction proof.

The weak convergence of α^n_t and strong convergence of N^n_t gives

$$\int_\Omega e^{-\delta t}A_t\alpha^n_t(y)N^n_t(y)dy \to \int_\Omega e^{-\delta t}A_t\alpha^*_t(y)N^*_t(y)dy \tag{5.9}$$

strongly in $L^2(\Omega)$. The weak convergence of α^n_t leads to the lower semicontinuity result for $V(\alpha^n_t)$, thus

$$\int_\Omega \frac{B_t}{2}V(\alpha^*_t(y))dy \le \liminf_{n\to\infty}\int_\Omega \frac{B_t}{2}V(\alpha^n_t(y))dy. \tag{5.10}$$

So we have

$$\begin{aligned}
J(\alpha^*) &= \sum_{t=0}^{T-1}\int_\Omega e^{-\delta t}[A_t\alpha^*_t(y)N_t(\alpha^*)(y)dy - \frac{B_t}{2}V(\alpha^*_t(y))]dy \\
&\ge \sum_{t=0}^{T-1}\int_\Omega e^{-\delta t}[A_t\alpha^*_t(y)N^*_t(y)dy - \frac{B_t}{2}V(\alpha^*_t(y))]dy \text{ (by induction argument)} \\
&\ge \lim_{n\to\infty}\sum_{t=0}^{T-1}\int_\Omega e^{-\delta t}[A_t\alpha^n_t(y)N^n_t(y)dy - \frac{B_t}{2}V(\alpha^n_t(y))]dy \\
&= \lim_{n\to\infty} J(\alpha^n),
\end{aligned} \tag{5.11}$$

which shows α^* is an optimal control. □

5.2 Characterization of an Optimal Control

Theorem 5.2. *We again differentiate the maps $\alpha \to N(\alpha)$ and $\alpha \to J(\alpha)$ to obtain our characterization.*

The mapping $\alpha \in U \to N \in (L^\infty(\Omega))^T$ is differentiable in the following sense:

$$\frac{N_t^\epsilon(x) - N_t(x)}{\epsilon} \rightharpoonup \psi_t(x)$$

weakly in $L^2(\Omega)$ as $\epsilon \to 0$ for any $\alpha \in U$ and $l \in (L^\infty(\Omega))^T$ such that $(\alpha + \epsilon l) \in U$ for ϵ small, where $N^\epsilon = N(\alpha + \epsilon l)$. Also ψ, depending on N, α and l, satisfies:

$$\psi_{t+1}(x) = \int_\Omega k(x,y) f_W\big((1-\alpha_t(y))N_t(y), y\big)\big(-l_t(y)N_t(y) + (1-\alpha_t(y))\psi_t(y)\big)dy \quad (5.12)$$

$$\psi_0(x) = 0$$

for $t = 0, 1, \cdots, T-1$, where f_W stands for the derivative of $f(\cdot, y)$ with respect to the first variable.

Remark 5.3. *Since the sensitivity function depends on N, α and l, we can use $\psi(\alpha, N(\alpha), l)$ to denote the directional derivative of $N(\alpha)$ along vector l with respect to α.*

Proof. In the proof, we omit the independent variable y in order to shorten the expressions, as long as no ambiguity exists. For instance, we use α_t for $\alpha_t(y)$, l_t for $l_t(y)$, N_t for $N_t(y)$, and so on.

Consider the control-to-solution map: $\alpha \to J(\alpha)$.

Let $N^\epsilon = N(\alpha + \epsilon l)$, then

$$\begin{aligned}\frac{N^\epsilon_{t+1}(x) - N_{t+1}(x)}{\epsilon} &= \int_\Omega k(x,y)\frac{f\big((1-\alpha_t-\epsilon l_t)N^\epsilon_t\big) - f\big((1-\alpha_t)N_t\big)}{\epsilon}dy \\ &= \int_\Omega k(x,y)\frac{f\big((1-\alpha_t-\epsilon l_t)N^\epsilon_t\big) - f\big((1-\alpha_t)N^\epsilon_t\big)}{-\epsilon l_t N^\epsilon_t} \\ &\quad (-l_t N^\epsilon_t) + \frac{f\big((1-\alpha_t)N^\epsilon_t\big) - f\big((1-\alpha_t)N_t\big)}{(1-\alpha_t)(N^\epsilon_t - N_t)} \\ &\quad \frac{(1-\alpha_t)(N^\epsilon_t - N_t)}{\epsilon}dy.\end{aligned}$$

Using $N^\epsilon_0 = N_0$ we get

$$N^\epsilon_1(x) = N_1(x).$$

For $t = 2$,

$$\begin{aligned}\frac{N^\epsilon_2(x) - N_2(x)}{\epsilon} &= \int_\Omega k(x,y)\frac{f\big((1-\alpha_1-\epsilon l_1)N^\epsilon_1\big) - f\big((1-\alpha_1)N_1\big)}{\epsilon}dy \\ &= \int_\Omega k(x,y)\bigg[\frac{f\big((1-\alpha_1-\epsilon l_1)N^\epsilon_1\big) - f\big((1-\alpha_1)N^\epsilon_1\big)}{-\epsilon l_1 N^\epsilon_1}(-l_1 N^\epsilon_1) \\ &\quad + \frac{f\big((1-\alpha_1)N^\epsilon_1\big) - f\big((1-\alpha_1)N_1\big)}{(1-\alpha_1)(N^\epsilon_1 - N_1)}\frac{(1-\alpha_1)(N^\epsilon_1 - N_1)}{\epsilon}\bigg]dy \\ &= \int_\Omega k(x,y)\frac{f\big((1-\alpha_1-\epsilon l_1)N^\epsilon_1\big) - f\big((1-\alpha_1)N^\epsilon_1\big)}{-\epsilon l_1 N^\epsilon_1}(-l_1 N^\epsilon_1)dy.\end{aligned}$$

From the boundedness of N_1 and Lipschitz Continuity of $f(\cdot, y)$ in $L^2(\Omega)$, we have

$$\left|\frac{N^\epsilon_2(x) - N_2(x)}{\epsilon}\right| \le C_2 \qquad \text{for all } x \in \Omega.$$

For $t = 3$,

$$\begin{aligned}\frac{N_3^\epsilon(x) - N_3(x)}{\epsilon} &= \int_\Omega k(x,y) \frac{f\big((1-\alpha_2-\epsilon l_2)N_2^\epsilon\big) - f\big((1-\alpha_2)N_2\big)}{\epsilon} dy \\ &= \int_\Omega k(x,y) \Bigg[\frac{f\big((1-\alpha_2-\epsilon l_2)N_2^\epsilon\big) - f\big((1-\alpha_2)N_2^\epsilon\big)}{-\epsilon l_2 N_2^\epsilon} (-l_2 N_2^\epsilon) \\ &\quad + \frac{f\big((1-\alpha_2)N_2^\epsilon\big) - f\big((1-\alpha_2)N_2\big)}{(1-\alpha_2)(N_2^\epsilon - N_2)} \frac{(1-\alpha_2)(N_2^\epsilon - N_2)}{\epsilon} \Bigg] dy.\end{aligned}$$

From the boundedness of N_2, $\dfrac{N_2^\epsilon(x) - N_2(x)}{\epsilon}$ and Lipschitz Continuity of $f(\cdot, y)$ in $L^2(\Omega)$, we have

$$\left|\frac{N_3^\epsilon(x) - N_3(x)}{\epsilon}\right| \le C_3 \qquad \text{for all } x \in \Omega.$$

And then by iteration,

$$\left|\frac{N_t^\epsilon(x) - N_t(x)}{\epsilon}\right| \le C_t \qquad \text{for all } x \in \Omega, t = 1, 2, \cdots, T.$$

From the *a priori* estimate, we have

$$\frac{N_t^\epsilon(x) - N_t(x)}{\epsilon} \rightharpoonup \psi_t(x) \qquad \text{weakly in } L^2(\Omega).$$

Similarly as in Theorem 1, by iteration, we have $\dfrac{N_t^\epsilon(x) - N_t(x)}{\epsilon}$ converges pointwise, and also strongly in L^2. which gives us the existence of $\psi \in (L^\infty(\Omega))^{T+1}$ such that

$$\psi_0(x) = 0$$

and

$$\begin{aligned}&\int_\Omega k(x,y) \frac{f\big((1-\alpha_t-\epsilon l_t)N_t^\epsilon\big) - f\big((1-\alpha_t)N_t^\epsilon\big)}{-\epsilon l_t N_t^\epsilon} (-l_t N_t^\epsilon) \\ &+ \frac{f\big((1-\alpha_t)N_t^\epsilon\big) - f\big((1-\alpha_t)N_t\big)}{(1-\alpha_t)(N_t^\epsilon - N_t)} \frac{(1-\alpha_t)(N_t^\epsilon - N_t)}{\epsilon} dy \\ &\to \int_\Omega k(x,y) f_W\big((1-\alpha_t)N_t\big)[(1-\alpha_t)\psi_t - l_t N_t] dy. \qquad (5.13)\end{aligned}$$

Passing to the limit, we get

$$\psi_{t+1}(x) = \int_\Omega k(x,y) f_W\big((1-\alpha_t(y))N_t(y), y\big)[(1-\alpha_t(y))\psi_t(y) - l_t N_t]dy,$$

for $t = 0, \cdots, T$. □

Now we differentiate the map $\alpha \to J(\alpha)$ to obtain a characterization of an optimal control.

Theorem 5.4. *Given an optimal control α^* and corresponding state solution $N^* = N(\alpha^*)$, there exists a solution $p \in (L^\infty(\Omega))^T$ satisfying the adjoint system:*

$$\begin{aligned} p_{t-1}(x) &= f_W\big((1-\alpha_t^*(x))N_t^*(x)\big)\big(1-\alpha_{t-1}^*(x)\big)\int_\Omega p_t(y)k(y,x)dy + e^{-\delta t}A_{t-1}\alpha_{t-1}^*(x) \\ p_T(x) &= 0 \end{aligned} \tag{5.14}$$

where $t = T, \cdots, 2, 1$. Furthermore, for $t = 0, 1, 2, \cdots, T-1$;

$$V'(\alpha_t^*(x)) = \frac{2}{B_t}(A_t - f_W\big((1-\alpha_t^*(x))N_t^*(x)\big)\int_\Omega e^{\delta t}p_{t+1}(y)k(y,x)dy)N_t^*(x)$$

on the interior of the control set.

Proof. Let α^* be an optimal control (which exists by Theorem 1) and $N^* = N(\alpha^*)$ be the corresponding state. For variation l with $(\alpha^* + \epsilon l) \in U$ for $\epsilon > 0$ sufficiently small, let N^ϵ be the corresponding solution of the state equation. Since the adjoint system is linear, there exists a solution p. We compute the directional derivative of the functional $J(\alpha)$ with respect to α in the direction l at α^*. Since $J(\alpha^*)$ is the

maximum value, we have

$$
\begin{aligned}
0 \geq & \lim_{\epsilon \to 0^+} \frac{J(\alpha^* + \epsilon l) - J(\alpha^*)}{\epsilon} \\
= & \lim_{\epsilon \to 0^+} \sum_{t=0}^{T-1} \frac{1}{\epsilon} \Big\{ \int_\Omega e^{-\delta t} \big[A_t(\alpha_t^* + \epsilon l_t) N_t^\epsilon(y) - \frac{B_t}{2} V(\alpha_t^* + \epsilon l_t) \big] dy \\
& - \int_\Omega e^{-\delta t} \big[A_t(\alpha_t^*) N_t^*(y) - \frac{B_t}{2} V(\alpha_t^*) \big] dy \Big\} \\
= & \lim_{\epsilon \to 0^+} \sum_{t=0}^{T-1} \int_\Omega e^{-\delta t} \big[A_t \alpha_t^* \frac{N_t^\epsilon(y) - N_t^*(y)}{\epsilon} + A_t l_t r N_t^\epsilon(y) - \frac{B_t}{2} \frac{V(\alpha_t^* + \epsilon l_t) - V(\alpha_t^*)}{\epsilon} \big] dy \\
= & \sum_{t=0}^{T-1} \int_\Omega e^{-\delta t} A_t \alpha_t^*(y) \psi_t(y) dy + \sum_{t=0}^{T-1} \int_\Omega e^{-\delta t} A_t l_t N_t^*(y) dy \\
& - \sum_{t=0}^{T-1} \int_\Omega e^{-\delta t} \frac{B_t}{2} V'(\alpha_t^*) l_t(y) dy.
\end{aligned}
$$

We use the coefficient of the ψ_t term as the non-homogeneous term in the adjoint system and transform that term:

$$
\begin{aligned}
&\sum_{t=0}^{T-1}\int_\Omega e^{-\delta t}A_t\alpha_t^*(y)\psi_t(y)dy \\
&=\sum_{t=0}^{T-1}\int_\Omega [p_t(y)-f_W\big((1-\alpha_t^*(y))N_t^*(y)\big)(1-\alpha_t^*(y))\int_\Omega p_{t+1}(x)k(x,y)dx]\psi_t(y)dy \\
&=\sum_{t=0}^{T-1}\int_\Omega p_t(y)\psi_t(y)dy \\
&-\sum_{t=0}^{T-1}\int_\Omega f_W\big((1-\alpha_t^*(y))N_t^*(y)\big)(1-\alpha_t^*(y))\psi_t(y)\int_\Omega p_{t+1}(x)k(x,y)dxdy \qquad (5.15)\\
&=\sum_{t=0}^{T-1}\int_\Omega p_{t+1}(y)\psi_{t+1}(y)dy-\int_\Omega p_T(y)\psi_T(y)dy+\int_\Omega p_0(y)\psi_0(y)dy \\
&-\sum_{t=0}^{T-1}\int_\Omega p_{t+1}(x)\int_\Omega f_W\big((1-\alpha_t^*(y))N_t^*(y)\big)(1-\alpha_t^*(y))\psi_t(y)k(x,y)dydx \\
&=\sum_{t=0}^{T-1}\int_\Omega p_{t+1}(x)[\psi_{t+1}(x)-\int_\Omega f_W\big((1-\alpha_t^*(y))N_t^*(y)\big)k(x,y)(1-\alpha_t^*(y))\psi_t(y)dy]dx \\
&=\sum_{t=0}^{T-1}\int_\Omega p_{t+1}(x)[-\int_\Omega k(x,y)f_W\big((1-\alpha_t^*(y))N_t^*(y)\big)l_t(y)N_t^*(y)dy]dx,
\end{aligned}
$$

where we used $p_T(x)\equiv 0$, $\psi_0(x)\equiv 0$, and the sensitivity equation (5.12).

Substituting out for the first term from our quotient calculation,

$$
\begin{aligned}
0\geq&\sum_{t=0}^{T-1}\int_\Omega p_{t+1}(x)[-\int_\Omega k(x,y)f_W\big((1-\alpha_t^*(y))N_t^*(y)\big)l_t(y)N_t^*(y)dy]dx \\
&+\sum_{t=0}^{T-1}\int_\Omega e^{-\delta t}A_t l_t(y)N_t^*(y)dy-\sum_{t=0}^{T-1}\int_\Omega e^{-\delta t}\frac{B_t}{2}V'(\alpha_t^*)l_t dy \\
&=\sum_{t=0}^{T-1}\int_\Omega [(\int_\Omega -p_{t+1}(x)f_W\big((1-\alpha_t^*(y))N_t^*(y)\big)k(x,y)dx+e^{-\delta t}A_t)N_t^*(y) \\
&-e^{-\delta t}\frac{B_t}{2}V'(\alpha_t^*)(y)]l_t(y)dy. \qquad (5.16)
\end{aligned}
$$

For any $t = 0, 1, \cdots, T-1$, on the set $\{x : 0 < \alpha_t^*(x) < M\}$, the variation l_t can be taken with support on this set, and have any sign, because the optimal control can be modified a little up or down and still stay inside the bounds. Thus on this set, the rest of the integrand must be zero, so that

$$V'(\alpha_t^*(x)) = \frac{2}{B_t}(A_t - f_W\big((1-\alpha_t^*(x))N_t^*(x)\big)\int_\Omega e^{\delta t}p_{t+1}(y)k(y,x)dy)N_t^*(x)$$

on the interior of the control set. □

Remark 5.5. *In the simplest case, if V is a quadratic function as $V(\alpha_t) = \alpha_t^2$ (the coefficient of α_t^2 could be included in B_t), then the characterization result before imposing bounds could be written as:*

$$\alpha_t^*(x) = \frac{1}{B_t}(A_t - \int_\Omega e^{\delta t}p_{t+1}(y)f_W\big((1-\alpha_t^*(x))N_t^*(x), x\big)k(y,x)dy)N_t^*(x).$$

5.2.1 Uniqueness Result

We obtain uniqueness of the optimal control under the assumption of a quadratic cost $V = \frac{B_t}{2}\alpha^2$ and largeness of the cost coefficients, B_t.

Theorem 5.6. *If B_t, $t = 0, 1, \cdots, T-1$ are sufficiently large, then the optimal control is unique.*

Proof. We show uniqueness by showing strict concavity of the map:

$$\alpha \in U \to J(\alpha)$$

The concavity follows from showing for all α, $l \in U$, and $0 < \epsilon < 1$,

$$g''(\epsilon) < 0$$

where $g(\epsilon) = J(\epsilon l + (1-\epsilon)\alpha)) = J(\alpha + \epsilon(l - \alpha))$.

For convenience we denote

$$N_t^\epsilon = N(\alpha + \epsilon(l-\alpha))$$

for $t = 0, 1, \cdots, T-1$, and similarly

$$N_t^{\epsilon+\tau} = N(\alpha + (\epsilon+\tau)(l-\alpha)),$$

for $t = 0, 1, \cdots, T-1$.

First, we calculate

$$\begin{aligned}
g'(\epsilon) &= \lim_{\tau\to 0} \frac{J(\alpha + (\epsilon+\tau)(l-\alpha)) - J(\alpha+\epsilon(l-\alpha))}{\tau} \\
&= \lim_{\tau\to 0} \sum_{t=0}^{T-1} \frac{1}{\tau} \Big(\int_\Omega e^{-\delta t} A_t(\alpha_t + (\epsilon+\tau)(l_t-\alpha_t)) N_t^{\epsilon+\tau} dy \\
&\quad - \int_\Omega e^{-\delta t} \frac{B_t}{2} (\alpha_t + (\epsilon+\tau)(l_t-\alpha_t))^2 dy \\
&\quad - \int_\Omega e^{-\delta t} [A_t(\alpha_t + \epsilon(l_t-\alpha_t)) N_t^\epsilon - \frac{B_t}{2}(\alpha_t + \epsilon(l_t-\alpha_t))^2] dy \Big) \\
&= \lim_{\tau\to 0} \sum_{t=0}^{T-1} \int_\Omega e^{-\delta t} [A_t(\alpha_t + \epsilon(l_t-\alpha_t)) \frac{N_t^{\epsilon+\tau} - N_t^\epsilon}{\tau} + A_t(l_t-\alpha_t) N_t^{\epsilon+\tau} \\
&\quad - \frac{B_t}{2}\tau(l_t-\alpha_t)^2 - B_t(\alpha_t + \epsilon(l_t-\alpha_t))(l_t-\alpha_t)] dy \\
&= \sum_{t=0}^{T-1} \int_\Omega e^{-\delta t} [A_t(\alpha_t + \epsilon(l_t-\alpha_t)) \psi_t^\epsilon + A_t(l_t-\alpha_t) N_t^\epsilon] dy \\
&\quad - \int_\Omega e^{-\delta t} B_t(\alpha_t + \epsilon(l_t-\alpha_t))(l_t-\alpha_t) dy.
\end{aligned}$$

Remark 5.3 indicates that the directional derivative of $N(\alpha+\epsilon(l-\alpha))$ along vector $l-\alpha$ with respect to $\alpha+\epsilon(l-\alpha)$ is $\psi(\alpha+\epsilon(l-\alpha), N(\alpha+\epsilon(l-\alpha)), l-\alpha)$. For convenience we use the following notation

$$\psi^\epsilon = \psi(\alpha + \epsilon(l-\alpha), N(\alpha+\epsilon(l-\alpha)), l-\alpha),$$

and similarly

$$\psi^{\epsilon+\tau} = \psi(\alpha + (\epsilon+\tau)(l-\alpha), N(\alpha + (\epsilon+\tau)(l-\alpha)), l-\alpha).$$

Later in the proof, we omit the independent variable y in order to shorten the expressions, as long as no ambiguity exists. For instance, we use α_t for $\alpha_t(y)$, l_t for $l_t(y)$, N_t for $N_t(y)$, and so on.

From Theorem 5.2 we obtain

$$\frac{N_t^{\epsilon+\tau} - N_t^{\epsilon}}{\tau} \rightharpoonup \psi_t^{\epsilon} \text{ as } \tau \to 0$$

with

$$\begin{aligned}\psi_{t+1}^{\epsilon}(x) = &\int_{\Omega} f_W\big((1-(\alpha_t + \epsilon(l_t-\alpha_t)))N_t^{\epsilon}\big)k(x,y)[(1-(\alpha_t+\epsilon(l_t-\alpha_t)))\psi_t^{\epsilon} \\ &- (l_t-\alpha_t)N_t^{\epsilon}]dy \qquad (5.17)\\ \psi_0^{\epsilon}(x) \equiv &0.\end{aligned}$$

Similarly,

$$\begin{aligned}\psi_{t+1}^{\epsilon+\tau}(x) = &\int_{\Omega} f_W\big((1-(\alpha_t + (\epsilon+\tau)(l_t-\alpha_t)))N_t^{\epsilon+\tau}\big)k(x,y) \\ &[(1-(\alpha_t+(\epsilon+\tau)(l_t-\alpha_t)))\psi_t^{\epsilon+\tau} - (l_t-\alpha_t)N_t^{\epsilon+\tau}]dy \qquad (5.18)\\ \psi_0^{\epsilon}(x) \equiv &0.\end{aligned}$$

Estimate $\psi_t^{\epsilon}(x)$ in terms of $l-\alpha$ by boundedness of f_W:

$$
\begin{aligned}
|\psi_1^\epsilon(x)| &= \left| \int_\Omega f_W\big((1-(\alpha_0+\epsilon(l_0-\alpha_0)))N_0^\epsilon\big)k(x,y)(l_0-\alpha_0)N_0^\epsilon dy \right| \\
&\le D_1 \int_\Omega |l_0-\alpha_0|\, dy, \\
|\psi_2^\epsilon(x)| &= | \int_\Omega f_W\big((1-(\alpha_1+\epsilon(l_1-\alpha_1)))N_1^\epsilon\big)k(x,y) \\
&\quad [(1-(\alpha_1+\epsilon(l_1-\alpha_1)))\psi_1^\epsilon - (l_1-\alpha_1)N_1^\epsilon]dy| \\
&\le D_2\big(\int_\Omega |l_0-\alpha_0|\, dy + \int_\Omega |l_1-\alpha_1|\, dy\big),
\end{aligned}
$$

and continuing to estimate, we obtain

$$
\left|\psi_{t+1}^\epsilon(x)\right| \le D_{t+1} \sum_{i=0}^{t} \int_\Omega |l_i-\alpha_i|\, dy,
$$

where the sequence D_{t+1} does not depend on ϵ.

Given (5.17) and (5.18), to get the second derivative of g we show the boundedness of $\dfrac{\psi_{t+1}^{\epsilon+\tau}(x)-\psi_{t+1}^\epsilon(x)}{\tau}$:

$$
\begin{aligned}
&\frac{\psi_{t+1}^{\epsilon+\tau}(x)-\psi_{t+1}^\epsilon(x)}{\tau} \\
&= \int_\Omega f_W\big((1-\alpha_t-(\epsilon+\tau)(l_t-\alpha_t)))N_t^{\epsilon+\tau}\big)k(x,y) \\
&\quad [(1-\alpha_t-(\epsilon+\tau)(l_t-\alpha_t))\psi_t^{\epsilon+\tau} - (l_t-\alpha_t)N_t^{\epsilon+\tau}]dy \\
&\quad - \int_\Omega f_W\big((1-\alpha_t-\epsilon(l_t-\alpha_t)))N_t^\epsilon\big)k(x,y) \\
&\quad [(1-\alpha_t-\epsilon(l_t-\alpha_t))\psi_t^\epsilon - (l_t-\alpha_t)N_t^\epsilon]dy \\
&= \int_\Omega k(x,y)(1-\alpha_t-\epsilon(l_t-\alpha_t))Q_1 dy \\
&\quad - \int_\Omega k(x,y) f_W\big((1-\alpha_t-(\epsilon+\tau)(l_t-\alpha_t)))N_t^{\epsilon+\tau}\big)(l_t-\alpha_t)\psi_t^{\epsilon+\tau} dy \\
&\quad - \int_\Omega k(x,y)(l_t-\alpha_t)Q_2 dy,
\end{aligned}
$$

where Q_1 stands for the quotient

$$\frac{f_W\big((1-\alpha_t-(\epsilon+\tau)(l_t-\alpha_t)))N_t^{\epsilon+\tau}\big)\psi_t^{\epsilon+\tau}-f_W\big((1-\alpha_t-\epsilon(l_t-\alpha_t)))N_t^{\epsilon}\big)\psi_t^{\epsilon}}{\tau}$$

and Q_2 stands for the quotient

$$\frac{f_W\big((1-\alpha_t-(\epsilon+\tau)(l_t-\alpha_t)))N_t^{\epsilon+\tau}\big)N_t^{\epsilon+\tau}-f_W\big((1-\alpha_t-\epsilon(l_t-\alpha_t)))N_t^{\epsilon}\big)N_t^{\epsilon}}{\tau}.$$

$$\begin{aligned}
Q_1 = & \\
& \frac{[f_W\big((1-\alpha_t-(\epsilon+\tau)(l_t-\alpha_t)))N_t^{\epsilon+\tau}\big)-f_W\big((1-\alpha_t-\epsilon(l_t-\alpha_t)))N_t^{\epsilon}\big)]\psi_t^{\epsilon+\tau}}{\tau} \\
& +\frac{f_W\big((1-\alpha_t-\epsilon(l_t-\alpha_t)))N_t^{\epsilon}\big)\psi_t^{\epsilon+\tau}-f_W\big((1-\alpha_t-\epsilon(l_t-\alpha_t)))N_t^{\epsilon}\big)\psi_t^{\epsilon}}{\tau} \\
= & \frac{f_W\big((1-\alpha_t-(\epsilon+\tau)(l_t-\alpha_t)))N_t^{\epsilon+\tau}\big)-f_W\big((1-\alpha_t-\epsilon(l_t-\alpha_t)))N_t^{\epsilon+\tau}\big)}{\tau}\psi_t^{\epsilon+\tau} \\
& +\frac{f_W\big((1-\alpha_t-\epsilon(l_t-\alpha_t)))N_t^{\epsilon+\tau}\big)-f_W\big((1-\alpha_t-\epsilon(l_t-\alpha_t)))N_t^{\epsilon}\big)}{\tau}\psi_t^{\epsilon+\tau} \\
& +f_W\big((1-\alpha_t-\epsilon(l_t-\alpha_t)))N_t^{\epsilon}\big)\frac{\psi_t^{\epsilon+\tau}-\psi_t^{\epsilon}}{\tau} \\
= & \frac{f_W\big((1-\alpha_t-(\epsilon+\tau)(l_t-\alpha_t)))N_t^{\epsilon+\tau}\big)-f_W\big((1-\alpha_t-\epsilon(l_t-\alpha_t)))N_t^{\epsilon+\tau}\big)}{-\tau(l_t-\alpha_t)} \\
& *[-(l_t-\alpha_t)\psi_t^{\epsilon+\tau}] \\
& +\frac{f_W\big((1-\alpha_t-\epsilon(l_t-\alpha_t)))N_t^{\epsilon+\tau}\big)-f_W\big((1-\alpha_t-\epsilon(l_t-\alpha_t)))N_t^{\epsilon}\big)}{(1-\alpha_t-\epsilon(l_t-\alpha_t))(N_t^{\epsilon+\tau}-N_t^{\epsilon})} \\
& *\frac{(1-\alpha_t-\epsilon(l_t-\alpha_t))(N_t^{\epsilon+\tau}-N_t^{\epsilon})}{\tau}\psi_t^{\epsilon+\tau} \\
& +f_W\big((1-\alpha_t-\epsilon(l_t-\alpha_t)))N_t^{\epsilon}\big)\frac{\psi_t^{\epsilon+\tau}-\psi_t^{\epsilon}}{\tau},
\end{aligned}$$

$$
\begin{aligned}
Q_2 = & \\
& \frac{[f_W\big((1-\alpha_t-(\epsilon+\tau)(l_t-\alpha_t))\big)N_t^{\epsilon+\tau}\big)-f_W\big((1-\alpha_t-\epsilon(l_t-\alpha_t))\big)N_t^{\epsilon}\big)]N_t^{\epsilon+\tau}}{\tau} \\
& +\frac{f_W\big((1-\alpha_t-\epsilon(l_t-\alpha_t))\big)N_t^{\epsilon}\big)N_t^{\epsilon+\tau}-f_W\big((1-\alpha_t-\epsilon(l_t-\alpha_t))\big)N_t^{\epsilon}\big)N_t^{\epsilon}}{\tau} \\
= & \frac{f_W\big((1-\alpha_t-(\epsilon+\tau)(l_t-\alpha_t))\big)N_t^{\epsilon+\tau}\big)-f_W\big((1-\alpha_t-\epsilon(l_t-\alpha_t))\big)N_t^{\epsilon+\tau}\big)}{\tau}N_t^{\epsilon+\tau} \\
& +\frac{f_W\big((1-\alpha_t-\epsilon(l_t-\alpha_t))\big)N_t^{\epsilon+\tau}\big)-f_W\big((1-\alpha_t-\epsilon(l_t-\alpha_t))\big)N_t^{\epsilon}\big)}{\tau}N_t^{\epsilon+\tau} \\
& +f_W\big((1-\alpha_t-\epsilon(l_t-\alpha_t))\big)N_t^{\epsilon}\big)\frac{N_t^{\epsilon+\tau}-N_t^{\epsilon}}{\tau} \\
= & \frac{f_W\big((1-\alpha_t-(\epsilon+\tau)(l_t-\alpha_t))\big)N_t^{\epsilon+\tau}\big)-f_W\big((1-\alpha_t-\epsilon(l_t-\alpha_t))\big)N_t^{\epsilon+\tau}\big)}{-\tau(l_t-\alpha_t)} \\
& *[-(l_t-\alpha_t)N_t^{\epsilon+\tau}] \\
& +\frac{f_W\big((1-\alpha_t-\epsilon(l_t-\alpha_t))\big)N_t^{\epsilon+\tau}\big)-f_W\big((1-\alpha_t-\epsilon(l_t-\alpha_t))\big)N_t^{\epsilon}\big)}{(1-\alpha_t-\epsilon(l_t-\alpha_t))(N_t^{\epsilon+\tau}-N_t^{\epsilon})} \\
& *\frac{(1-\alpha_t-\epsilon(l_t-\alpha_t))(N_t^{\epsilon+\tau}-N_t^{\epsilon})}{\tau}N_t^{\epsilon+\tau} \\
& +f_W\big((1-\alpha_t-\epsilon(l_t-\alpha_t))\big)N_t^{\epsilon}\big)\frac{N_t^{\epsilon+\tau}-N_t^{\epsilon}}{\tau}.
\end{aligned}
$$

We can get the boundedness of (5.19) and (5.19) from the boundedness of N_t, ψ_t, $\frac{\psi_t^{\epsilon+\tau}(x)-\psi_t^{\epsilon}(x)}{\tau}$, $\frac{N_t^{\epsilon+\tau}(x)-N_t^{\epsilon}(x)}{\tau}$ and Lipschitz continuity of $f(\cdot,y)$ in $L^2(\Omega)$.

Thus (5.19) and iteration leads to the following boundedness:

$$
|\frac{\psi_t^{\epsilon+\tau}(x)-\psi_t^{\epsilon}(x)}{\tau}| \le E_t \qquad \text{for all } x\in\Omega, t=1,2,\cdots,T,
$$

where the sequence E_{t+1} does not depend on τ or ϵ.

From the *a priori* estimate, we have the existence of $\sigma^{\epsilon}\in(L^{\infty}(\Omega))^{T+1}$ such that

$$
\frac{\psi_t^{\epsilon+\tau}(x)-\psi_t^{\epsilon}(x)}{\tau} \rightharpoonup \sigma_t^{\epsilon}(x) \qquad \text{weakly in } L^2(\Omega), \text{ as } \tau\to 0,
$$

where

$$\begin{aligned}\sigma_{t+1}^{\epsilon}(x) &= \int_{\Omega} k(x,y)(1-\alpha_t-\epsilon(l_t-\alpha_t))\Big(f_{WW}\big((1-\alpha_t-\epsilon(l_t-\alpha_t))N_t^{\epsilon}\big)\\ &\quad *\big[-N_t^{\epsilon}(l_t-\alpha_t)\psi_t^{\epsilon}+(1-\alpha_t-\epsilon(l_t-\alpha_t))\big(\psi_t^{\epsilon}\big)^2\big]\\ &\quad +f_W\big((1-\alpha_t-\epsilon(l_t-\alpha_t))N_t^{\epsilon}\big)\sigma_t^{\epsilon}\Big)dy\\ &\quad -\int_{\Omega} k(x,y)f_W\big((1-\alpha_t-\epsilon(l_t-\alpha_t))N_t^{\epsilon}\big)(l_t-\alpha_t)\psi_t^{\epsilon}dy\\ &\quad -\int_{\Omega} k(x,y)(l_t-\alpha_t)\Big(f_{WW}\big((1-\alpha_t-\epsilon(l_t-\alpha_t))N_t^{\epsilon}\big)\\ &\quad *\big[-(l_t-\alpha_t)\big(N_t^{\epsilon}\big)^2+(1-\alpha_t-\epsilon(l_t-\alpha_t))\psi_t^{\epsilon}N_t^{\epsilon}\big]\\ &\quad +f_W\big((1-\alpha_t-\epsilon(l_t-\alpha_t))N_t^{\epsilon}\big)\psi_t^{\epsilon}\Big)dy\end{aligned}$$

$$\sigma_0^{\epsilon}(x)\equiv 0$$

for $t=0,1,\cdots,T-1$.

Now we obtain

$$g''(\epsilon)=\sum_{t=0}^{T-1}\int_{\Omega} e^{-\delta t}[2A_t(l_t-\alpha_t)\psi_t^{\epsilon}+A_t(\alpha_t+\epsilon(l_t-\alpha_t))\sigma_t^{\epsilon}-B_t(l_t-\alpha_t)^2]dy.$$

We now use an iterative method to estimate σ_{t+1}^{ϵ} in terms of $(l_k-\alpha_k)^2$, $k=0,1,\cdots,T-1$:

$$\int_{\Omega}|\sigma_t^{\epsilon}|\,dy\le F_t\sum_{k=0}^{t-1}\int_{\Omega}(l_k-\alpha_k)^2dy,$$

where the sequence of constants F_{t+1} does not depend on ϵ.

First, using $\sigma_0^{\epsilon}\equiv 0$ and $\psi_0^{\epsilon}\equiv 0$, we obtain

$$\begin{aligned}|\sigma_1^{\epsilon}(x)| &= \left|\int_{\Omega} k(x,y)(l_0-\alpha_0)\big(N^{\epsilon}\big)^2 f_{WW}\big((1-\alpha_0-\epsilon(l_0-\alpha_0))N_t^{\epsilon}\big)dy\right|\\ &\le F_1\int_{\Omega}|(l_0-\alpha_0)|^2\,dy.\end{aligned}$$

Then we have

$$\begin{aligned}|\sigma_2^\epsilon(x)| =& \leq L_1\left|\int_\Omega (l_1-\alpha_1)\psi_1^\epsilon dy\right| + L_2\left|\int_\Omega \left(\psi_1^\epsilon\right)^2 dy\right| \\ &+ L_3\left|\int_\Omega \sigma_1^\epsilon dy\right| + L_4\left|\int_\Omega (l_1-\alpha_1)^2 dy\right| \\ &\leq F_2\Big(\int_\Omega |(l_1-\alpha_1)|^2\, dy + \int_\Omega |(l_0-\alpha_0)|^2\, dy\Big),\end{aligned}$$

from

$$\begin{aligned}\sigma_2^\epsilon(x) \;=\; & \int_\Omega k(x,y)(1-\alpha_1-\epsilon(l_1-\alpha_1))\Big(f_{WW}\big((1-\alpha_1-\epsilon(l_1-\alpha_1))N_1^\epsilon\big) \\ & *\big[-N_1^\epsilon(l_1-\alpha_1)\psi_1^\epsilon + (1-\alpha_1-\epsilon(l_1-\alpha_1))\big(\psi_1^\epsilon\big)^2\big] \\ & + f_W\big((1-\alpha_1-\epsilon(l_1-\alpha_1))N_1^\epsilon\big)\sigma_1^\epsilon\Big)dy \\ & - \int_\Omega k(x,y) f_W\big((1-\alpha_1-\epsilon(l_1-\alpha_1))N_1^\epsilon\big)(l_1-\alpha_1)\psi_1^\epsilon dy \\ & - \int_\Omega k(x,y)(l_1-\alpha_1)\Big(f_{WW}\big((1-\alpha_1-\epsilon(l_1-\alpha_1))N_1^\epsilon\big) \\ & *\big[-(l_1-\alpha_1)\big(N_1^\epsilon\big)^2 + (1-\alpha_1-\epsilon(l_1-\alpha_1))\psi_1^\epsilon N_1^\epsilon\big] \\ & + f_W\big((1-\alpha_1-\epsilon(l_1-\alpha_1))N_1^\epsilon\big)\psi_1^\epsilon\Big)dy.\end{aligned}$$

where L_1, L_2,L_3 and F_1 are constants that does not depend on ϵ.

Continuing the iteration, we can get the estimate for σ_t^ϵ.

Using the estimates,

$$g''(\epsilon) \leq \sum_{t=0}^{T-1}(H-B_t)\int_\Omega (l_t-\alpha_t)^2 dy,$$

which gives the desired concavity for B_t's sufficiently large. Here H is a constant that does not depend on ϵ. □

5.3 Conclusion

This chapter completes the analysis and characterization results for Case 6 of the order of events. We now have completed control results for all six cases. Whatever order a manager would choose to use in harvesting a particular species, the optimal control analysis is available for all possible orders. These techniques could also be extended to harvesting of an invasive species using an objective functional to minimize the population and the cost of harvesting controls.

Chapter 6

Investigating Optimal Vaccination Strategies in a Cholera Model

6.1 Introduction

Cholera is an intestinal infection that is caused by the bacterium *Vibrio cholerae* and can lead to death in its untreated victims within hours. The main symptoms are profuse watery diarrhea and vomiting, with severe cases leading to rapid dehydration. Cholera is primarily spread through the consumption of feces-contaminated drinking water or food, and the majority of infected individuals can be treated successfully with oral rehydration salts, with more extreme cases requiring intravenous fluids [42]. There is a huge discrepancy between the cases of cholera that are reported annually worldwide (around 200,000) and the actual number of infected people (3 - 5 million), as well as the reported (4000-6300) versus actual (more than 100,000) deaths due to cholera [42].

Cholera is a disease that affects communities with lack of sanitation and poor infrastructure, and thus long-term solutions would involve improvements in water supply, sanitation, and food safety. Current vaccines have improved efficacy and

safety and as such are being considered as valuable tools to be used along with measures that for clean drinking water and food [4].

In 2001, Codeço formulated an ODE cholera model which considered the interplay between infected humans and the concentration of cholera bacteria in the surrounding environment and the resulting disease dynamics [10]. Then Merrell and Butler reported that freshly shed cholera bacteria from human intestines are as much as 700 times more infectious than bacteria shed only hours previously [37]. For this pathway of infection, Hartley et al. [18] proposed a model with hyperinfective vibrios introduced into the water reserves by the infected people in the population; that new model explained the frequent explosive nature of the disease due to the human contribution to the environment [40].

King et al. [24] proposed a two-patch cholera ODE model including classes for 'mild' infections and waning immunity. Miller Neilan et al. [39] studied optimal control of three strategies to slow the spread of the disease in ODE model with hyperinfectious vibrios, asymptomatic infecteds and waning immunity. That work considered antibiotic treatment as one of the controls, as well as sanitation and vaccination. In the 1990s, Angola cleaned up all strains within 1 year but antibiotic resistance caused serious problems in the following year. Thus antibiotic treatment is no longer considered in this model. Furthermore, since oral rehydration is given to everyone, the variable for oral rehydration combined with antibiotic treatment is eliminated. There is another modeling approach with a compartment for pathogen level in the water; this SIWR system of four ODEs was used to simulate cholera in the 19th century in London [48, 49]. A recent review of cholera transmission by Nelson et al. suggests that questionable parameter assumptions in previous models, including a high assumption of the percentage of asymptomatic infections, can affect from model results. The work also states that future models should consider decay rates from protective immunity and seasonal variation [40].

We combine the key ideas of asymptomatic infecteds, hyperinfectious vibrios and optimal control from [10, 24, 39]. We seek to develop insight in this work

by including a new mechanism for tracking protective immunity, and a concern for how parameter assumptions influence model outcomes with an exploration for how vaccination might optimally be distributed in a population. In Section 6.2 we present a model which includes two classes of susceptible humans, with and without partial immunity, which are then infected at differing rates as symptomatic or asymptomatic in infection. The model allows for waning of protective immunity to differ in the population depending on whether an infection was with our without symptoms [24, 40]. Additionally, the model uses the assumption that hyperinfectious cholera bacteria contribute to the dynamics of a cholera outbreak [18, 37]. Our focus is to investigate the effect of model assumptions on optimal vaccination schedule, and to determine the sensitivity of potential policy advice to the hidden dynamics of cholera that may not be easily measured, especially in the affected areas that typically have poor infrastructure. Because vaccination implementation would require at least a rudimentary infrastructure, the model assumes that all individuals suffering from symptomatic cholera would be given oral rehydration therapy, and thus we assume a low death rate of infected individuals.

In particular, in Section 6.3 we investigate the sensitivity of the model to its parameters through a Latin Hypercube Sampling (LHS) analysis. In Section 6.4 we derive the basic reproductive number corresponding to the new model. In Section 6.5 we introduce the optimal control problem: we seek to simultaneously minimize the human cost of disease as well as the financial cost of vaccination. We establish the existence of a solution to the optimal control problem and we characterize the optimal solutions. We consider various numerical simulations of the optimal control problem. We analyze the effects of the choice of weights between human cost and vaccination cost on optimal control advice, and then turn our attention to populations which share similar visible infection rates, but whose underlying dynamics differ in the choice of the certain parameters. Do the disease dynamics that we cannot easily observe change the advice of the amount and duration of the optimal vaccination strategy? We also vary the parameters found to be most sensitive in our LHS analysis.

6.2 Description of Cholera Model

Susceptible humans are divided into two classes, susceptible humans S without partial immunity and susceptible humans $\hat{S}$ that have gained partial immunity either genetically or from previous infection. For susceptible humans without partial immunity, a proportion p of possible infections will become symptomatic, while for susceptible humans with partial immunity, infections are always asymptomatic. Humans recovered from asymptomatic infection and symptomatic infection are distinguished as R_A and R_S. We introduce a control ν and a vaccinated class V into which all susceptible individuals can be sent directly.

As suggested by Nelson et al. [40], our model considers the rates at which various types of protective immunity are lost. We assume that individuals in R_A who have recovered from asymptomatic infections return at rate ω_1 to the partially immune class $\hat{S}$, and that individuals recovering from fully symptomatic cholera, those in the R_S class, also wane to the partially immune class $\hat{S}$ but at a slower rate ω_2. We assume a very slow waning from the partially immune class $\hat{S}$ into the fully susceptible class S with rate ω_3. We assume as well that vaccination wanes at rate ω_4 into the fully susceptible class S. In the current model, B_L and B_H represent the concentrations of non-HI and HI vibrios in environment.

The nine ODEs of this cholera model with corresponding initial conditions are shown below, with notation and parameter descriptions given in Table 6.1.

$$
\begin{aligned}
\frac{dS}{dt} &= -\big[\beta_L \frac{B_L(t)}{\kappa_L + B_L(t)} + \beta_H \frac{B_H(t)}{\kappa_H + B_H(t)}\big] S(t) \\
&\quad + b\big(S(t) + \hat{S}(t) + I_S(t) + I_A(t) + R_S(t) + R_A(t) + V(t)\big) \\
&\quad - dS(t) + \omega_3 \hat{S}(t) + \omega_4 V(t) - \nu S(t) \\
\frac{dI_S}{dt} &= p\big[\beta_L \frac{B_L(t)}{\kappa_L + B_L(t)} + \beta_H \frac{B_H(t)}{\kappa_H + B_H(t)}\big] S(t) \\
&\quad - dI_S(t) - \gamma_2 I_S(t) - e_2 I_S(t) \\
\frac{dR_S}{dt} &= -dR_S(t) + \gamma_2 I_S(t) - \omega_2 R_S(t) \\
\frac{d\hat{S}}{dt} &= -\big[\beta_L \frac{B_L(t)}{\kappa_L + B_L(t)} + \beta_H \frac{B_H(t)}{\kappa_H + B_H(t)}\big] \hat{S}(t) - d\hat{S}(t) \\
&\quad - \omega_3 \hat{S}(t) + \omega_1 R_A(t) + w_2 R_S(t) - \nu \hat{S}(t) \\
\frac{dI_A}{dt} &= \big[\beta_L \frac{B_L(t)}{\kappa_L + B_L(t)} + \beta_H \frac{B_H(t)}{\kappa_H + B_H(t)}\big] \hat{S}(t) - dI_A(t) - e_1 I_A(t) \\
&\quad - \gamma_1 I_A(t) + (1-p)\big[\beta_L \frac{B_L(t)}{\kappa_L + B_L(t)} + \beta_H \frac{B_H(t)}{\kappa_H + B_H(t)}\big] S(t) \\
\frac{dR_A}{dt} &= -dR_A(t) + \gamma_1 I_A(t) - \omega_1 R_A(t) \\
\frac{dV}{dt} &= \nu(\hat{S}(t) + S(t)) - \omega_4 V(t) - dV(t) \\
\frac{dB_H}{dt} &= \eta_1 I_A(t) + \eta_2 I_S(t) - \chi B_H(t) \\
\frac{dB_L}{dt} &= \chi B_H(t) - \delta B_L(t)
\end{aligned}
$$

with initial conditions

$$
S(0) = S_0, \hat{S}(0) = \hat{S}_0, I_S(0) = I_{S_0}, I_A(0) = I_{A_0}, R_S(0) = R_{S_0}, R_A(0) = R_{A_0},
$$

$$
V(0) = V_0, B_L(0) = B_{L_0}, B_H(0) = B_{H_0}.
$$

Table 6.1: Notation assigned to parameters

Notation	Description
S_0	Initial number of susceptible humans
$\hat{S}_0$	Initial number of susceptible humans with partial immunity
I_{A0}	Initial number of asymptomatic infecteds
I_{S0}	Initial number of symptomatic infecteds
R_{A0}	Initial number of recovered humans (asymptomatic)
R_{S0}	Initial number of recovered humans (symptomatic)
V_0	Initial number of humans with vaccinated immunity
B_{L0}	Initial concentration of non-HI vibrios in environment
B_{H0}	Initial concentration of HI vibrios in environment
p	Probability of infected individual without partial immunity originally to be symptomatic
β_L	Ingestion rate of non-HI vibrio from environment
β_H	Ingestion rate of HI vibrio from environment
κ_L	Half saturation constant of non-HI vibrios
κ_H	Half saturation constant of HI vibrios
e_1	Cholera-related death rate for asymptomatic infecteds
e_2	Cholera-related death rate for symptomatic infecteds
γ_1	Cholera recovery rate (asymptomatic)
γ_2	Cholera recovery rate (symptomatic)
ω_1	Rate of waning cholera immunity from asymptomatic infecteds to susceptible humans with partial immunity
ω_2	Rate of waning cholera immunity from symptomatic infecteds to susceptible humans with partial immunity
ω_3	Rate of waning cholera immunity from susceptible humans without partial immunity to susceptible humans with partial immunity
ω_4	Rate of waning cholera immunity from humans with vaccinated immunity to susceptible humans without partial immunity
η_1	Rate of contribution to HI vibrios in environment by asymptomatic infecteds
η_2	Rate of contribution to HI vibrios in environment by symptomatic infecteds
χ	Transaction rate of vibrios from HI to non-HI state
δ	Death rate of vibrios
ν	Rate at which susceptible and asymptomatic infecteds are vaccinated on day
b	Natural birth rate of humans
d	Natural death rate of humans

6.3 Parameters and Latin Hypercube Sampling Analysis

In modeling cholera, we have many unknown parameters, and a limited amount of data to determine if our parameters and model structures are appropriate.

King et al. [24] point out that the effect on the epidemic dynamics from so-called "inapparent infections" may be an important factor in explaining the pattern of outbreaks. The immunity from an asymptomatic infection most likely lasts a significantly shorter period of time than does the immunity from symptomatic infection, which indicates $\omega_1 << \omega_2$. More recently, Nelson et al. [40] suggests that the very high rate of asymptomatic infecteds in [24] that work maybe significantly higher than current studies suggest. Nelson et al. report the symptomatic rate across age brackets in Bangladesh is about 57%, contrasting much lower rates for symptomatic infections in the same region in the 1970s. Indeed, the World Health Organization factsheet for cholera reports that the only 25% would be expected to show symptoms [1], while the Centers for Disease Control and Prevention states on their General Information page for cholera that only 1 in 20 people would show severe symptoms [7]. Thus, values for the parameters p, and in turn ω_1 and ω_2, the proportion of symptomatic illnesses from the S class, and the waning asymptomatic and symptomatic recoveries, respectively, are clearly in doubt. The choice for values of p is additionally complicated by our model structure which seeks to explain some proportion of asymptomatic illness through the process of gaining partial immunity through recovery from disease. The vaccination rates are based on work of Legros et al. [30]. In areas without infrastructure we might see $1-2\%$ but in areas with infrastructure, such as a refuge came, we expect up to 4% daily. We choose ranges for the death rates from symptomatic and asymptomatic illnesses based on potential case fatality rates and an assumption that while we would expect no deaths to result directly from an asymptomatic infection, we do suspect cholera could be a confounding element in seemingly-unrelated deaths. From the year 2007 to 2008,

globally, the majority of countries reported an overall $CFR > 1\%$; the CFR was $< 1\%$ in 9 countries, it ranged from 1% to 4.9% in 22 countries and in 5 countries it was between 5.5% and 14.3% [12]. Here we use a CFR of 4%. A recent cost analysis by Jeuland [20] assumes the length of illness is 2 - 8 days, combining with the work of Nelson et al. [40], we assume $\gamma_1 = 0.5$ and $\gamma_2 = 0.2$. e_2, the cholera-related death rate for symptomatic infecteds is calculated from:

$$e_1 = ln(1 - CFR) * \gamma_1, \;\; e_2 = ln(1 - CFR) * \gamma_2.$$

We choose the waning rate for vaccination and partial immunity to be $\omega_3 = \omega_4 = 1/(10 * 365)$, deduced from a mathematical model by [25], suggesting a 10-year-long period before the immunities completely wane out. We also assume $\omega_1 = 0.01$, $\omega_2 = 0.0022$, according to the work by King et al. [24].

We use estimates consistent with Hartley et al.[18] and Codeço [11]. The half satuartion constant for non-HI vibrios κ_L is estimated to be 10^3 cells/ml. According to laboratory experiments, when inoculated into the intestines of mice, freshly shed Vibrio cholerae greatly outcompete bacteria grown in vitro, by as mush as 700-fold. So for HI vibrios estimations, we assume the ratio of saturation constants for non-HI vibrios and HI vibrios is $1 : 700$. i.e., $\kappa_H = 10^3/700$ cells/ml. Freshly shred Vibrio cholerae stay at a hyper-infectious state for approximately 5 days, and then reduce to non-hyper-infectious vibrios. Average lifespan of the non-HI vibrios is around 30 days. Thus we set $\chi = 1/5 = 0.2$, and $\delta = 1/30$.

There are several other parameter values whose values cannot be expected to be known independent of the intuition gained from model simulation. One is the contact rate β_L of humans with less-infectious bacteria, and the proportion r of that rate which we expect to describe contact with hyper-infectious bacteria. Prior attempts at describing contact rate have depended on quantifying the amount of water consumed by an individual in a day, and assuming that the only contact with cholera bacteria is through ingestion of drinking water [18], but it is well understood that contact with

cholera bacteria can actually occur through contact with contaminated household items [40]. While we think loosely of the environmental reservoir of bacteria as inhabiting a literal reservoir of water, the true picture is actually more complicated and difficult to quantify. In addition, it is also difficult to quantify the contribution of humans to cholera contamination in the environment. We can quantify the shedding rate of symptomatic and asymptomatic humans, but how much of the shedding actually makes it into the environmental reservoir, and what is the volume of that reservoir remain in question. In fact, we can only quantify the the difference in shedding between the humans [40]. But numerical results in Section 6.6.2 illustrate that for parameter sets with different β, η, and S_0 values, even though the population dynamics underneath might be different, as long as the Infection Rate remains on the same level, the optimal control strategies will be almost identical to each other.

We analyze parameter sensitivity by using the Latin Hypercube Sampling (LHS) scheme (Marino et al 2008; Blower and Dowlatabadi, 1994). This scheme estimates the uncertainty of a parameters by treating each parameter as a random variable and defining a probability density function for it using a biologically realistic range (see Table 6.2). The n sampled values for each parameter are then randomly chosen and the model is simulated. We run our simulations for 180 days and calculate three outcome measures for each run: Total Infecteds, Total Symptomatic Infecteds, and Maximum Number of Symptomatic Infecteds, respectively. Here "total infecteds" refers to the accumulated total of all individuals who have entered either of the two infected classes, and "total symptomatic infecteds" refers to the accumulated total of all individuals who have entered the symptomatic infected class. For each parameter, we confirm that the outcome measures are monotone. Subsequently, we compute Partial Rank Correlation Coefficients (PRCC) and accompanying p-values to determine the level of sensitivity of each sampled parameter. If, for a given outcome measure, a parameter has a PRCC value ranging from 0.5 to 1.0 or from -1.0 to -0.5, along with a corresponding low p-value, then the parameter is considered sensitive and, thus, deemed to affect that outcome measures significantly were slight changes to

be made to that parameter during the simulation. Sensitive parameters are selected for further study in optimal control analysis.

Our simulations show that the outcome measures are sensitive to changes in parameters p, γ_2, S_0 and β_L. We find that p, the proportion of the infected population who are asymptomatic; and S_0, the susceptible population without partial immunity; is significant in determining the total number of symptomatic infected people, as well as the maximum population size for the symptomatic infecteds. Note γ_2, the recovery rate from symptomatic infection, is significant for maximum number of symptomatic infecteds. Unlike p, S_0 and γ_2, however, β_L, which measures ingestion rate of non-highly infectious vibrio from environment, is significant for all three outcome measures.

Table 6.2: Sensitivity analysis of the initial model without controls

LHS sensitivity analysis: initial model without control (n = 400, time = 180 days)					
Parameters	Ranges		PRCC		
	Min	Max	Total infecteds	Total symptomatic infecteds	Max symptomatic infecteds
ω_1	0.0098	0.027	0.211	0.015	−0.009
ω_2	0.0012	0.0034	−0.021	0.016	0.041
ω_3	0.00001	0.01	0.109	0.329	0.094
p	0.05	0.15	0.214	0.613*	0.519*
r	0.01	1	0.554*	0.380	0.471
β_L	0.001	0.08	0.881*	0.757*	0.808*
e_1	0.00003	0.0005	0.025	−0.009	0.002
e_2	0.0006	0.01	0.005	−0.018	−0.071
γ_1	0.1	0.9	−0.122	−0.034	−0.004
γ_2	0.01	0.50	−0.523*	−0.348	−0.762*
η_1	0.001	0.015	0.559*	0.343	0.247
s	1	200	0.533*	0.331	0.233
B_{L0}	$\kappa_L/500$	κ_L	0.279	0.190	0.301
S_0	1000	10000	−0.362	−0.767*	−0.797*

$*$ Denotes a parameters having a p-value below 0.001.

6.4 Calculate the Basic Reproduction Number, $\mathcal{R}_0$

The next generation method, set forth by van den Driessche and Watmough [50], is used to calculate the basic reproduction number, $\mathcal{R}_0$, which helps determine whether or not this infectious disease will spread through a population. Consider the system consisting of all disease-free states to be ordered such that $x = (I_A, I_S, B_H, B_L, R_A, R_S, S, \hat{S})$, and let N denote the total human population before the disease attacks. The disease-free equilibrium is $x_0 = (0, 0, 0, 0, 0, 0, S_0, \hat{S}_0)$. New infections only occur in the first and second compartments. For $1 \leq i \leq 8$, let $\mathbb{F}_i(x)$ be the rate of new infections in the ith compartment, $V_i^+(x)$ be the rate of transfer of population, either humans or vibrios, into compartment i by all other means, and $V_i^-(x)$ be the rate of transfer of population, either humans or vibrios, out compartment i. Then $\mathbb{V}_i(x)$ is defined as the difference $V_i^+(x) - V_i^-(x)$. Our system is $X_i' = \mathbb{F}_i - \mathbb{V}_i$, where $i = 1, 2, \cdots, 8$. The reproduction number $\mathcal{R}_\prime$ is the spectral radius of the next generation matrix, FV^{-1}, where F and V are the components of the Jacobian matrix corresponding to $\mathbb{F}$ and $\mathbb{V}$ for infected components.

We calculate F and V^{-1} below,

$$F = \begin{vmatrix} 0 & 0 & \dfrac{\beta_H(S_0(1-p)+\hat{S}_0)}{\kappa_H} & \dfrac{\beta_L(S_0(1-p)+\hat{S}_0)}{\kappa_L} \\ 0 & 0 & \dfrac{\beta_H S_0 p}{\kappa_H} & \dfrac{\beta_L S_0 p}{\kappa_L} \\ 0 & 0 & 0 & 0 \\ 0 & 0 & 0 & 0 \end{vmatrix},$$

$$V^{-1} = \begin{vmatrix} \dfrac{1}{d+e_1+\gamma_1} & 0 & 0 & 0 \\ 0 & \dfrac{1}{d+e_2+\gamma_2} & 0 & 0 \\ \dfrac{\eta_1}{(d+e_1+\gamma_1)\chi} & \dfrac{\eta_2}{(d+e_2+\gamma_2)\chi} & \dfrac{1}{\chi} & 0 \\ \dfrac{\eta_1}{(d+e_1+\gamma_1)\delta} & \dfrac{\eta_2}{(d+e_2+\gamma_2)\delta} & 1 & \dfrac{1}{\delta} \end{vmatrix}.$$

Thus the basic reproduction number is given by

$$\mathcal{R}_0 = \left(\frac{\eta_1 \big(S_0(1-p) + S_1\big)}{d + e_1 + \gamma_1} + \frac{\eta_2 S_0 p}{d + e_2 + \gamma_2} \right) \left(\frac{\beta_L}{\delta \kappa_L} + \frac{\beta_H}{\chi \kappa_H} \right).$$

When $\mathcal{R}_0 < 1$, the disease free equilibrium is locally stable. But if $\mathcal{R}_0 > 1$, the infection will be able to spread in a population.

6.5 Optimal Control Formulation and Analysis

We seek an optimal vaccination strategy to minimize both the social loss due to disease and the cost of vaccination during the time interval. In our model, the social loss is assumed to be proportional to the number of symptomatic infecteds. The cost consists of a linear term, measuring the total price of vaccination used, and a quadratic term, indicating non-linear costs potentially arising at high intervention levels.

Thus our objective functional is the following,

$$J(\nu) = \int_0^T \big\{ AI_S(t) + B\nu(t)\big(S(t) + \hat{S}(t) + I_A(t) + R_A(t)\big) + C(S_0 + \hat{S}_0)\nu^2(t) \big\} dt, \quad (6.1)$$

where A, B, and C are positive balancing coefficients which transform the integrand into units of dollars. In the third term, we multiply C by the initial total population to balance the size of the three terms.

The vaccination rate ν is positive and not more than 1. Thus the control set is $U = \big\{ \nu \in L^\infty([0,T]) | 0 \leq \nu(t) \leq \nu_{max}, t \in [0,T] \big\}$ for $\nu_{max} < 1$. The optimal control problem is stated as:

Find $\nu^* \in U$ such that

$$J(\nu^*) = \min_{\nu \in U} J(\nu) \quad (6.2)$$

subject to the state system (6.1)-(6.1) and initial conditions (6.2).

Figure 6.1 shows transmissions of cholera disease between seven human population classes, effected by concentrations of two vibrio population classes in the environment, while vaccination is enforced.

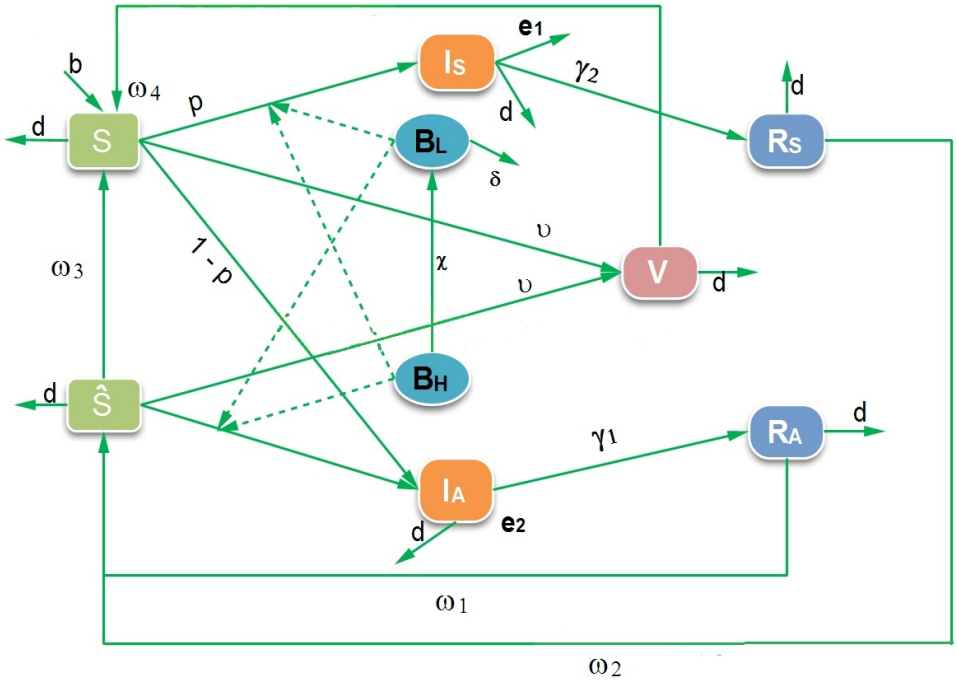

Figure 6.1: Diagram for the Cholera model with vaccination as control.

Using a result in Lukes [35], one can show that given a control, there exists a unique solution to the state system. The structure of the system gives boundedness and non-negativity of those solutions.

Theorem 6.1. *There exist an optimal control* ν^* *with corresponding states* $(S^*, \hat{S}^*, I_A^*, I_S^*, R_A^*, R_S^*, V^*, B_H^*, B_L^*)$ *that minimizes the objective functional* $J(\nu)$ *defined by* (6.1).

Proof. Since the controls and the state solutions are non-negative, the objective functional is bounded below by 0 and there exists a corresponding minimizing sequence ν_n such that

$$\lim_{n\to\infty} J(\nu_n) = inf_{\nu\in U} J(\nu).$$

Given that the controls are uniformly bounded, the state solution sequence corresponding to the sequence of minimizing controls are uniformly bounded.

That gives uniform bounds on the derivatives of those state solution sequence, resulting in uniform boundedness and equicontinuity of the corresponding state solution sequence. On a sequence, the control sequence x converges weakly in $L^2(0,T)$ and the state solution sequence converges uniformly. Passing to the appropriate limit in the system of differential equations and the objective functional, we can deduce that the limit of the those sequences are an optimal control and its corresponding state solutions. □

The Pontryagin's Maximum principle [43] is used to characterize the optimal control. The Hamiltonian is formed as the following,

$$
\begin{aligned}
H = \\
& AI_S(t) + B\nu(t)\big(S(t) + \hat{S}(t) + I_A(t) + R_A(t)\big) + C(S_0 + \hat{S}_0)\nu^2(t) \\
& +\lambda_S\Bigg(- \Big(\big[\beta_L \frac{B_L(t)}{\kappa_L + B_L(t)} + \beta_H \frac{B_H(t)}{\kappa_H + B_H(t)}\big] - b + d + \nu\Big)S(t) \\
& +b\big(\hat{S}(t) + I_S(t) + I_A(t) + R_S(t) + R_A(t) + V(t)\big) + \omega_3\hat{S}(t) + \omega_4 V(t)\Bigg) \\
& +\lambda_{\hat{S}}\Bigg(- \Big(\big[\beta_L \frac{B_L(t)}{\kappa_L + B_L(t)} + \beta_H \frac{B_H(t)}{\kappa_H + B_H(t)}\big] + d + \omega_3 + \nu\Big)\hat{S}(t) \\
& +\omega_1 R_A(t) + w_2 R_S(t)\Bigg) \\
& +\lambda_{I_S}\Bigg(p\big[\beta_L \frac{B_L(t)}{\kappa_L + B_L(t)} + \beta_H \frac{B_H(t)}{\kappa_H + B_H(t)}\big]S(t) - (d + \gamma_2 + e_2)I_S(t)\Bigg) \\
& +\lambda_{I_A}\Bigg(\big[\beta_L \frac{B_L(t)}{\kappa_L + B_L(t)} + \beta_H \frac{B_H(t)}{\kappa_H + B_H(t)}\big]\hat{S}(t) - (d + e_1 + \gamma_1)I_A(t) \\
& +(1-p)\big[\beta_L \frac{B_L(t)}{\kappa_L + B_L(t)} + \beta_H \frac{B_H(t)}{\kappa_H + B_H(t)}\big]S(t)\Bigg) \\
& +\lambda_{R_S}\big(- (d + \omega_2)R_S(t) + \gamma_2 I_S(t)\big) \\
& +\lambda_{R_A}\big(- (d + \omega_1)R_A(t) + \gamma_1 I_A(t)\big) \\
& +\lambda_V\big(\nu(\hat{S}(t) + S(t)) - (\omega_4 + d)V(t)\big) \\
& +\lambda_{B_H}\big(\eta_1 I_A(t) + \eta_2 I_S(t) - \chi B_H(t)\big) \\
& +\lambda_{B_L}\big(\chi B_H(t) - \delta B_L(t)\big),
\end{aligned}
$$

where the λ's are the adjoint variables associated with their respective states. For example, λ_S is the adjoint variable corresponding to state S. Since an optimal control exists by Theorem 6.1, we can now obtain the necessary condition for optimality using Pontryagin's Maximum Principle [43].

Theorem 6.2. , *Given an optimal control* $\nu^* \in U$, *and corresponding states* $(S, \hat{S}, I_A, I_S, R_A, R_S, V, B_H, B_L)$, *there exist adjoint functions satisfying*

$$\begin{aligned}
\frac{d\lambda_S}{dt} &= -B\nu + \big[\beta_L \frac{B_L(t)}{\kappa_L + B_L(t)} + \beta_H \frac{B_H(t)}{\kappa_H + B_H(t)}\big](\lambda_S - p\lambda_{I_S} - (1-p)\lambda_{I_A}) \\
&\quad +(d - b + \nu)\lambda_S - \lambda_V \nu, \qquad (6.3)\\
\frac{d\lambda_{\hat{S}}}{dt} &= -B\nu + \big[\beta_L \frac{B_L(t)}{\kappa_L + B_L(t)} + \beta_H \frac{B_H(t)}{\kappa_H + B_H(t)}\big](\lambda_{\hat{S}} - \lambda_{I_A}) \\
&\quad +(d + \omega_3 + \nu)\lambda_{\hat{S}} - (\omega_3 + b)\lambda_S - \lambda_V \nu, \qquad (6.4)\\
\frac{d\lambda_{I_S}}{dt} &= -A + (d + \gamma_2 + e_2)\lambda_{I_S} - b\lambda_S - \gamma_2\lambda_{R_S} - \eta_2\lambda_{B_H}, \qquad (6.5)\\
\frac{d\lambda_{I_A}}{dt} &= -B\nu + (d + \gamma_1 + e_1)\lambda_{I_A} - b\lambda_S - \gamma_1\lambda_{R_A} - \eta_1\lambda_{B_H}, \qquad (6.6)\\
\frac{d\lambda_{R_S}}{dt} &= -\omega_2\lambda_{\hat{S}} - b\lambda_S + (d + \omega_2)\lambda_{R_S}, \qquad (6.7)\\
\frac{d\lambda_{R_A}}{dt} &= -B\nu - \omega_1\lambda_{\hat{S}} - b\lambda_S + (d + \omega_1)\lambda_{R_A}, \qquad (6.8)\\
\frac{d\lambda_V}{dt} &= -\omega_4\lambda_S - b\lambda_S + (d + \omega_4)\lambda_V, \qquad (6.9)\\
\frac{d\lambda_{B_H}}{dt} &= \beta_H \frac{\kappa_H(t)}{(\kappa_H + B_H)^2}\big(S(\lambda_S - p\lambda_{I_S} - (1-p)\lambda_{I_A}) + \hat{S}(\lambda_{\hat{S}} - \lambda I_A)\big) \\
&\quad +\chi\lambda_{B_H} - \chi\lambda_{B_L}, \qquad (6.10)\\
\frac{d\lambda_{B_L}}{dt} &= \beta_L \frac{\kappa_L(t)}{(\kappa_L + B_L)^2}\big(S(\lambda_S - p\lambda_{I_S} - (1-p)\lambda_{I_A}) + \hat{S}(\lambda_{\hat{S}} - \lambda I_A)\big) \\
&\quad +\delta\lambda_{B_L}, \qquad (6.11)
\end{aligned}$$

with transversality conditions

$$\lambda_S = \lambda_{\hat{S}} = \lambda_{I_A} = \lambda_{I_S} = \lambda_{R_A} = \lambda_{R_S} = \lambda_V = 0$$

at $t = T$. *And this optimal control is characterized by*

$$\nu^* = max\bigg(0, min\bigg(\frac{-B(S + \hat{S} + I_A + R_A) + S\lambda_S + \hat{S}\lambda_{\hat{S}} - (S + \hat{S})\lambda_V}{2C(S_0 + \hat{S}_0)}, \nu_{max}\bigg)\bigg).$$

Proof. The differential equations for the adjoints are standard results from Pontryagin's Maximum Principle [43]. The right hand sides of the differential equations can

be easily computed by

$$\begin{aligned}
\frac{d\lambda_S}{dt} &= -\frac{\partial H}{\partial S}, \\
\frac{d\lambda_{\hat{S}}}{dt} &= -\frac{\partial H}{\partial \hat{S}}, \\
\frac{d\lambda_{I_S}}{dt} &= -\frac{\partial H}{\partial I_S}, \\
\frac{d\lambda_{I_A}}{dt} &= -\frac{\partial H}{\partial I_A}, \\
\frac{d\lambda_{R_S}}{dt} &= -\frac{\partial H}{\partial R_S}, \\
\frac{d\lambda_{R_A}}{dt} &= -\frac{\partial H}{\partial R_A}, \\
\frac{d\lambda_V}{dt} &= -\frac{\partial H}{\partial V}, \\
\frac{d\lambda_{B_H}}{dt} &= -\frac{\partial H}{\partial B_H}, \\
\frac{d\lambda_{B_L}}{dt} &= -\frac{\partial H}{\partial B_L}.
\end{aligned}$$

The final time conditions are due to the transversality conditions. Because there is no salvage term in the objective functional, the final time conditions are zero.

The necessary condition for an optimal control ν^* on the set $\{t|0 < \nu^*(t) < \nu_{max}\}$ is

$$0 = \frac{\partial H}{\partial \nu} = B(S + \hat{S} + I_A + R_A) + 2C(S_0 + \hat{S}_0)\nu^* - \lambda_{\hat{S}} S - \lambda_S S + \lambda_V (S + \hat{S}). \quad (6.12)$$

Thus we have

$$\nu^* = \frac{-B(S + \hat{S} + I_A + R_A) + S\lambda_S + \hat{S}\lambda_{\hat{S}} - (S + \hat{S})\lambda_V}{2C(S_0 + \hat{S}_0)}.$$

The necessary condition for an optimal control ν^* on the set $\{t|\nu^*(t) = 0\}$ is

$$0 \leq \frac{\partial H}{\partial \nu} = B(S + \hat{S} + I_A + R_A) + 2C(S_0 + \hat{S}_0)\nu^* - \lambda_{\hat{S}} S - \lambda_S S + \lambda_V (S + \hat{S}). \quad (6.13)$$

Since $2C > 0$ and $S_0 + \hat{S}_0 > 0$, we have

$$\frac{-B(S + \hat{S} + I_A + R_A) + S\lambda_S + \hat{S}\lambda_{\hat{S}} - (S + \hat{S})\lambda_V}{2C(S_0 + \hat{S}_0)} \leq 0.$$

The necessary condition for an optimal control ν^* on the set $\{t|\nu^*(t) = \nu_{max}\}$ is

$$0 \geq \frac{\partial H}{\partial \nu} = B(S + \hat{S} + I_A + R_A) + 2C(S_0 + \hat{S}_0)\nu^*_{max} - \lambda_{\hat{S}}S - \lambda_S S + \lambda_V(S + \hat{S}). \quad (6.14)$$

Since $2C > 0$ and $S_0 + \hat{S}_0 > 0$, we have

$$\frac{-B(S + \hat{S} + I_A + R_A) + S\lambda_S + \hat{S}\lambda_{\hat{S}} - (S + \hat{S})\lambda_V}{2C(S_0 + \hat{S}_0)} \geq \nu_{max}.$$

In conclusion of the above three cases, the optimal control is

$$\nu^* = max\left(0, min\left(\frac{-B(S + \hat{S} + I_A + R_A) + S\lambda_S + \hat{S}\lambda_{\hat{S}} - (S + \hat{S})\lambda_V}{2C(S_0 + \hat{S}_0)}, \nu_{max}\right)\right).$$

□

Note the uniqueness result for the optimal control for small time T can be obtained as in [39] using boundedness of solution of the state and adjoint systems and the continuity in the structure of the differential equations.

6.6 Simulation of an Outbreak

We start with the set of parameters shown in Table 6.3 to simulate an outbreak. Here we assume a scenario of a refugee camp with an initial population of $10,000$, 1000 out of which have partial immunity. A non-hyperinfectious vibrios population of $\kappa_L/100$ is introduced into the environment. Figure 6.2 shows the simulation of an outbreak during a 100 day time period. The basic reproduction number R_0 is calculated as 6.096, and the disease will spread in this population.

Table 6.3: Base parameters for simulations

β_H	.002 day^{-1}	β_L	.02 day^{-1}	κ_L	10^3 cells/ml
κ_H	$\kappa_L/700$	b	0.03149/365 day^{-1}	d	0.01619/365 day^{-1}
p	.1	ω_1	0.01 day^{-1}	ω_2	0.0022 day^{-1}
ω_3	1/(10*365) day^{-1}	ω_4	1/(10*365) day^{-1}	r_1	.5 day^{-1}
r_2	.2 day^{-1}	e_1	.000205 day^{-1}	e_2	.0041 day^{-1}
η_1	$.008\frac{cells}{ml-day-human}$	η_2	$0.8\frac{cells}{ml-day-human}$	χ	5 day^{-1}
δ	1/30 day^{-1}	S_0	9000	$\hat{S}_0$	1000
I_{A_0}	0	I_{S_0}	0	R_{A_0}	0
R_{S_0}	0	V_0	0	B_{L_0}	$\kappa_L/100$
B_{H_0}	0	T	100 day		

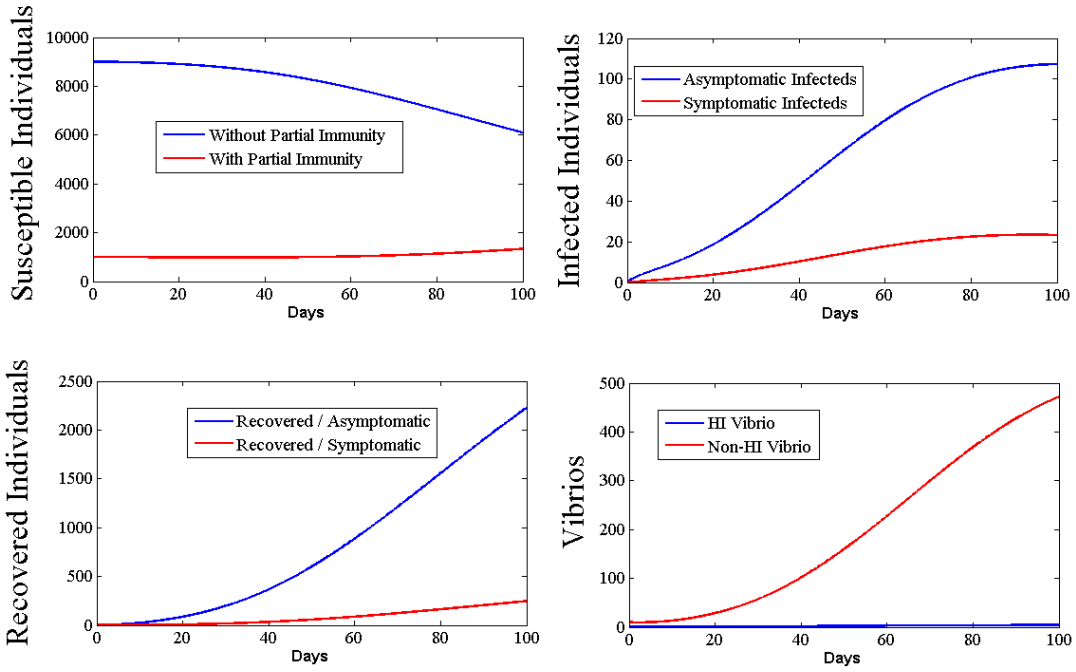

Figure 6.2: Outbreak Simulation

6.6.1 Effect of Weights on Optimal Control

Now we add vaccination as a control and find the optimal vaccination rate. The maximum vaccination rate is set as 0.04. We choose three sets of the weights in the objective functional from Table 6.4, to show the effects of varying weights on optimal control result. Compared to Set 1, Set 2 has a bigger C value, indicating a larger quadratic cost and Set 3 has a smaller B value, indicating a smaller linear vaccination cost.

Table 6.4: Three sets of weights.

	A	B	C
Set 1	1	0.04	1
Set 2	1	0.04	2
Set 3	1	0.25	1

Figure 6.3, 6.4 and 6.5 show the best vaccination plans and populations in different classes under control, using the three sets of weights in Table 6.4. We observe declining vaccination rates in all three cases, and no vaccination is suggested during later period of time. Figure 6.3 shows a vaccination rate around 0.035 at the beginning of the time and vaccines are applied during the first 60 days. Both infected populations are significantly reduced by control, and the number of symptomatic infected individuals stays at level lower than 5. Figure 6.4 shows that with a bigger quadratic cost in Set 2, the optimal vaccination rate is reduced correspondingly. The initial vaccination rate drops to 0.025 yet the vaccination period is still around 60 days. Symptomatic infecteds are control at the same level while number of asymptomatic infecteds is larger compared to the first case. Figure 6.5 suggests a lower initial vaccination rate of 0.025 and a much shorter vaccination period around 15 days, effected by a larger vaccination linear cost in Set 3. Because less vaccination is applied, symptomatic infecteds can reach as many as 20 and asymptomatic infecteds reaches 80.

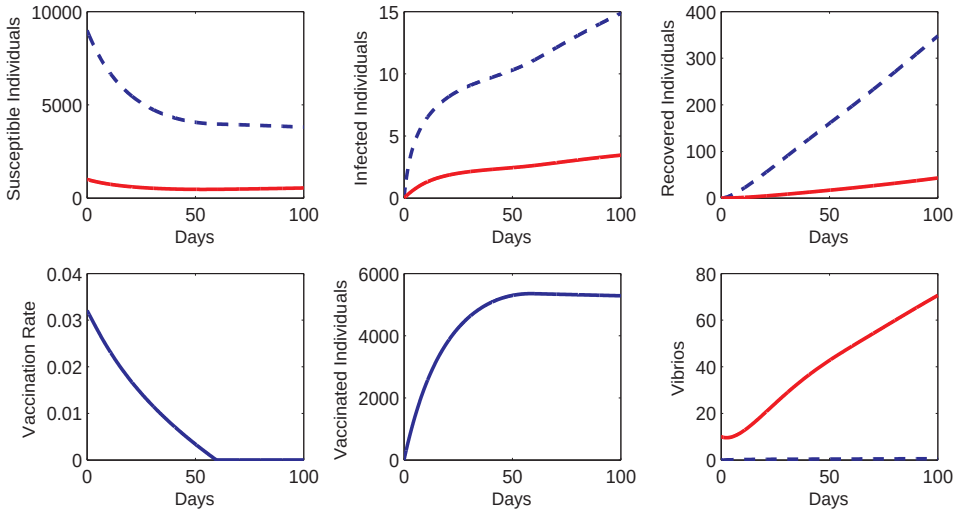

Figure 6.3: Set 1: $A = 1, B = 0.04, C = 1$

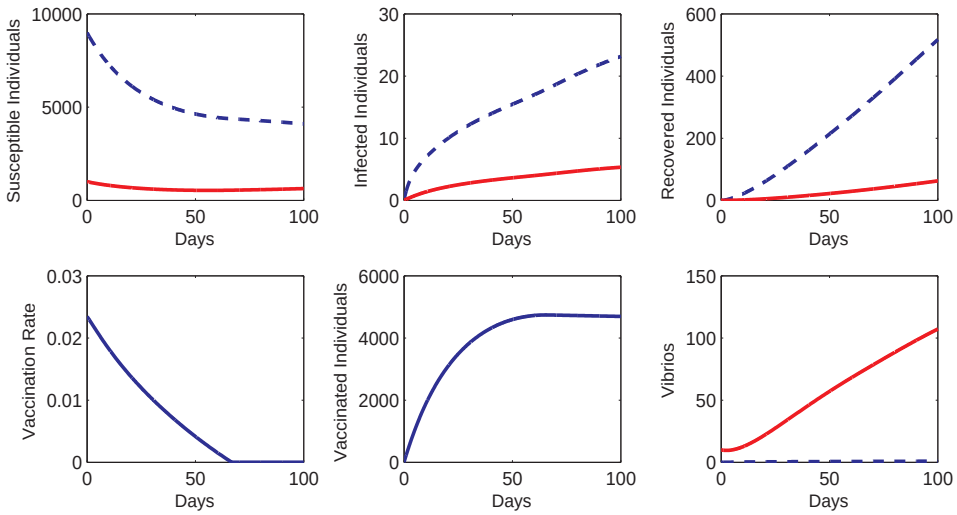

Figure 6.4: Set 2: $A = 1, B = 0.04, C = 2$

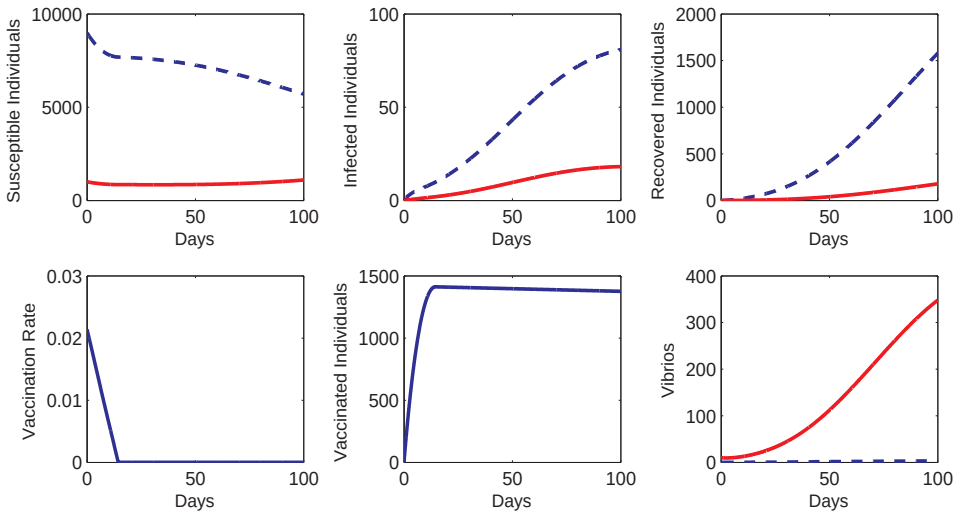

Figure 6.5: Set 3: $A = 1, B = 0.25, C = 1$

6.6.2 Effect of Infection Rate on Optimal Control

We define the infection rate as the ratio of total number of symptomatic infecteds to total number of population. During the time period we study, the total population will not have significant change, thus we use

$$\frac{\textbf{total number of sympotomatic infecteds}}{\textbf{total number of initial population}}$$

as infection rate to measure the intensity of the outbreak. The total number of symptomatic infecteds is calculated by counting the flux into that class at each time step.

It is possible to simulate outbreaks with approximately same infection rates using different sets of parameters. For instance, by the four set of parameters in Table 6.5 we obtain infection rates around 0.26.

Figure 6.6, 6.7, 6.8, and 6.9 show the populations of both humans and vibrios as vaccination is applied, as well as optimal vaccination rates. For each simulation we use the same set of weights, $A = 1, B = 0.04, C = 1$. Maximum vaccination rate is set as 4%. We observe that those parameter sets give similar vaccination advices,

Table 6.5: Four sets of parameters giving similar infection rates.

Parameters	Case 1	Case 2	Case 3	Case 4
S_0	9000	5000	7000	6000
$\hat{S}_0$	1000	5000	3000	4000
β_L	0.02	0.04	0.02	0.03
η_1	0.008	0.007	0.01	0.008
Total Attacked	298	270	231	276
Infection Rate	0.298	0.269	0.230	0.275

with a starting rate around 3.5% and a time duration of around 60 days. In fact, we tried more sets of parameters and those numerical results also suggest the infection rate plays a key rule in making optimal vaccination plans.

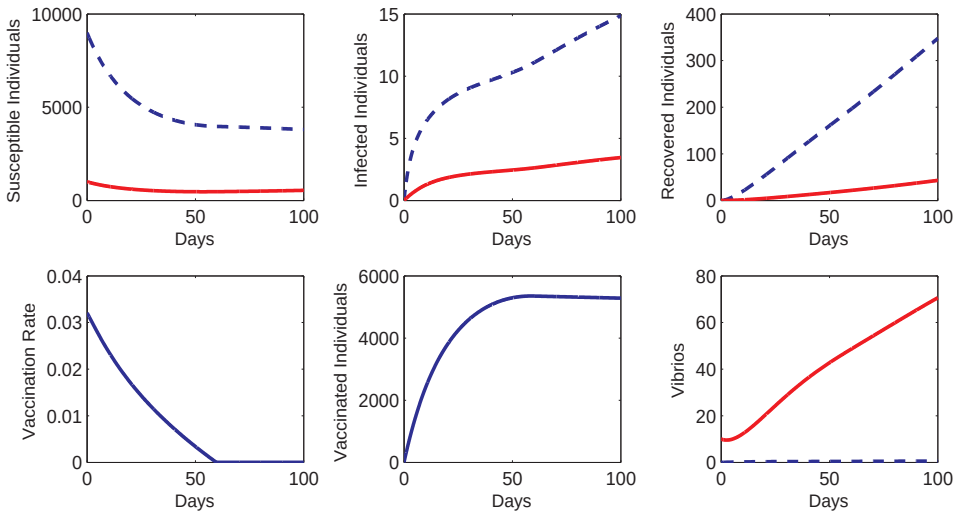

Figure 6.6: Case 1

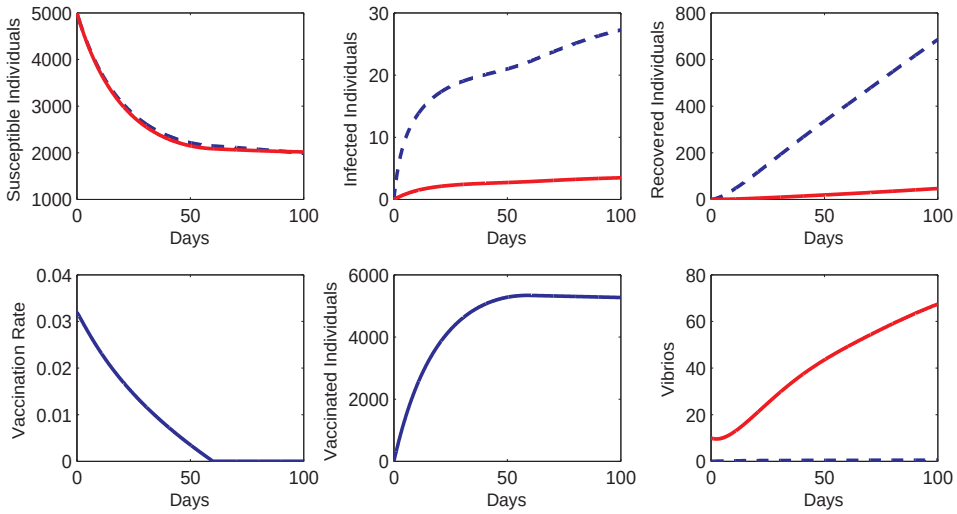

Figure 6.7: Case 2

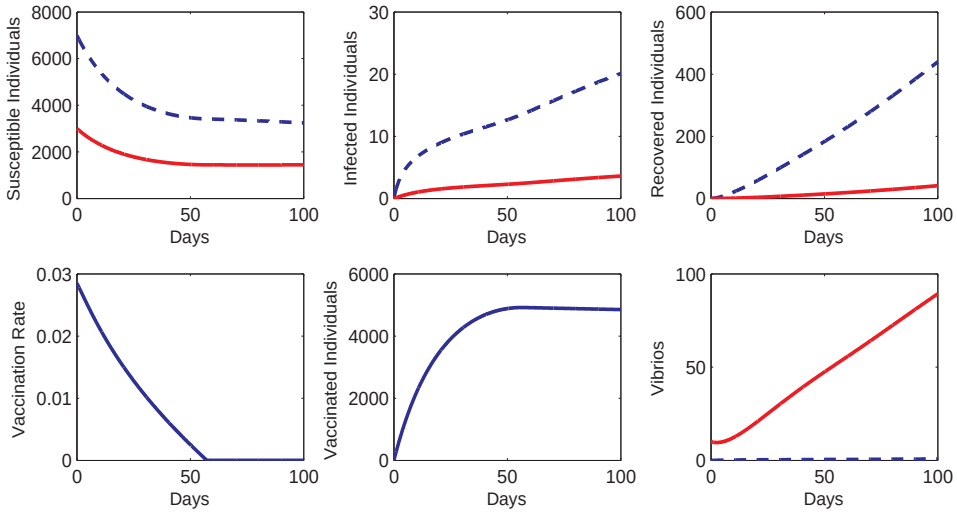

Figure 6.8: Case 3

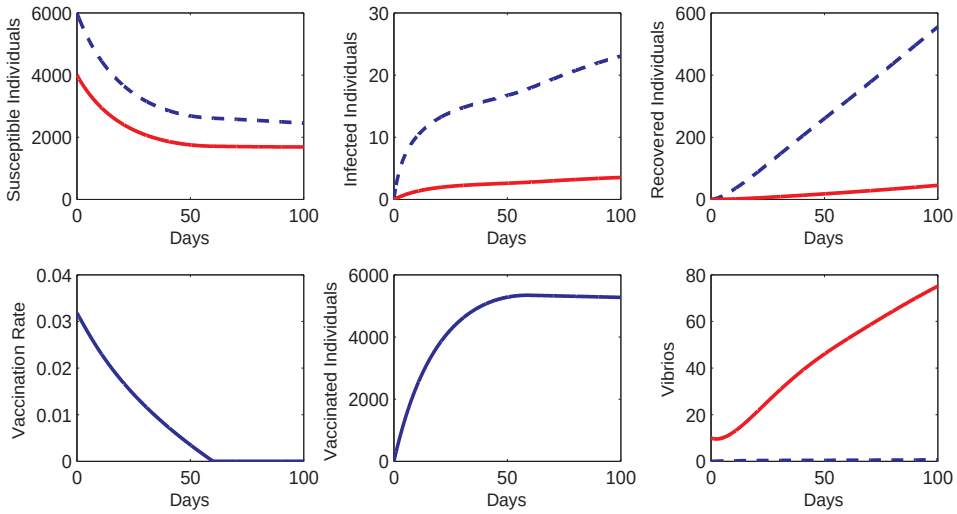

Figure 6.9: Case 4

6.6.3 Effect of LHS-sensitive Parameters on Optimal Control

We now study the effect of LHS-sensitive parameters on optimal control.

We use a set of weights as in Set 1 of Table 6.4. Based on the parameter table, Table 6.5, we study the effect of LHS-sensitive parameters β_L, p, γ_2 and S_0, as suggested in Section 6.3.

We vary one of the three parameters each time while keeping others the same values as shown in Table 6.5. The remaining parameters are from Table 6.3.

Figures 6.10, 6.11, 6.13 and 6.12 show the effect of changing the sensitive parameters for Case 1 in Table 6.6. In Figure 6.10, β_L is increased from 0.02 to 0.04, which brings in a higher infection rate, causing the vaccination rate reaches the upper bound 0.04 for about 10 days, and the duration of vaccination is extended to around 70 days. Figure 6.11 shows a strong effect caused by raising p from 0.1 to 0.8. The maximum population of symptomatic infecteds are 30 times larger, and the effort of vaccination almost lasts through the whole 100 days time period, with the vaccination largest rate for more than half of the time. At the end of the time approximately 8000 people are vaccinated, together with almost 1200 people in the recovered classes, nearly everyone is immune to the disease. Figure 6.13 shows a much smaller infected population with much less effort in vaccination, not more than 2.5% in the beginning and lasting only for 50 days, when more people, from 1000 to 3000, are with partial immunities. Figure 6.12 also shows a much smaller infected population with much less effort in vaccination, not more than 0.1% in the beginning and lasting not more than for 30 days, when the recovery rate from symptomatic infection, γ_2, is increased from 0.2 to 0.4.

Figures 6.14, 6.15, 6.16, and 6.15 for Case 2, Figures 6.17, 6.18, 6.19, and 6.18 for Case 3, Figures 6.20, 6.21, 6.22 and 6.21 for Case 4 in Table 6.5, show the outcomes by changing β_L into 0.04, p into 0.8, S_0 into 7000 and γ_2 into 0.4. In those figures, We observe similar effects of the sensitive parameters on populations of different classes and the optimal vaccination strategies.

Remark 6.3. *In the numerical results, the dashed lines are susceptibles without partial immunity, asymptomatic infecteds, recovered individuals from asymptomatic infections, and hyperinfectious vibrio populations. The solid lines are susceptibles with partial immunity, symptomatic infecteds, recovered individuals from symptomatic infections, and non-hyperinfectious vibrio populations.*

Remark 6.4. *In the numerical results, populations of hyperinfectious vibrios are low relative to the non-hyperinfectious vibrios, which raises a question whether the hyperinfectious vibrio population class is actually needed in this model. Our calculations show that sympotomatic infecteds caused by hyperinfectious vibrios is a large proportion (generally 30% to 50%) in total infecteds. So the B_H variable is needed in order to accurately mimic the infection.*

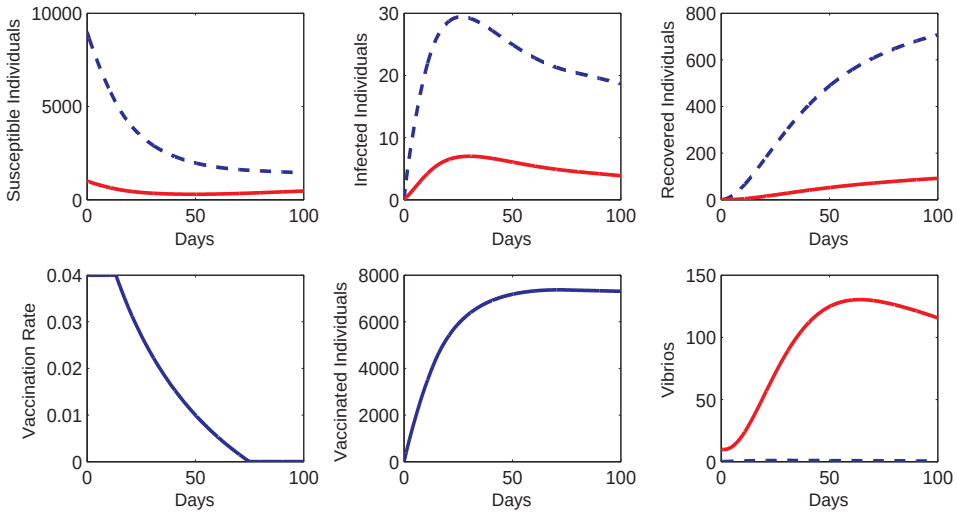

Figure 6.10: β_L changed into 0.04. Case 1

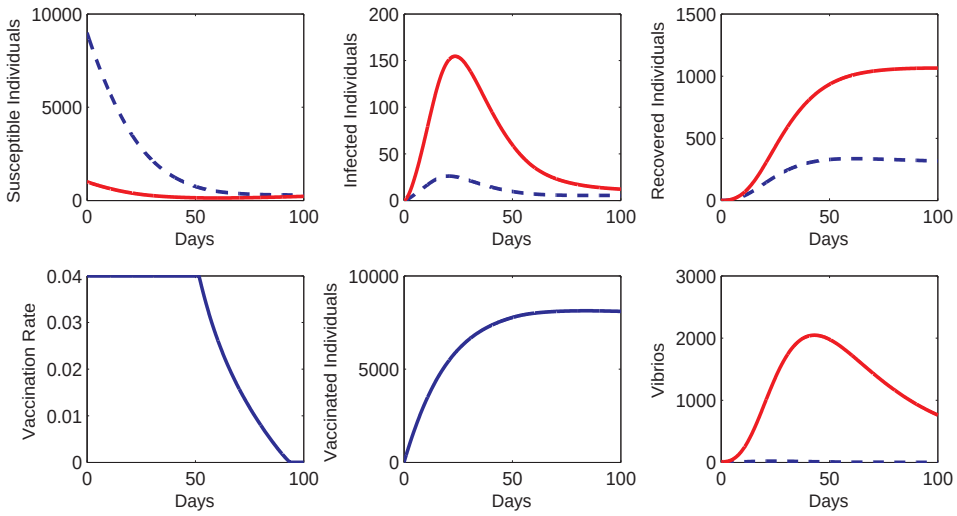

Figure 6.11: p changed into 0.8. Case 1

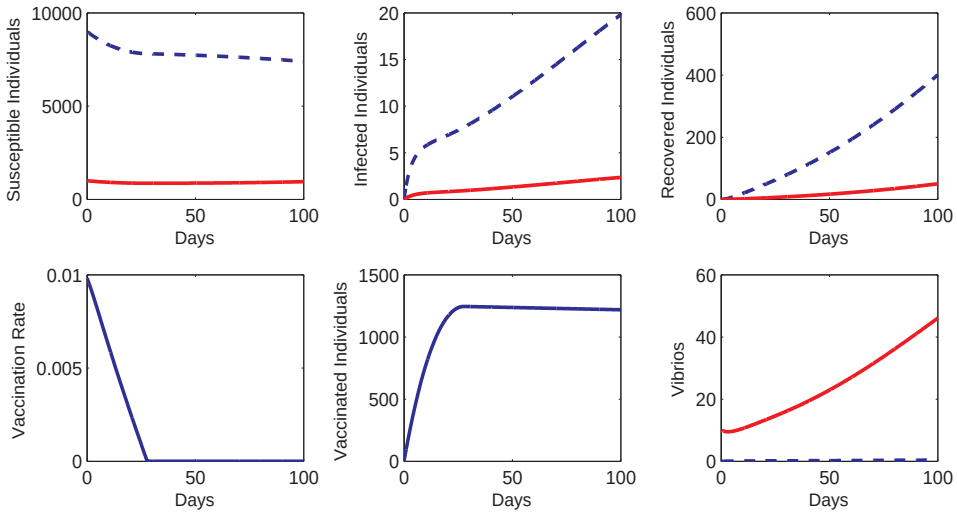

Figure 6.12: γ_2 changed into 0.4, Case 1.

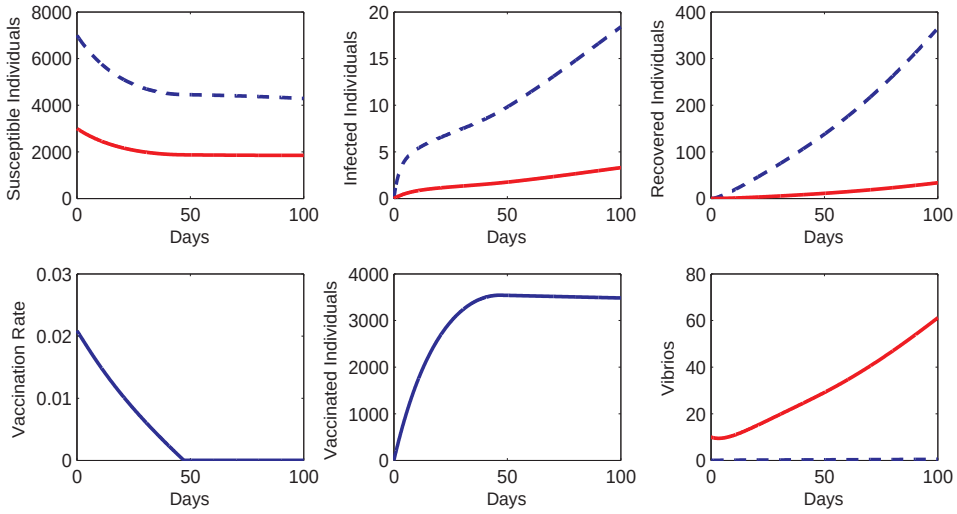

Figure 6.13: S_0 changed into 7000. Case 1

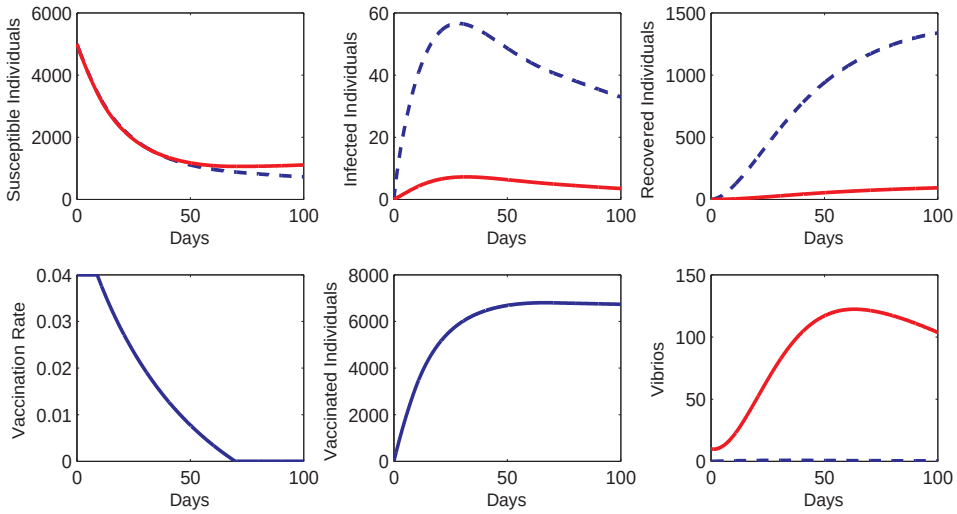

Figure 6.14: β_L changed into 0.04. Case 2

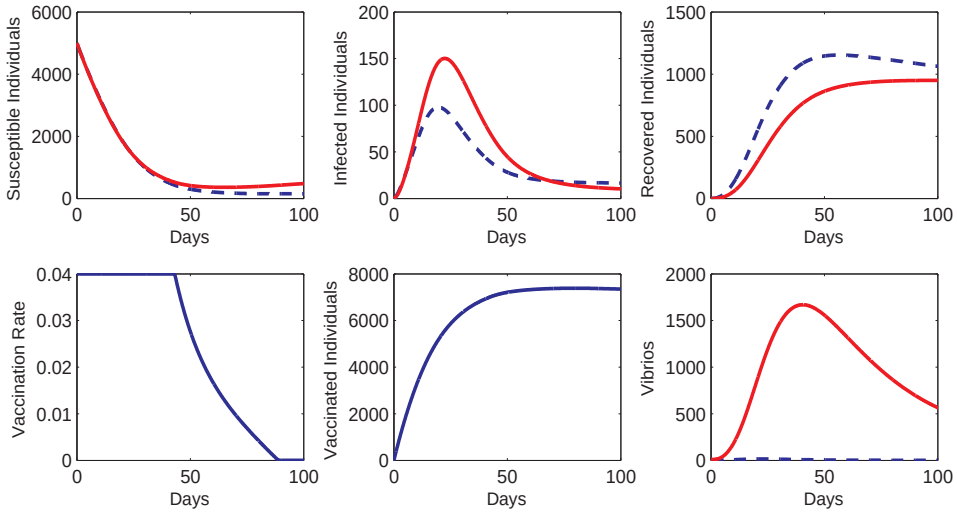

Figure 6.15: p changed into 0.8. Case 2

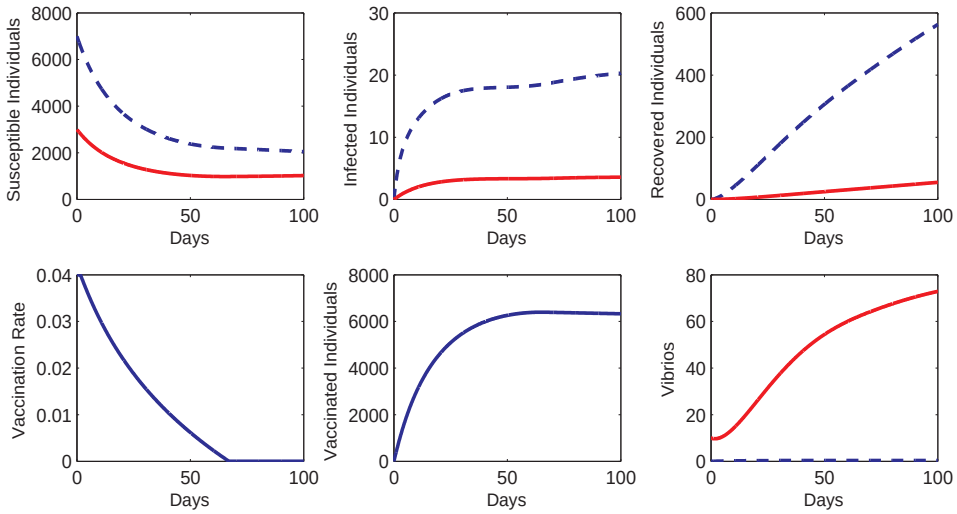

Figure 6.16: S_0 changed into 7000. Case 2

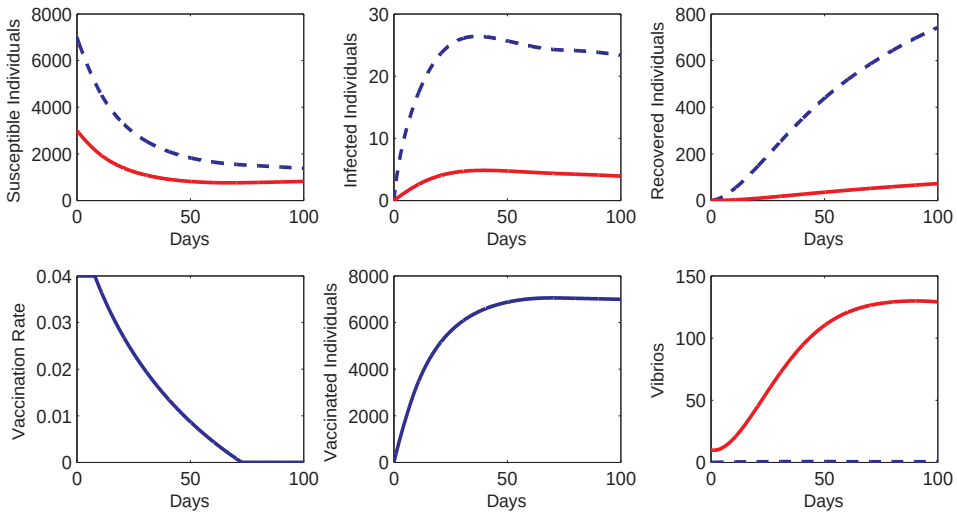

Figure 6.17: β_L changed into 0.04. Case 3

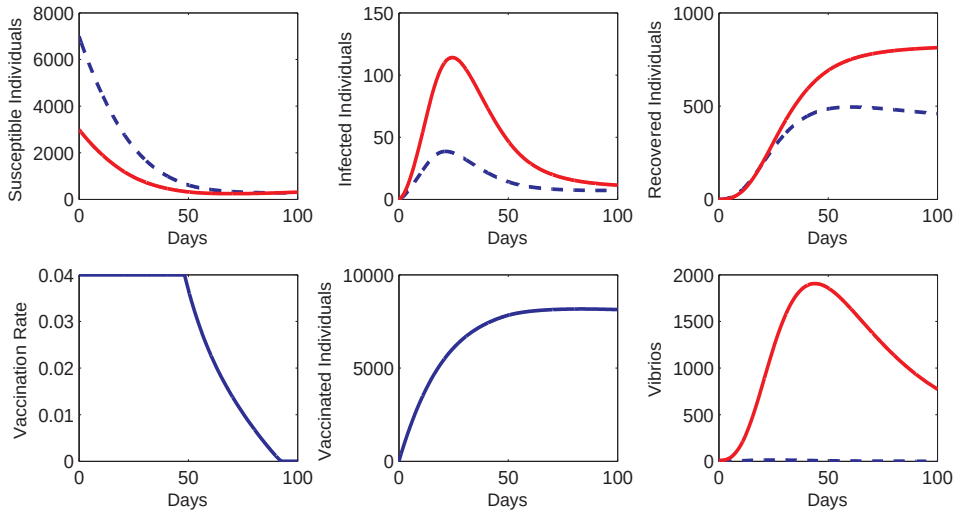

Figure 6.18: p changed into 0.8. Case 3

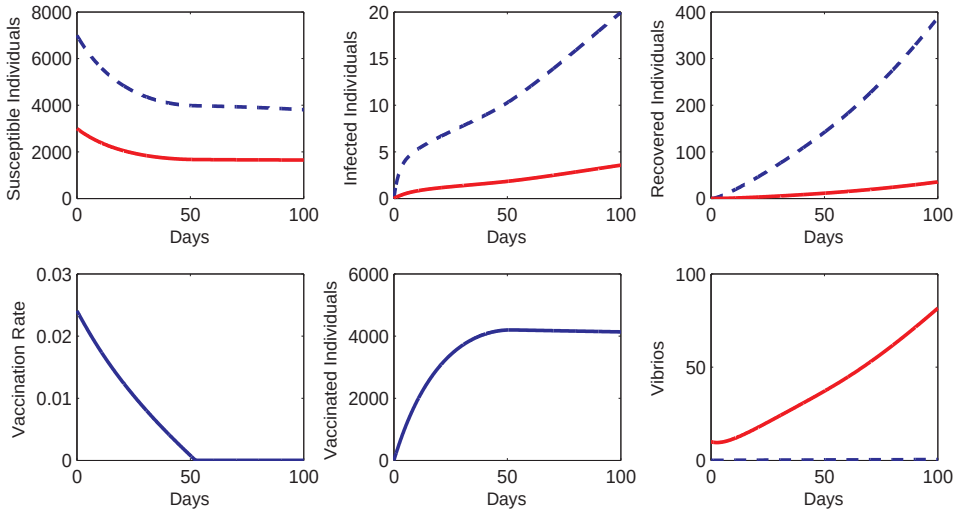

Figure 6.19: S_0 changed into 7000. Case 3

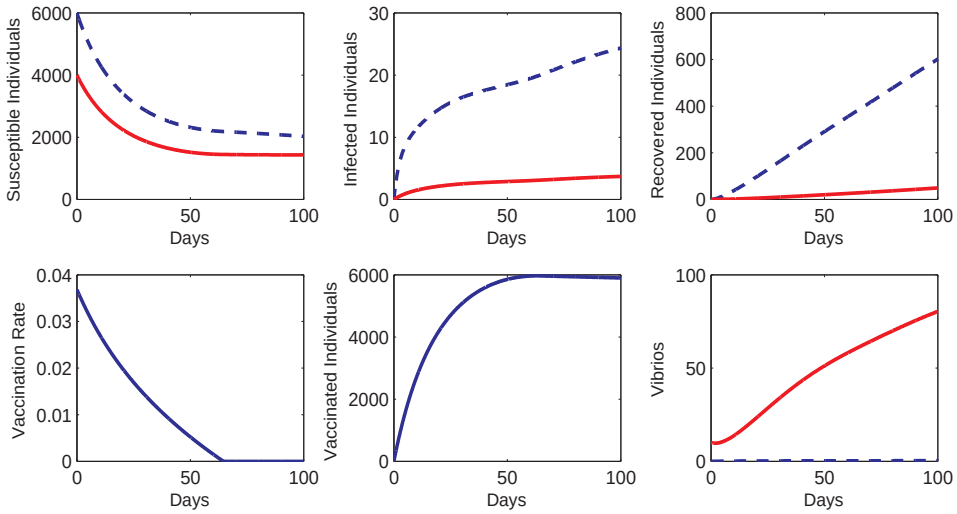

Figure 6.20: β_L changed into 0.04. Case 4

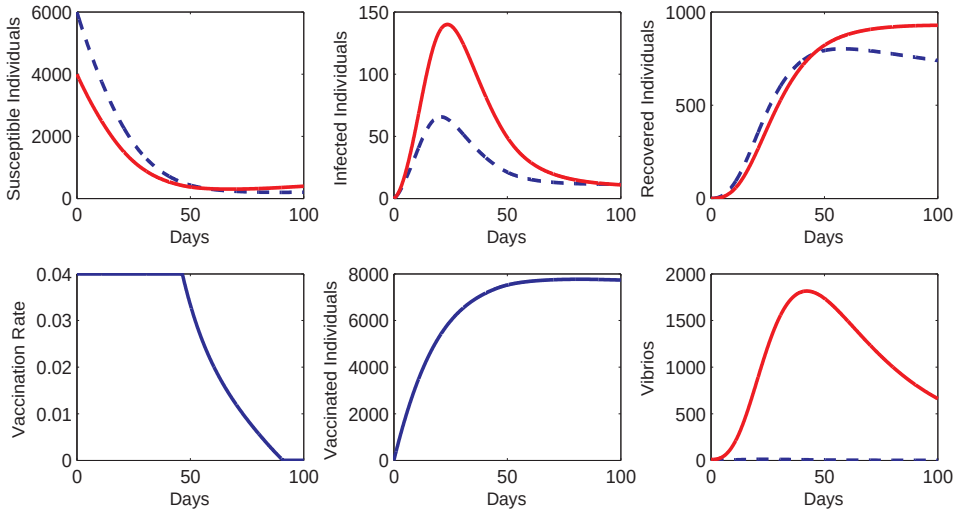

Figure 6.21: p changed into 0.8. Case 4

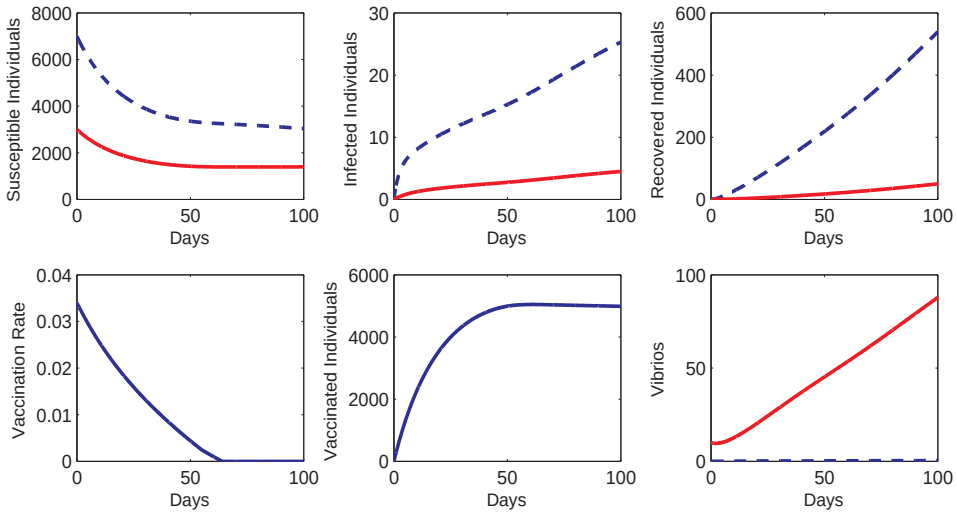

Figure 6.22: S_0 changed into 7000. Case 4

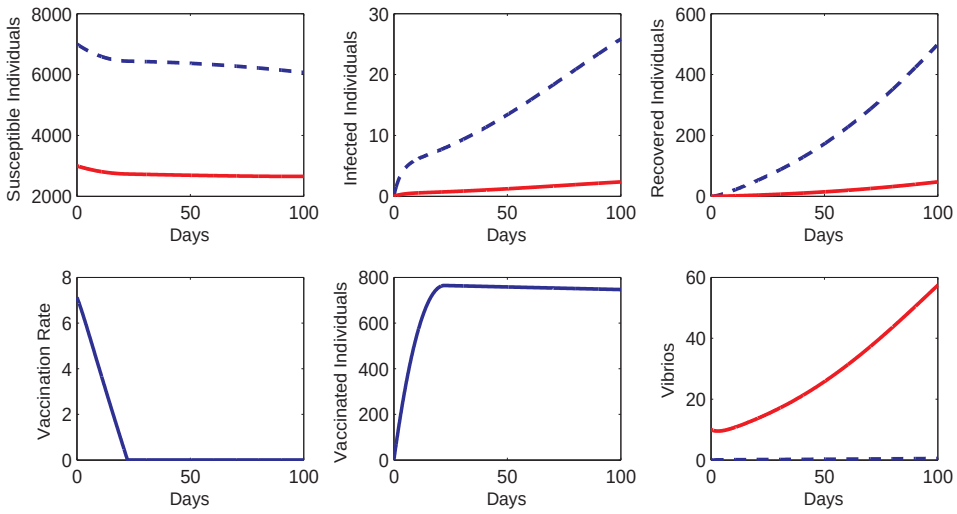

Figure 6.23: γ_2 changed into 0.4, Case 3.

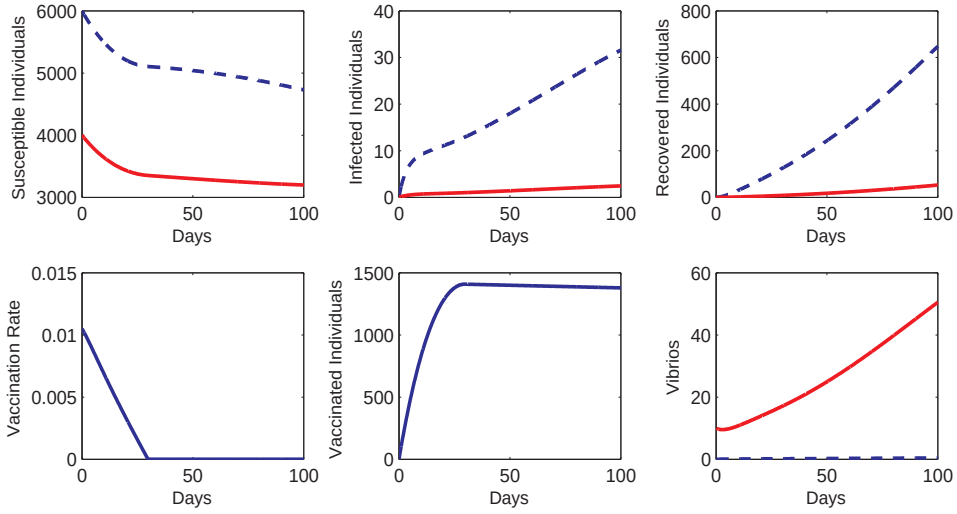

Figure 6.24: γ_2 changed into 0.4, Case 4.

6.7 Conclusion

This work provides an ordinary differential equation model for the spread of cholera that incorporates symptomatic and asymptomatic infections, hyperinfectious and non-hyperinfectious vibrios, susceptibles with partial immunity and susceptibles without partial immunity, and different rates of loss of immunity.

Our work on the application of the optimal control theory on this model also presents both theoretical and numerical analysis of the most economical vaccination strategies. Numerical results based on Latin Hypercube Sampling analysis determines the effects on the optimal control arising from variation in sensitive parameters.

An important result of this work is the role played by infection rate in decision making. This work shows that there are different sets of parameters that can give the same infection rate, and even though the population dynamics arising from those sets of parameters are different, the optimal vaccination strategy remains about the same. We have not developed provide rigorous proofs of this result, but we do observe this pattern in numerical results for many sets of parameters. This result can be very helpful in determining vaccination schedules, because some parameters, such as the ingestion rates of vibrios, are hard to quantify in real life, and are sensitive parameters in the system, yet the infection rate is more easily measured.

Bibliography

Bibliography

[1] (2008). World health organization, cholera, fact sheet no. 107. 87

[2] Andersen, M. (1991). Properties of some density-dependent integrodifference equation population models. *Mathematical Biosciences*, 104:135–157. 7

[3] Andow, D. A., Kareiva, P. M., Levin, S. A., and Okubo, A. (1990). Spread of invading organisms. *Landscape Ecology*, 4:177–188. 6

[4] Auckerman, J. N., Rombo, L., and Fisch, A. (2007). The true burden and risk of cholera: implications for prevention and control. *Lancet Infect. Dis.*, 7:521–30. 82

[5] Bateman, A. J. (1950). Is gene dispersion normal? *Heredity*, 4:353–363. 7

[6] Bhat, M. G., Fister, K. R., and Lenhart, S. (1999). An optimal control model for surface runoff contamination of a large river basin. *Natural Resource Modeling Journal*, 12:175–195. 25

[7] CDC (June 2010). Cholera general information, last revived 6-15-2011, http://www.cdc.gov/cholera/general/. *Nature*. 87

[8] Chandrasekhar, S. (1943). Stochastic problems in physics and astronomy. *Rev.Mod. Phys.*, 15:1–91. 6

[9] Clark, J. S. (1998). Why trees migrate so fast: Confronting theory with dispersal biology and the paleorecord. *American Naturalist*, 152:204–224. 6

[10] Codeço, C. (2001). Endemic and epidemic dynamics of cholera: the role of the aquatic reservoir. *BMC Infect Dis.*, 1(1). 82

[11] Codeço, C. and Coelho, F. (2000). Trends in cholera epidemiology. *PLoS Med.*, 1(1):e42. 88

[12] Corporation, B. D. (2010). Cholera. 88

[13] Easterling, M. R., Ellner, S. P., and Dixon, P. M. (2000). Size-specific sensitivity: Applying a new structured population model. *Ecological Society of America*, 81(3):694–708. 7

[14] Ekeland, I. and Témam, R. (1976). *Convex Analysis and Variational Problems*. Society fro Industrial and Applied Mathematics, Philadelphia, PA. 12

[15] Fleming, W. H. and Rishel, R. W. (2005). *Deterministic and Stochastic Optimal Control*. Springer-Verlag, New York. 1

[16] Gaff, H., Joshi, H. R., and Lenhart, S. (2007). Optimal harvesting during an invasion of a sublethal plant pathogen. *Environment and Development Economics Journal*, 12:673–686. 2, 7

[17] Hackbush, W. (1978). A numerical method for solving parabolic equations with opposite orientations. *Computing*, 20(3):229–40. 42

[18] Hartley, D. M., Morris, J. G., and Simth, D. L. (2006). Hyperinfectivity: a critical element in the ability of v. cholerae to cause epidemics? *PLoS Med.*, 3(1):63–69. 4, 82, 83, 88

[19] Holmes, E. E., Lewis, M. A., Banks, J. E., and Veit, R. R. (1994). Partial differential equations in ecology spatial interactions and population dynamics. *Ecology*, 75:18–29. 6

[20] Jeuland, M., Cook, J., Poulos, C., Clemens, J., Whittington, D., and Group, D. C. E. S. (2009). Cost-effectiveness of new-generation oral cholera vaccines: A multisite analysis. *Value in Health*, 12:899908. 88

[21] Joshi, H. R., Lenhart, S., and Gaff, H. (2006). Optimal harvesting in an integrodifference population model. *Optimal Control Applications and Methods*, (27):135–157. 2, 3, 7, 18, 39, 40, 42, 50

[22] Joshi, H. R., Lenhart, S., Lou, H., and Gaff, H. (2007). Harvesting control in an integrodifference population model with concave growth term. *Nonlinear Anal. Hybrid Syst*, 3:417–429. 2, 3, 7, 39, 41, 42, 50

[23] Kean, J. M. and Barlow, N. D. (2001). A spatial model for the successful biological control of sitona discoideus by microctonus aethiopoides. *The Journal of Applied Ecology*, 1(38):162–169. 7

[24] King, A., Ionides, E. L., Pascual, M., and Bouma, M. (2008). Inapparent infections and cholera dynamics. *Nature*, 454:877–880. 4, 82, 83, 87, 88

[25] Koelle, K., Rod, X., Pascual1, M., Yunus, M., and Mostafa, G. (4 August 2005). Refractory periods and climate forcing in cholera dynamics. *Nature*, 436:696 700. 88

[26] Kot, M. (1992). Discrete-time travelling waves: Ecological examples. *Journal of Mathematical. Biology*, 30:413–436. 6, 43

[27] Kot, M. (2002). Do invading organisms do the wave? (english summary). *Can. Appl. Math. Q.*, 1(10):139–170. 2, 6

[28] Kot, M., Lewis, M., and van den Driessche, P. (1996). Dispersal data and the spread of invading organisms. *Ecology*, 77:2027–2042. 2, 6

[29] Kot, M. and Schaffer, W. (1986). Discrete-time growth-dispersal models. *Math. BiosciMathematical Biosciences*, 80:109–136. 6

[30] Legros, D., Paquet, C., Perea, W., Marty, I., Mugisha, N., Royer, H., Neira, M., and Ivanoff, B. (1999). Mass vaccination with a two-dose oral cholera vaccine in a refugee camp. *Bull World Health Organ.*, 77(10):837–42. 87

[31] Lenhart, S. and Workman, J. (2007). *Optimal Control Applied to Biological Models*. CRC Press. 4

[32] Lewis, M. A. (1997). Variability, patchiness, and jump dispersal in the spread of an invading population. in spatial ecology: The role of space in population dynamics and interspecific interactions, d. tilman and p. kareiva, editors. *Princetion University Press*, Princetion , New Jersey, USA,:46–69. 6

[33] Lewis, M. A. and RW, V. K. (1997). Integrodifference models for persistence in fragmented habitats. *Bulletin of Mathematical Biology*, 59:107–137. 6

[34] Li, X. and Yong, J. (1995). *Optimal Control Theory for Infinite Dimensional Systems*. Birkhäuser, Boston. 3

[35] Lukes, D. L. (1982). *Differential Equations: Classical to Controlled*. Academic Press, New York. 93

[36] MacDonald, G. M. (1993). Fossil pollen analysis and the reconstruction fo plant invasions. *Advances in ecological research*, 24:67–109. 6

[37] Merrell, D. S. and Bulter, S. M. (2002). Host-induced epidemic spread of the cholera bacterium. *Nature*, 417:642–645. 82, 83

[38] Murray, J. D., Stanley, E. A., and Brown, D. L. (1986). On the spread of rabies among foxes. *Proc. Roy. Soc. London Ser*, 229:111–150. 6

[39] Neilan, R. M., Schaefer, E., Gaff, H., Fister, K., and Lenhart, S. (2007). Modeling optimal intervention strategies for cholera. *Bulletin of Math, . Biol.*, 1(4):379–393. 4, 82, 98

[40] Nelson, E. J., Harris, J. B., Jr, J. G. M., Calderwood, S. B., and Camilli, A. (October 2009). Cholera transmission: the host, pathogen and bacteriophage dynamic. *Nature Reviews: Microbiology*, 7:693702. 82, 83, 84, 87, 88, 89

[41] Neubert, M., Kot, M., and Lewis, M. A. (1995). Dispersal and pattern formation in a discrete-time predator-prey model. *Theoretical population biology*, 48:7–43. 7, 43

[42] Organization, W. H. (26 March 2010). Cholera vaccines: Who position paper, weekly epidemiological record. *Nature*, 85(13):117 128. 81

[43] Pontryagin, L. S., Boltyanskii, V. G., Gamkrelize, R. V., and Mishchenko, E. F. (1956). *Modeling optimal intervention strategies for cholera, The Mathematical Theory of Optimal Processes*. Wiley, New York. 1, 95, 96

[44] Reid, C. (1899). *The origin of the British Flora*. Dualu, London, UK. 6

[45] Sethi, S. P. and Thompson, G. L. (2000). *Optimal Control Theory; Applications to Management Science and Economics*. Kluwer, Boston. 3

[46] Slatkin, M. (1973). Gene flow and selection in a cline. *Genetics*, 75:733–756. 6

[47] Slatkin, M. (1975). Gene flow and selection in a two-locus system. *Genetics*, 81:787–802. 6

[48] Tien, J., Poinar, H., Fisman, D., and Earn, D. (2011). Herald waves of cholera in nineteenth century london. *J. of Royal Society, Interface*, 8:756–760. 82

[49] Tien, J. H. and Earn, D. J. D. (2010). Multiple transmission parthways and disease dynamics in a waterborne pathgen. *Bulletin of Math, . Biol.*, 72(6):1506–1533. 82

[50] van den Driessche, P. and Watmough, J. (2002). Reproduction numbers and sub-threshold endemic equilibria for compartmental models of disease transmission. *Mathematical Biosciences*, 180:2948. 91

[51] Weinberger, H. F. (1978). Asymptotic behavior of a model in population genetics. *Nonlinear partial differential equations and applications*, 648:47–96. 6

[52] Yosida, K. (1980). *Functional Analysis, 6th ed.* Springer-Verlag, Berlin. 62, 63

Vita

Peng Zhong was born in Shandong province, China on February 22, 1985, the daughter of Zhong Zhenhua and Chen Fengyun. After completing high school at Pingyuan Yizhong High School, Shandong, China in 2000, she attended the University of Science and Technology of China, in Hefei, China from 2000-2004. She graduated with A Bachelor of Mathematics degree in 2004. From 2005-2011, she attended the University of Tennessee in Knoxville, Tennessee. Zhong's graduate schooling was supported by a graduate teaching assistantship. On this teaching assistantship, she taught several semesters of Calculus.

Zhong graduated with her PhD in Mathematics in August 2011. She continues her work in mathematical ecology as a postdoc with Prof. Nina Fefferman at Rutgers University in New Jersey.